Antonino Quattrone

Assessment of structural reliability: a dynamic monitoring approach

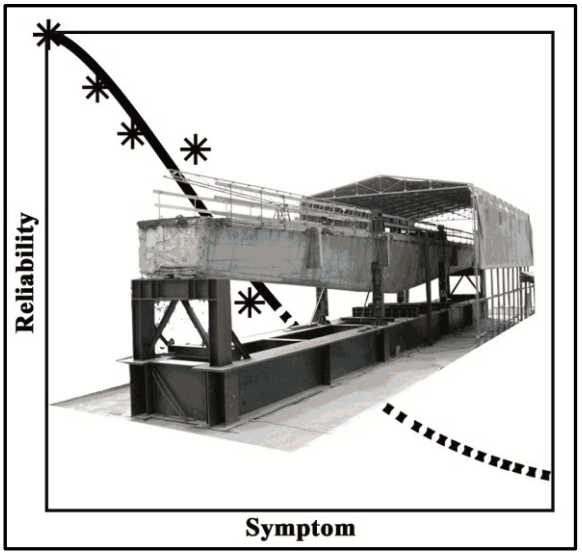

Dottorato di Ricerca in Ingegneria delle Strutture
Politecnico di Torino

Antonino Quattrone

Assessment of structural reliability: a dynamic monitoring approach

Tesi per il conseguimento del titolo di Dottore di Ricerca
XXIV Ciclo (A.A. 2009, 2010, 2011)

Dottorato di Ricerca in Ingegneria delle Strutture
Politecnico di Torino

APRILE 2012

Dottorato di Ricerca in Ingegneria delle Strutture
Politecnico di Torino
10129 Torino, Italy
Tutore: Prof. Alessandro De Stefano
Coordinatore: Prof. Alberto Carpinteri

Ringraziamenti

A Rosa e Maria Giovanna,
che hanno sempre
lottato insieme a me.

Desidero ringraziare tutti coloro che sono stati coinvolti, a volte loro malgrado, in questo lavoro. Ringrazio in particolare il prof. Alessandro De Stefano per il supporto e la fiducia che ha dimostrato nei miei riguardi in tutti questi anni; il prof. Rosario Ceravolo, per il suo aiuto alla comprensione di alcune tematiche trattate in questo lavoro.

Un ringraziamento speciale lo rivolgo ai miei amici con cui ho avuto la fortuna, il piacere e l'onore di lavorare fianco a fianco: li ringrazio di cuore per i loro consigli, il loro supporto costante e per i tantissimi momenti trascorsi insieme.

Gianluca, Emiliano, Luca, Francesco, Giacomo, Giovanna, Maria Elena, Barbara, Alessandro, Maria, Alex, Luisa e gli altri che ho dimenticato sono senza alcun dubbio la parte migliore di questo percorso. Non avrei potuto chiedere compagni migliori.

Abstract

The subject of this thesis is framed in the field of vibration based monitoring. In particular the work is focused on: implementing techniques of extraction of features, the use of collected data to recognize damages and the combined application of knowledge coming from monitoring systems with the classical structural safety formulations to a real case study. The thesis can be divided in three parts, which cover three of the main topics of SHM.

1. The first step consists in a proposal for an improved modal frequency identification procedure based on time-frequency estimators. The proposed method exploits the properties of Principal Component Analysis in identifying the stationary components of the instantaneous time-frequency estimators, and then the modal frequencies, analysing non-stationary signals. The method was validated trough numerical examples and then applied to a real complex case study: the Holy Shroud Chapel in Turin.

2. In the second part, the results of extensive experimental test campaign performed on a masonry arch bridge model are presented. A proposal for an on-line application of novelty detection technique is formulated and the application based on instantaneous modal parameters identified during the application of pier settlements is presented.

3. The last point investigated in this thesis is the combined application of knowledge coming from dynamic tests and the classical structural safety formulations to a set of concrete bridge beams, recently dismounted after 50 years of service life. Both static and dynamic tests have been carried out on five beams and modal parameters identified. The tests highlight the connection among residual strength and dynamic characteristics, as the periods.

Riassunto

Il soggetto di questa tesi si inserisce nell'ambito di ricerca riguardante il monitoraggio strutturale dinamico. La ricerca ha riguardato tre aspetti principali: l'implementazione di tecniche di estrazione di parametri sensibili dai dati di monitoraggio, l'utilizzo di tali parametri al fine di identificare l'insorgere di un danno ed, infine, l'applicazione combinata dei dati di monitoraggio con le procedure di valutazione della sicurezza di strutture esistenti.

La tesi tratta tre argomenti principali riguardanti il tema del monitoraggio strutturale diagnostico:

1. Il primo argomento consiste nella proposta di una procedura di identificazione dei paramentri modali basata su stimatori nel dominio tempo – frequenza. Il metodo proposto sfrutta le proprietà della Principal Component Analysis al fine di identificare le componenti stazionarie di stimatori istantanei t-f e , da queste, le frequenza modali della struttura. Il metodo è stato validato su esempi numerici e quindi applicato ad un caso studio reale, la Cupola della S.S. Sindone di Torino.

2. Nella seconda parte si presentano i risultati della sperimentazione condotta su un modello di ponte ad arco in muraturaE' formulate una proposta per l'applicazione on-line di tecniche di novelty detection basate sulla identificazione istantanea dei parametric modali. La metodologia è stata validate sulla base dei segnali ottenuti durante l'applicazione di un danneggiamento imposto al modello di ponte.

3. L'ultimo argomento trattato consiste nell'applicazione combinata dei dati di prove dinamiche con le procedure di valutazione della sicurezza ad un set di travi da ponte, rimosse dopo 50 anni in opera. Sono state eseguite sia prove dinamiche che statiche, finalizzate alla valutazione della resistenza residua. I risultati delle analisi evidenziano la correlazione tra resistenza residua e le caratteristiche dinamiche, Quindi, sulla base dei dati sperimentali, sono state applicate le formulazioni di stima dell'affidabilità strutturale riscontrate in letteratura.

INDEX

Chapter 1

Introduction

The network of infrastructures of a nation constitutes an asset of strategic importance to the life of the community. Its management requires periodic monitoring, through both short-term and long-term programs. In particular, the actual serviceability conditions, the assessment of the safety conditions and the vulnerability to natural catastrophic events must be checked, also resorting to experimental techniques.

Interest in Structural Health Monitoring (SHM) has been growing in recent years, especially in view of the potential social and economic benefits that might be obtained through a controlled management of the infrastructural asset. A thorough knowledge of the effective operational conditions and the residual safety margins of an infrastructure, achievable implementing a monitoring system, may lead to a rational scheduling of the interventions, and hence to an optimal management of economic resources.

The development of a SHM system is a complex, multidisciplinary task. It requires a detailed knowledge of the structure and a preliminary risk analysis based on several damage scenarios. On the basis of a sensitive analysis, appropriate features can be observed and in this context the implementation of a effective measurement system represent a crucial step.

The massive amount of data collected must be elaborated trough appropriate algorithms, sifting the useful information to be used in the decision-making process.

A generalised lack of knowledge is experienced starting the evaluation process of the condition of a structure, in particular for historical buildings or large complex systems. The uncertainties usually concern material properties, interaction between the structural elements, presence of hidden defects and the development of degradation phenomena. The recourse to

innovative technologies can help reaching an exhaustive comprehension of the structural behaviour and a reliable assessment of the structural health state. In the last years, the development of information technology, with increasing of data storage capacity, fast processing and transfer rate, associated with a general cost reduction, has addressed more and more studies into the development of vibration-based SHM systems.

Extensive research has been carried out on the development of non-destructive assessment methods based on the changes of the dynamic structural response. The adoption of vibration monitoring procedures and other non-destructive damage evaluation techniques represents a particularly appealing perspective for existing structures. In vibration-based monitoring, it is assumed that the vibration characteristics of the structure change due to damage, and by identifying these characteristics and comparing them to those of a healthy structure the existence of damage can be detected.

The residual reliability of the structure can then be defined as a function of the measurable symptoms used in damage detection. The knowledge of the current value of a symptom makes it possible to determine the residual damage capacity and the residual lifetime of a structure. One of the main purpose of a monitoring system should be detecting the damage and assessing the residual structural reliability over time. The effect of aging in structures, the evolution of degradation and the consequent reduction of safety were extensively studied in literature.

The subject of this research is framed in the field of vibration based monitoring. In particular the work is focused on: implementing techniques of extraction of features, the use of collected data to recognize damages and the application of reliability evaluation procedures based on symptoms evolution. Experimental test campaigns on different typologies of structures have been performed along past years, and each issue here threated has been applied on a real case study.

The first step consists in the proposal of an improved modal frequency identification procedure based on time-frequency estimators. Modal frequencies are widely used as features in a number of damage detection techniques. The proposed method exploits the properties of Principal Component Analysis in identifying the stationary components of the instantaneous time-frequency estimators, and then the modal frequencies, analysing non-stationary signals. The method was validated trough numerical examples and then applied to a real complex case study: the Holy Shroud Chapel in Turin. This structure is particularly challenging due to his geometrical configuration and the presence of damages caused by a destructive fire broke out in 1997 during some restoration works.

In the second part, the results of extensive experimental test campaign performed on a masonry arch bridge model are presented. In previous works (Ruocci, 2010), this model was tested to propose the application of SHM methodologies, based on novelty detection, to the protection of historical bridges from scour. In this thesis, a proposal for an on-line application of novelty detection technique is formulated and the application based on instantaneous modal parameters identified during the application of pier settlements is presented.

The last point investigated in this thesis is the combined application of knowledge coming from monitoring systems and the classical structural safety formulations to a real case study. The formulated approach presented ties ultimate strength and features extracted by dynamic test of ageing structures. The effects of corrosion or carbonation in the life time of structure, especially bridges, are widely studied and some mathematical models can be found in literature. An extensive experimental campaign was performed to evaluate the residual load-bearing capacity of nine precast post-tensioned concrete bridge beams showing different levels of degradation, recently dismounted after 50 years of service life. Dynamic tests have been carried out on five beams and modal parameters identified. The tests highlight the connection among residual strength and dynamic characteristics, as the periods.

The evolution of dynamic characteristics as a function of the ultimate bearing capacity has been evaluated. The residual resistance of the of the beams has been expressed as a function of measured symptoms and the evolution in time is estimated. Nevertheless the reliability of the beams has been also estimated.

Chapter 2

Vibration-based structural health monitoring and reliability assessment

This chapter introduces the concept of the Structural Health Monitoring (SHM), describing its common components and presenting the motivations which encourage its adoption in managing important infrastructures. A general classification of the available experimental technologies is provided and the most important issues which must be considered in the design of a diagnostic monitoring system are addressed.

Nowadays, most of the SMH applications make effective use of vibrational data acquired by means of different kind of sensors permanently applied or during periodical on field tests. A complete vibration-based SHM system needs the evaluation of the following steps:

1. Instrumentation
2. Data acquisition
3. Signal processing
4. Feature extraction
5. Pre-processing and data cleaning
6. Damage detection techniques
7. Alarms and data transfer
8. Prognosis evaluation

In particular, features extraction and damage detection techniques will be here treated. Nowadays, the integration between the knowledge coming from the monitoring systems (diagnosis) and the and the structural safety formulations (prognosis) is one of the most challenging issue. The aim is the improvement of structural systems maintenance practices by increasing the accuracy of the predictions, improving the structural safety and reducing the life-cycle cost. The symptom- based reliability assessment approach, proposed by Cempel [30] in the field of mechanical engineering, is here presented in details.

2.1 Introduction

Structures are inevitably subjected to ageing effects and require expensive maintenance acts and surveillance against accidental events. The availability of a permanent assessment of the structural conditions is essential to assure an appropriate level of reliability and safety. In addition to the traditional visual inspection methods, several experimental procedures have been proposed in order to provide accurate information about the structural behaviour and integrity.

This process has been risen by the rapid development in the sensing, data analysing and information sciences fields. In [1] Farrar and Worden broadly define *structural health monitoring* (SHM) as a process which involves the periodic monitoring of a structure through measurements, the extraction of features able to capture the phenomena under investigation and their statistical analysis to determine the actual state of the system. A diagnostic monitoring system is therefore the result of the integration of several sensors, devices and auxiliary tools, like:

- a measurement system;
- an acquisition system;
- a data processing system;
- a communication/warning system;
- an identification/modelling system;
- a decision making system.

Even if it is based on innovative measuring, analysing, modelling and communication techniques, SHM shares the same goals of traditional visual inspections. The health monitoring can be considered an extension of the well-established investigation practices since it integrates these novel technologies in a unique smart system, trying to overcome the limitations of traditional visual inspections.

There are several reasons which let prefer an automatic monitoring system working in real or at least nearly-real time rather the investigations performed periodically. First of all, a matter of economic convenience. Visual inspections must be carried out by high qualified personnel with a periodic recurrence which is not related to the actual state of the

structure. A permanent monitoring system is much more cost-effective on a long period of time because of the amortization of the initial costs due to the ideation, design and execution. The vibration-based damage assessment method has proved its potentialities in different applications.

At present, several issues should be investigated or developed. The use of different typologies of less expansive sensors in networks will provide a continuous flow of data that will require a capability to process and analyse different sources of information and to take the environmental and operating conditions variability into account.
Furthermore, an effective integration between the knowledge coming from SHM and the formulation of structural reliability represents one of the most challenging issue to investigate.

2.2 Structural health monitoring

Different authors have given different definitions for SHM. For example, Aktan et al. [2] defined SHM as follows: "SHM is the measurement of the operating and loading environment and the critical responses of a structure to track and evaluate the symptoms of operational incidents, anomalies, and/or deterioration or damage indicators that may affect operation, serviceability, or safety reliability".

Rytter, in his PHD thesis, Sohn et al. [3] classified the purposes for which a monitoring system is set up, in increasing order of complexity and difficulty to achieve:

1) damage identification;
2) damage localisation;
3) damage classification;
4) estimation of the magnitude of damage;
5) evaluation of residual service life (prognosis).

In terms of the identification and localisation of structural damage, so far the most significant results have been obtained in the field of Condition Monitoring of rotating machines, mostly thanks to a variety of factors, including very low variability in the operational conditions, a deep knowledge of possible damage scenario, a clear-cut correlation between damage and structural response and, not least, the widely acknowledged economic benefits that the managers of such systems can obtain from monitoring activities [1].

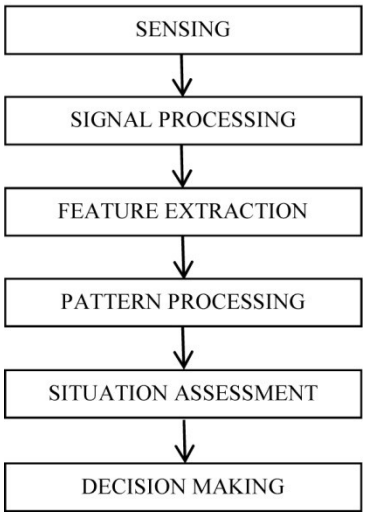

Figure 1 Waterfall model of a SHM process

Several experimental technologies can be adopted at the purpose to grown the knowledge of structural condition (

Table 1).

Class	Name	Description
Static test	Non-destructive static tests	Measurement of the response in a limited portion of the structure under the application of controlled loads, used for the mechanical characterisation of the materials.
	Destructive static tests	Laboratory tests carried out to characterise the strength of collected samples or *in-situ* destructive tests. The latter are expensive and their results are difficult to generalise: their execution is usually limited to the realm of a scientific research project.
Dynamic tests	Non-destructive dynamic tests	Vibration analysis performed to extract the modal properties of the structure and characterise its dynamic behaviour. They can employ a forced excitation or the environmental vibrations produced by wind, traffic or micro-earthquakes. The forced excitation can be provided impulsively through the impact of a sledge hammer or the drop of a weight, or regulated by an electro-dynamic or electro-hydraulic actuator.
	Permanent monitoring	The most innovative and ambitious development of the

Hybrid tests		experimental technologies: the measuring system is permanently placed on the structure acquiring periodically different quantities referred to the structural behaviour and the operational and environmental conditions. This allows to study their correlation in order to provide reliable early warnings.
	Geometric monitoring	Its most common objective is to track changes in the geometry produced by phenomena delayed in time. Geometry monitoring technologies include laser scanning, global positioning systems, photogrammetry and remote sensing technologies.
	Non-destructive evaluation	A wide range of non-destructive technologies used to investigate limited portion of the structure in order to acquire information of different nature. Commonly used to detect hidden construction details, defects or damage or to determine the physical and chemical properties of the materials.

Table 1 Principal experimental technologies employed in SHM

In the field of civil engineering, the need of monitoring the actual operational conditions became evident with the construction of huge structures, such as dams, suspended bridges, nuclear power plants. In the field of dams and nuclear power plants, the execution of monitoring activities is mandatory by law and is governed by specific regulations (Brownjohn [4], Fanelli [5]).

In the field of bridges, the collapse of the Tacoma bridge put in evidence the need of monitoring the operational conditions of suspended bridges, and, in particular, to experimentally check the wind-structure interaction effects. The huge investments involved in building these structures justified the adoption of highly sophisticated and costly monitoring systems and careful inspection programs, as has been described for experiences in Japan, Hong Kong, North America (Wong [6]). Currently, the best results have been obtained in laboratory applications or applications confined to the field of research, such as, for instance, the *Z24 bridge* [8].

On smaller bridges – such as those built in Italy in the 1950s and 60s – the use of monitoring systems is not as common; the need to provide a maintenance program for these bridges began to be felt in the 1970s/80s, when major phenomena of structural damaging and deterioration of the materials occurred. The incidence of structural deterioration phenomena increases with the average age of a structure, giving rise to more and more urgent requests for repair and restoration interventions. Moreover, the ever greater performance levels required by the technical laws have claimed to the structural assessment of a considerable proportion of pre-existing bridges and require ad hoc interventions to restore the minimum safety level specified for new structures. Finally, interventions may be required, in some cases, due to the greater knowledge acquired on the

seismicity of the various regions, or even due to changes in the hydrogeological situation of a territory.
Ageing and damaging bring about variations in a structure, affecting the properties of its constituent materials, its geometric configuration, boundary conditions, the connectivity between the different structural elements, loading conditions. Damage may be the result of a process of accumulation, that develops continuously over time (as in the case of ageing, for instance) or be due to localised events (e.g., an earthquake).
In planning scheduled ordinary and, above all, extraordinary maintenance works, it is indispensable to possess detailed information on the actual conditions of an existing structure: this consideration bears out the importance of Structural Health Monitoring as well as experimental investigations and numerical analyses for the determination of mechanical properties, for diagnostic purposes and for a reliable estimate of residual safety levels. In the field of structural monitoring, the following aspects constitute problems still awaiting an effective solution:

- lack of a quantitative evaluation of economic benefits based on precise cost-benefit analyses;
- general inadequacy of the monitoring systems commonly used, in terms of type and number of sensors employed;
- ineffective handling and interpretation of the data supplied by the measuring instruments;
- need for reliable and economical systems to transfer the data collected;
- insufficient capability and reliability in damage detection and identification from the experimental measurements and discrimination from variations in ambient conditions.

The final aim of a monitoring system is to provide information about the health of the monitored object. The information gathered would then be used within a decision-making regarding the management of the structure. The integration of the monitoring in structural reliability assessment process would allow to optimize the scheduling of interventions needed to ensure the required performance with the safety levels demanded by the legislation over the years.

2.2.1 Vibration-based health monitoring

Dynamic monitoring of civil engineering structures (e.g. bridges, buildings, dams) has gained a lot of interest over the past few years, due to the rather cheap instrumentation and the development of new powerful system identification techniques.
Environmental conditions are a very relevant source of noise and uncertainty. Tests on real structures show the dramatic influence they have on the eigenfrequencies. Long term

temperature changes are closely correlated with the eigenfrequencies changes, but for short term the correlation lowers strongly. To get rid of the disturbance of the short term oscillation of eigenfrequencies, only predictive black-box model are available.

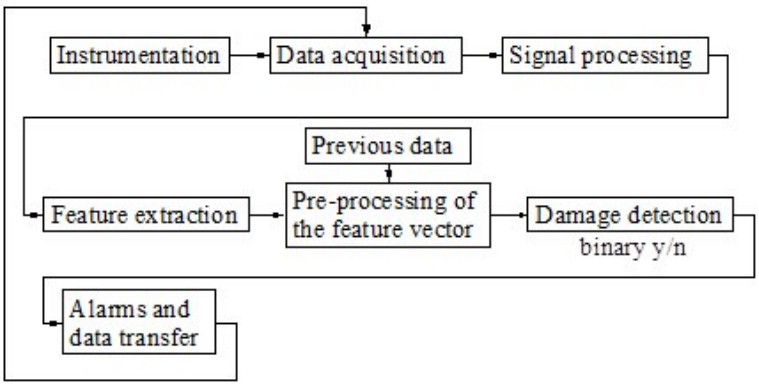

Figure 2 Flow chart of a structural health monitoring system (from Kullaa, 2005)

2.3 Experimental modal analysis

Structural diagnostics is often associated to experimental modal analysis techniques, since deviations in modal parameters may reflect changes in local mechanical properties. In civil engineering applications measurements carried out in environmental excitation conditions assume a special importance, in fact: a) measurements can be performed during the structure's regular service; b) they require no special excitation equipment; c) it is not necessary to measure the excitation.

2.3.1 Classification of modal identification techniques

The experimental modal analysis is the estimation of the structural modal parameters based on the excitation and response measurements. A schematic representation of the experimental modal identification is provided in Figure 3.The available modal identification techniques can be classified according to different criteria. First of all, a main distinction is between identification methods that use data in the time domain and those that use data in the frequency domain. Recently, some methods have been proposed, which employ data in the coupled time-frequency domain. In each case one

ore more locations for the input force and the output response can be investigated, leading to the distinction between the methods:

- SISO (single-input single-output): single response due to single force;
- SIMO (single-input multiple-output): multi responses due to single force;
- MIMO (multiple-input multiple-output): multi responses due to various forces;
- MISO (multiple-input single-output): single response due to many forces.

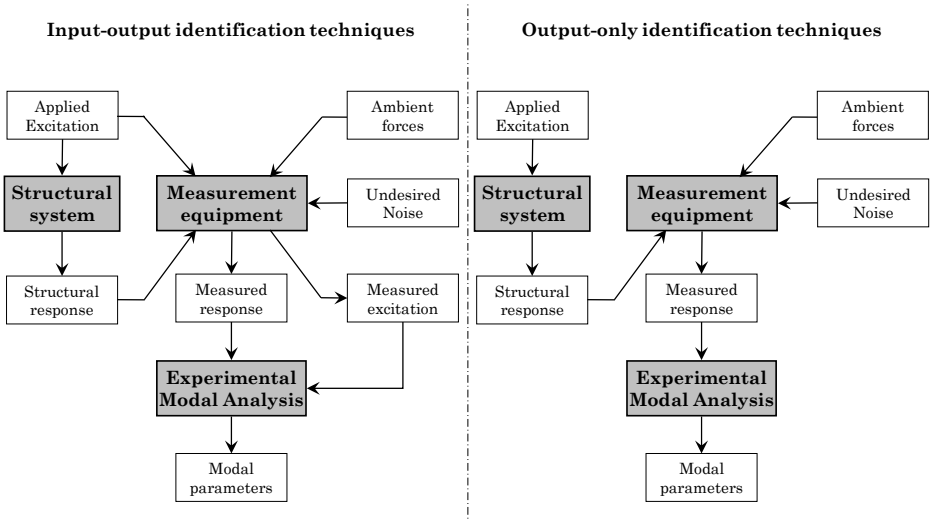

Figure 3 Schematic representation of the input-output and output-only identification methods

Further, the type of the identified dynamic properties distinguishes between direct and indirect methods. The former methods estimate directly the stiffness, mass and damping coefficients (or matrices in the multi-degree-of-freedom case). The indirect methods evaluate the modal parameters, i.e. the natural frequencies, mode shapes and damping ratios.

Another general classification criterion is related to the type of excitation source which is used in the experimental tests. As mentioned in the preceding sections of this chapter, vibration tests can be carried out either exciting the structure by means of actuators, shakers, sledge hammer impacts and dropping weights or exploiting the environmental vibrations provided by wind or traffic in the case of bridges. The forced vibrations allows the measurement of both the input force and the output response while only the structural response is measured in the ambient vibrations tests because the external loading may be unknown or very difficult to quantify. The free vibration tests,

where the systems are induced with an initial deformation and then are quickly released, can be pooled with the second group.

Therefore, in the logic of the diagnostic monitoring design, the choice of the excitation source also entails the adopted modal identification technique. In the case of input-output identification techniques the target is the determination of the Frequency Response Function (FRF) of the system. The techniques operating in the frequency domain generally try to approximate the FRF by means of procedures like the curve fitting, whereas in the time domain identification methods are based on autoregressive models [25] or Markov processes, as in the case of the realization algorithms.

Domain	Excitation	Methods
Time	known	Ibrahim Time Domain (ITD)
		Auto-Regressive Moving Average (ARMA)
	unknown	Eigenvalue Realization Algorithm (ERA)
		Stochastic Subspace Identification (SSI)
		PolyReference Time Domain (PRTD)
		Second Order Blind Identification (SOBI)
Frequency	known	Rational Fractional Polynomial (RFP)
		Goyder method
	unknown	Spectral Analysis
		Frequency Domain Decomposition (FDD)
Time-frequency	unknown	Time-Frequency Instantaneous Estimators (TFIE)

Table 2 Classification of the modal identification techniques

2.3.2 The output-only methods

The output-only methods require the fulfilment of some hypotheses referred to the nature of the excitation and the dynamic response. According to these characteristics several algorithms can be derived. For example, the spectral analysis can be used to identify the modal parameters in the case of stationary excitation [26]. In the time domain Auto-Regressive eXogenous (ARX) models employ exogenous noise [20] while Random Decrement (RD) techniques are used to determine the Impulse Response Function (IRF) [27].

In recent years, time domain techniques have been widely used successfully, thanks to the great spectral resolution offered by these methods in the analysis of complex systems, and thanks to their modal uncoupling capability.

Frequency domain techniques, though affected by the disturbance due to the needing of an edge-smoothing time window on digital samples, are again made interesting by the powerful cleaning effect of SVD tool [30]. The common limitation of time and frequency approaches lies in the fact that they have both been conceived for the analysis of response signals that do not deviate much from stationarity, though in actual fact they are widely used for the analysis of signals whose main characteristic is far from being stationarity (bridges excited by vehicle traffic, towers exposed to wind gusts, etc.).

In structural response signals, the main characteristic appears to be the slow variation in modal energy; the response might be viewed as a time-varying combination of modulated harmonic functions. Furthermore, in non-stationary conditions, classical Fourier analysis should be replaced by the more general time-frequency analysis. To cope with non-stationary excitation is possible to implement methods operating in the time-frequency domain [28,29]. A method has been recently proposed that works out instantaneous quantities, such as the phase difference and the amplitude ratio between channels, as a function of frequency. In linear systems, modal components are recognised since they show estimator values that are characterised by stability over time. The estimators are defined on the basis of the time-frequency analysis of vibration response signals, so these techniques might be placed into a new class of time-frequency domain methods. In the next chapters both time domain and time –frequency domain identification methods will be applied. A brief theoretical explanation of the time domain methods used is provided in the following. A more detailed explanation of time – frequency domain methods is reported in chapter 3, where an improved frequency extraction procedure will be proposed.

2.3.3 The ERA method

The ERA method, due to Juang et. al. ,adopts the state space formulation associated to the equation of motion which, written in the discrete time form, leads to:

$$\{u_{k+1}\} = [A]\{u_k\} + [B]\{\delta_k\} \tag{1}$$

where [A] is the "state matrix", [B] is the "input matrix", $\{u_k\}$ is the state vector and $\{\delta_k\}$ is the impulse excitation.

Assuming that at the initial time it is $\{u_k\} = \{0\}$ and knowing that $\{\delta_0\} = \{1,0,\ldots 0\}^T$ and $\{\delta_k\} = \{0\}$ at $k > 0$, for all subsequent time intervals it is possible to write:

$$\{u_k\} = [A]^{k-1}\{B\} \tag{2}$$

and by considering all the loading points, it is possible to find:

$$[X_k] = [A]^{k-1}[B] \tag{3}$$

where $[X_k]$ represents the "Markov parameters".

The k Markov parameters, which represent the measured signals (or their RD functions when working with ambient measurements), can be organised in a Hankel matrix. A Single Value Decomposition (SVD) is performed on the Hankel matrix to reconstruct Equation 3 from redundant data. This process is known as realisation and it entails the determination of the [A] and [B] matrices. There is an infinite number of sets of matrices that satisfy Equation 3 since there is an infinite number of realisations for the system. The aim is to obtain the realisation which, while characterised by the smallest state space dimension, still represents the dynamic behaviour of the structure. Accordingly, the modal quantities will be extracted from the following eigenvalue and eigenvector problem:

$$[s[I] - [A]]\{\Psi_u\} = \{0\} \tag{4}$$

where s is the eigenvalue, $\{\Psi_u\}$ is the eigenvector and $[I]$ is the identity matrix.

2.3.4 The CVA method

When an ambient excitation is considered, the input is unmeasured and Equation 6.5 becomes:

$$\{u_{k+1}\} = [A]\{u_k\} + \{e_k\} \tag{5}$$

where $\{e_k\}$ is the excitation vector.

A Stochastic Subspace Identification (SSI) starts by building large block Hankel matrices from the output sequence, divided up in 'past' and 'future' data matrices as shown in Equation 5:

$$\left[\begin{array}{cccc} \{u_0\} & \{u_1\} & \cdots & \{u_{j-1}\} \\ \cdots & \cdots & \cdots & \cdots \\ \{u_{i-2}\} & \{u_{i-1}\} & \cdots & \{u_{i+j-3}\} \\ \{u_{i-1}\} & \{u_i\} & \cdots & \{u_{i+j-2}\} \\ \hline \{u_i\} & \{u_{i+1}\} & \cdots & \{u_{i+j-1}\} \\ \{u_{i+1}\} & \{u_{i+2}\} & \cdots & \{u_{i+j}\} \\ \cdots & \cdots & \cdots & \cdots \\ \{u_{2i-1}\} & \{u_{2i}\} & \cdots & \{u_{2i+j-2}\} \end{array}\right] = \left[\begin{array}{c} [U_p] \\ [U_f] \end{array}\right] = \begin{array}{c} "past" \\ "future" \end{array} \tag{6}$$

The Kalman filter state sequence can be obtained by projecting the row space of the future block Hankel matrix, into the row space of the past block Hankel matrix. This can be done using the concept of angles between subspaces, which is a generalization of the angle between two vectors. Once that state sequence is obtained, the estimation of the system follows from solving a least squares problem.

The SSI methods require the assumption that $\{e_k\}$ is constituted by white noise. If this assumption is violated, the main frequencies contained in the input signals cannot be separated from the authentic modal components, when solving the eigenvalue problem. The technique used for this application is the third algorithm considered in the unifying theorem proposed by Van Overschee and DeMoor. This method is often referred to as the "Canonical Variate Analysis" (CVA) and is due to Larimore.

2.4 Damage assessment based on vibration measurements

The identification of damage using vibration measurements is a well-established practice and its application to civil engineering structures dates back to early Eighties. Its theoretical foundation derives from the principle that the dynamic response of the structural system is affected by the alteration of the stiffness, mass or energy dissipation properties when damage occurs. The most widely accepted interpretation of the damage identification problem is that of statistical pattern recognition. In this approach the system is represented by a statistical model whose parameters are directly derived from the data. Each data (here referred as pattern) is condensed and expressed in terms of selected damage-sensitive features. The features extraction is generally recognised as the most crucial step in the diagnostic procedure.

Its role is essential and it can highly bias the damage recognition stage. Indeed, most of the damage identification methods are unable to deal with the raw data records because their massive dimension does not fit with the inputs limitation requirement common to every pattern recognition algorithm. Moreover, the selected features shall maximise the capability of the diagnostic method to discriminate among the different

structural states. The most sensitive information are condensed in low-dimension arrays while discarding further parts which could be source of noise and affect the accuracy of the damage assessment. Several damage symptoms have been identified to detect the anomalous behaviour of the system due to damage. For an extensive documentation about the parameters that can be employed within the vibration-based SHM the reader may refer to [1]. The features extracted from vibration measurements can be subdivided into three main domains: the time, frequency (or spectral) and modal domains. This classification is not only philosophical but entails substantial distinctions in the implementation of the damage identification algorithm depending on the selected features. In the time domain, the coefficients estimated by means of the Auto-Regressive (AR) or the Auto-Regressive Moving Average (ARMA) models are commonly used to fit the time histories acquired from the undamaged state of the structure. A base line is derived from these features and damage is detected when the coefficients estimated from new acquisitions are seen to deviate from it. In [3] Sohn and Farrar applied a control chart based on the coefficients extracted from the vibration test data acquired from a concrete column progressively damaged.

The features selection in the frequency domain rely on the application of the Fourier Frequency Transform (FFT) which allows to reduce drastically the volume of data and compensate the little loss of information averaging the effects of random noise. The selected features are commonly the shift in the resonance and anti-resonances or changes affecting the amplitudes. Alternative approaches consider limited portions of the frequency spectrum sampled around the resonance peaks. When the input force is unknown like in the output-only measurements, the computation of the Frequency Response Function (FRF) is substituted by the Power Spectral Density (PSD) or the Transmissibility Functions (TF). In [3] the transmissibility spectra computed by Fourier transforming the signals acquired from couples of piezoelectric accelerometers are sampled to detect, localise and assess damage simulated on an aircraft wing by the removal of pre-installed panels. A pattern recognition approach is pursued and an artificial neural network is trained to classify the patterns into damage classes corresponding to the removed panel.

The modal domain provides a large set of damage sensitive features. The first are the natural frequencies of the system whose shifts are commonly employed to compute damage detection indices. Methods based on modal displacements can be used to objectively measure the similarity between two mode shapes. The Modal Assurance Criterion (MAC) compares sets referred to the undamaged and damaged states of the structure. Low values of the index represent a dissimilarity between the modes and can be interpreted as an indication of damage.

Information about the localisation of structural changes due to damage can be obtained also by means of mode shape curvatures or strain mode shapes. Since they are derivatives of mode shapes their changes are highly localised to the region of damage and their sensitiveness is more pronounced compared to modal displacements. Modal curvatures are also employed in the determination of the modal strain energy to define an index for damage localisation in off-shore platforms. In [32], both spectral and modal

parameters have been successfully used in the identification of increasing damages applied to a masonry arch bridge model.

Several other features can be used for damage identification but, up to now, none of them has proved to work satisfactorily for every type of structure and for every type of damage. Unfortunately, the best features for damage detection are typically application specific. A large variety of possible damage scenarios may occur and the selection of the best features depends on the extraction of the most explanatory information related to the most likely damage events. This crucial stage of the diagnostic procedure requires a priori knowledge about the structure, the expected damage scenario and their interaction, i.e. the response of the structure to that specific type of damage. This amount of required information varies depending on the selected features but does not automatically imply an handicap for the damage assessment. The evidence of an expected structural behaviour represents a precious proof of the method's reliability and should not be considered secondary. From a different point of view, we can say that the physical meaningfulness is a further condition which should be satisfied in order to prevent erroneous misclassifications due to the scarce interpretability of the results. Finally, one can claim that the optimality in the features selection resides in a trade-off between their damage sensitiveness and the concrete possibility to ensure their consistency with the expected structural response to damage.

2.5 Monitoring-oriented reliability assessment

The integration of SHM and reliability analysis as a part of an efficient structural management and decision-making tool is nowadays a great challenge. Integrating visual inspections, diagnostic instrumentation and monitoring data allow updating the knowledge on the structural performance and can significantly affect, for example, the planning of interventions, allowing an optimization of maintenance and repair costs.

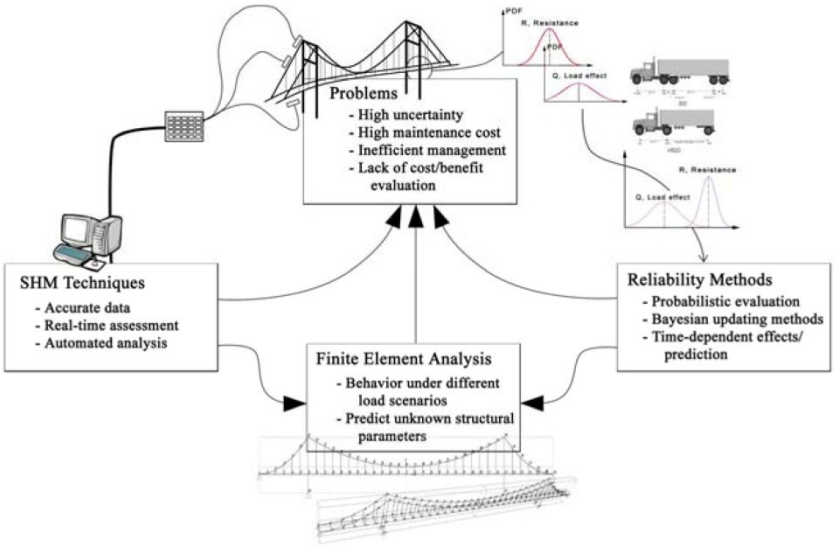

Figure 4 Approaches for Bridge Management (including SHM), Susoy et al.(2008) [29]

Reliability analysis in civil structures is usually associated with limit states and utilised for assessing the safety of the structural system at design stage. This approach however is not suitable for the reliability analysis of existing structural systems. These are inevitably subjected to ageing and show the performance deterioration over time. A reliability analysis based only on design parameters could be unable to predict the safety and performance in the future.

2.5.1 Symptom-based reliability

The symptom-based reliability, originally adopted for assessing the engine conditions [34], is more appropriate than the traditional time-based reliability for existing structural members and system as the monitoring process can provide useful data (symptoms) for further assessing current condition and predicting future performance. An application of symptom-based formulation to civil structures has been proposed by Ceravolo et al. [36].

Reliability is defined as the probability of the structure attaining a limit state during a predetermined period of time. In many instances, this assessment is summarised by an ad hoc reliability index. In last years, several studies has been produced in order to take into account the presence of monitoring system.

If the degradation of reliability over time is taken into account, the lifetime of a structure can be considered as a random variable and reliability can be characterised in relation to the so-called "hazard function" (the damage rate in the infinitesimal time interval), which assumes various forms depending on the distribution model adopted (Weibull, Gamma. etc.). In this connection, a monitoring-oriented approach is of great interest, as the monitoring process is able to supply useful data both to plot the reliability curves, defined as a function of the symptom, and to interpret the diagrams obtained. Structural monitoring, construed as a system that provides on request data regarding a specific change, or damage, occurring in a structure, can be a valid tool to fine-tune reliability estimates in the light of the actual conditions of a structure. In this paragraph the symptom-based approach is analysed, in order to evaluate its applicability to the typical problems of structural engineering. This constitute the basis of the reliability estimation performed in following chapters.

Let us now examine a symptomatic approach to the evaluation of the performance of a structure. Reliability will depend on measurable quantities. If the reliability of a structure, R(t), is defined as the probability that the time it takes a system to reach a damage limit state associated to the structure's lifetime, t_b, is greater than a generic time t:

$$R(t) = P(t \le t_b)\,, \tag{7}$$

then reliability can be rewritten as a function of the symptom variable, S; in this case, it is defined as the probability that a system, which is still able to meet the requirements for which it has been designed ($S<S_l$), is active and displays a value of the S smaller than S_b, where S_l is the maximum value that a symptom that can reach in a system according to statistical decision theory, and S_b is the value of the symptom corresponding to the reference limit state. Accordingly, reliability is defined as:

$$R(S) = P(S \le S_b \mid S < S_l) = \int_S^{\infty} f_S \, dS \tag{8}$$

i.e., $R(S)$ can be expressed by the integral of the symptom's distribution probability density f_S. With the symptomatic approach it is also possible to work out, for the $R(S)$ function, expressions similar to those used by the time-based approach, that is to say for $R(t)$; the hazard function, $h(t)$, specifies the instantaneous rate of reliability deterioration during the infinitesimal time interval, Δt, assuming that integrity is guaranteed up to time t [7]

$$h(t) = \lim_{\Delta t \to 0} \frac{P\left(t \le t_b < t + \Delta t \mid t_b \ge t\right)}{\Delta t} \tag{9}$$

$h(t)$ is correlated to the reliability function, $R(t)$, by the following relationship:

$$R(t) = \exp\left(-\int_0^t h(x)\,dx \right). \tag{10}$$

In a similar manner, the so-called symptom hazard function, $h(S)$, is defined as the reliability deterioration rate per unit of increment of the symptom:

$$R(S) = \exp\left(-\int_0^S h(x)\,dx \right). \tag{11}$$

For example, if the time law of the evolution of the symptom can be approximated with Pareto's model, we get:

$$S(t) = S_{(t=0)} \left(1 - t/t_b\right)^{-1/\gamma} \tag{6}$$

where $S_{(t\,=\,0)}$ is the value of the symptom at time t = 0, and t_b is the time of attainment of a damage limit state or the total lifetime. Hence:

$$R(S) = 1 - t/t_b = \left(S_{(t=0)}/S\right)^{\gamma} \quad \gamma > 0 \tag{7}$$

where the γ coefficient determines the law of evolution of the symptom over time.

Reliability as a function of the symptom gives the residual damage capacity, ΔD, of the structure:

$$R(S) = \left(S_{(t=0)}/S\right)^{\gamma} = 1 - D \equiv \Delta D(S), \tag{14}$$

where $D = t/t_b$ represents the system's aging as well as the measure of the damage. Assuming that one knows the evolution of reliability through the observation of a set of systems, the value of the symptom as observed in a given unit makes it possible to determine the residual lifetime of the unit itself.

References

[1] Farrar, C. R., Worden, K. (2007); "*An introduction to structural health monitoring*", Phil. Trans. R. Soc. A. 15, 365, pp. 303-315

[2] Aktan A.E., Catbas F.N., Grimmelsman K.A., Tsikos C.J(2000);" *Issues in Infrastructure Health Monitoring for Management."* Journal of Engineering Mechanics, ASCE; 126(7): 711-724.

[3] Sohn, H., Farrar, C. R., Hemez, F. M., Shunk, D. D. (2003) *A Review of Structural Health Monitoring Literature*: 1996–2001. Los Alamos National Laboratory Report, LA-13976-MS.

[4] Brownjohn, J. M. W., (2007); "*Structural health monitoring of civil infrastructure"*. Phil. Trans. R. Soc. A. 365, pp. 589-622

[5] Fanelli, M.A. 1992. "*The Safety of Large Dams*". Engineering Safety, Ed. D. Blockly, McGraw-Hill Book Company Europe, Maidenhead, Berkshire,England. pp. 205-223.

[6] Wong, K.Y., Lau, C.K., and Flint, A.R. (2000a) "*Planning and Implementation of the Structural Health Monitoring System for Cable-Supported Bridges in Hong Kong*," Nondestructive Evaluation of Highways, Utilities and Pipelines IV, A.E. Aktan and S.R. Gosselin, Editors, Proceedings of SPIE Vol. 3995, pp.288-289.

[7] Maeck J., Peeters B., De Roeck G. (2001), "*Damage identification on the Z24 bridge using vibration monitoring",Smart Materials and Structures.* **10** 512

[8] Worden, K., Dulieu_Barton, J. M., (2004); "*An Overview of Intelligent Fault Detection in Systems and Structures"*. Structural Health Monitoring, 3, 85.

[9] Worden, K., Burrows, A. P., (2001); "*Optimal sensor placement for fault detection"*. Engineering Structures, 23, pp. 885-901.

[10] Meo, M., Zumpano, G., (2005); "*On the optimal sensor placement techniques for a bridge structure"*. Engineering Structures, 27, pp. 1488-1497.

[11] Kammer, D. C., (1991); "*Sensor placement for on-orbit modal identification and correlation of large space structures"*. J Guidance, Control Dynam, 14.

[12] Imamovic, N., (1998) "*Model validation of large finite element model using test data*". Ph.D. dissertation. Imperial College London.

[13] Heo G., Wang M.L., Satpathi D., (1997) "*Optimal transducer placement for health monitoring of long span bridge*". Soil Dynamics and Earthquake Engineering, 16, pp. 495–502.

[14] Lynch J. P., (2007) "*Embedded data processing wireless sensors networks*". Smart Structures short course notes, University of Trento, Italy.

[15] Cooley, J.W., Tukey, J.W., (1965) "*An Algorithm for the Machine Calculation of Complex Fourier Series*". Mathematics of Computation, 19(90), pp. 297-311.

[16] Welch, P.D., (1967) "*The Use of Fast Fourier Transform for the Estimation of Power Spectra: A Method Based on Time Averaging Over Short, Modified Periodograms* ". IEEE Transactions on Audio Electroacoustics, AU-15, pp. 70-73.

[17] Sun, Z., Chang, C.C., (2004) "*Statistical Wavelet-Based Method for Structural Health Monitoring*". Journal of Structural Engineering, 130(7), pp. 1055-1062.

[18] Sun, Z., Chang, C.C., (2002) "*Structural damage assessment based on wavelet packet transform*". Journal of Structural Engineering, 128(10), pp. 1354-1361.

[19] Huang, N.E., Shen, Z., Long, S.R., Wu, M.C., Shih, H.H., Zheng, Q., Yen, N.-C., Tung, C.C., Liu, H.H., (1998) "*The empirical mode decomposition and the Hilbert spectrum for nonlinear and non-stationary time series analysis*". Proceedings of the Royal Society of London, 454, pp. 903–995.

[20] Yang, J. N., Lei, Y., Pan, S., Huang, N., (2003) "*System identification of linear structures based on Hilbert-Huang spectral analysis. Part 1: normal modes*". Earthquake Eng. and Structural Dynamics, 32, pp. 1443-1467.

[21] Yang, J. N., Lei, Y., Pan, S., Huang, N., (2003) "*System identification of linear structures based on Hilbert-Huang spectral analysis. Part 2: complex modes*". Earthquake Eng. and Structural Dynamics, 32, pp. 1533-1554.

[22] Xu, Y. L., and Chen, J., (2004) "*Structural damage detection using empirical mode decomposition: Experimental investigation*". Journal of Engineering Mechanics, 130(11), pp. 1279-1288.

[23] Yang, J. N., Lei, Y., Lin, S., and Huang, N., (2004) "*Hilbert-Huang based approach for structural damage detection*". Journal of Engineering Mechanics, 130(1), pp. 85-95.

[24] Ljiung, J, (1999) "*System Identification, Theory for the User*". 2nd ed., Prentice-Hall Inc., Englewood Cliffs, NJ.

[25] Juang, J. N., (1994) "*Applied System Identification*". Prentice Hall PTR, Upper Saddle River, NJ 07458.

[26] Bendat, J. S., Piersol, A. G., (1980) "*Engineering Application of Correlation and Spectral Analysis*". New York: Wiley-Interscience.

[27] Asmussen, J. C., Brincker, R., Ibrahim, S. R., (1999) "*Statistical Theory of the Vector Random Decrement Technique*". Journal of Sound and Vibration 226(2), pp. 329-344.

[28] Argoul, P., Hans, S., Conti, F., Boutin, C., (2000) "*Time-frequency analysis of free oscillations of mechanical structures. Application to the identification of the mechanical behavior of buildings under shocks*". Proceedings of the European COST F3 Conference on System Identification & Structural Health Monitoring, Madrid, pp. 283-292.

[29] Bonato, P., Ceravolo, R., De Stefano, A., Molinari, F., (2000) "*Cross-time frequency techniques for the identification of masonry buildings*". Mechanical systems and signal processing, 14(1), pp. 91-109.

[30] Brincker R., Zhang L., Andersen P. (2001), *"Modal identification of output-only systems using frequency domain decomposition"* , Smart Materials and Structures 10, 441-445

[31] Demarie, G. V., (2006) "*Identificazione istantanea di strutture con non-linearità di Volterra*". PhD Thesis, Politecnico di Torino, Italy (in Italian).

[32] Ruocci, G. (2010) "*Application of the SHM methodologies to the protection of masonry arch bridges from scour",* Politecnico di Torino, PHD thesis

[33] Susoy, M., Catbas , F.N., Frangopol, D.M., *Evaluation of Time-Variant Bridge Reliability Using Structural Health Monitoring*. IMAC-XXVI Conference & Exposition on Structural Dynamics - Technologies for Civil Structures.

[34] Cempel, C., Natke, H.G., Yao, J.T.P., (2000); *Symptom reliability and hazard for systems condition monitoring*. Mechanical Systems and Signal Processing, 14(3), pp. 495 – 505.

[35] Stewart, M.G., Rosowsky, D.V., (1998); *Time-dependent reliability of deteriorating reinforced concrete bridge decks*. Structural Safety,(20), pp. 91-109.

[36] Ceravolo, R., Pescatore, M., De Stefano, A., (2009); *Symptom based reliability and generalized repairing cost in monitored bridges*. Reliability engineering & System safety, 94(8), pp. 1331-1339.

[37] Shull, P. J., (2002); "*Nondestructive evaluation theory, techniques, and applications*", New York, NY: Marcel Dekker, Inc.

Chapter 3

Modal identification in time-frequency domain

The ambient vibration measurements are extensively used in civil engineering field to evaluate the structural integrity of constructions in a non-destructive manner. The extraction of sensitive features from massive amount of collected data is an important challenge designing a reliable monitoring system. Most of the techniques currently used in structural identification under ambient excitation typically require the hypothesis of stationarity, though, in the field of civil engineering, excitation may be markedly non stationary. This consideration prompted in the past some proposals for identification methods that, being based on time-frequency transformations, were designed to handle current types of non-stationary excitation.

In TF representation, the amplitude ratio and the phase difference between any two measured signals are determined by means of TF estimators. In frequency intervals where a single modal component is predominant for both signals, the phase difference instantaneous estimator tend to become steady in time. Therefore, modal frequencies can be identified by searching for the minima of the estimators' standard deviation as a function of frequency.

This procedure may fail in recognizing a modal frequency when at least one pair is weakly correlated around it, because its large standard deviation prevents the average from being small. Recurring to Principal Component Analysis (PCA), the method is here improved by substituting the average of standard deviations with the smallest principal component variance extracted from the set of time-frequency estimators.

The improved method has been tested on both numerical and real cases study.

The recent achievements in the sensing and information technologies are pushing towards the development of on-line monitoring systems capable to provide an instantaneous assessment of structural health state. To assess the variation in time of modal parameters of a monitored structure, an optimization procedure based on the instantaneous curve fitting applied directly to time–frequency representations of dynamic response signals can be used.

3.1 Time – frequency identification through instantaneous estimators

The monitoring of systems in normal service conditions is of paramount importance in a variety of fields where fault or damage detection is an issue. In some sectors, including civil structures, the use of techniques exploiting environmental excitation may avoid problems such as obstruction of road bridges or breaks in production processes. The use of environmental input gives rise to the need for analyzing non-stationary response signals, generally from accelerometers, which constitute the typical output of monitored systems. When bi-linear transforms from Cohen's class are used, the system response is perceived in the TF plane as the evolution of spectral components corresponding to the energy of the individual vibration modes (Cohen 1995).

Classical time-domain and frequency-domain identification methods assume that the modal parameters do not evolve versus time and vibration amplitude, and that the input is at least weakly stationary. In Civil Engineering applications, where the excitation is generally non-stationary and the presence of noise during the data acquisition phase unavoidable, TF-domain techniques may offer several advantages, including: accuracy in parameter estimation; effective handling of non-stationary signals and moderate non-linearities; robustness against noise.

An effective TF identification method for use in non-stationary conditions under unknown excitation was presented in [**1**], improving an earlier technique proposed by the same authors and based on model filters. The new method utilizes auto- and cross-TF transforms from Cohen's class which, beyond possessing valuable properties for the analysis of mechanical signals, lend themselves to a clear interpretation in energy terms. It does not require strict conditions about stationarity, but its performance is tied to modal component separability in the TF plane, only requiring that the input spans the frequency range of vibration modes.

With such method, the estimation of amplitude and phase information is based directly on the analysis of the auto- and cross-TF transforms of the signals. Amplitude ratios are directly determined from the ratio between the instantaneous amplitudes of the TF representations of the signals. Phase relationships are estimated based on the phase of the cross-TF representation of pairs of channels. Since the estimators are derived directly from two-dimensional functions of the time and frequency variables, they retain their dependence on time variables. Therefore they make it possible to determine the time evolution of the

modal shape associated with a given frequency component and hence to establish *a posteriori*, i.e., at the end of the process, whether a given frequency value may or may not be a structural vibration mode. In linear time-invariant systems, modal signals are characterized by their amplitude and phase relationships being constant and their consequent modal shape being thus stable over time. The identification of modal frequencies therefore reduces to a search for the particular values at which the estimators remain constant with respect to the time variable, in general by resorting to multiple criteria techniques. Having identified the frequencies, the estimators supply directly the temporal evolution of the amplitude and phase ratios, i.e., the modal shapes.

Without entering into the details of the method, let us assume that the structure, subjected to an unknown excitation, is instrumented with N simultaneous acquisition channels according to some of its degrees of freedom. In the TF representation of the response signals, the energy appears to be concentrated around the modal frequencies and modulated according to the evolution of the time-frequency transform of the modulating waveform. Due to the fact that in the TF plane the shape of the modulating waveform is maintained, it can be easily demonstrated that the amplitude ratio and phase difference between any two measured signals $s_i(t)$ and $s_j(t)$ can be determined directly from their bilinear TF auto and cross representations $D_i(t,f)$, $D_j(t,f)$, and $D_{ij}(t,f)$ according to:

$$A_{ij}(t,f) = \sqrt{\frac{D_i(t,f)}{D_j(t,f)}} \qquad \Phi_{ij}(t,f) = phase\{D_{ij}(t,f)\} \tag{1}$$

where $A_{ij}(t,f)$ represents the Time-Frequency Instantaneous Estimator (TFIE) for the amplitude ratio, and $\Phi_{ij}(t,f)$ the TFIE for the phase difference, between the i-th and the j-th channels. In frequency intervals where a single modal component is predominant, the estimators tend to become steady in time. As this property increases progressively up to a peak at the modal frequencies, the latter can be identified by searching for the minima of the estimators' standard deviation as a function of frequency. Since the phase difference estimator proves more stable than the amplitude ratio estimator for the purposes of frequency localization, modal frequencies are typically identified as the minima of the standard deviation of the phase difference estimator along the time axis, defined as:

$$S_{ij}(f) = \sqrt{\frac{1}{T}\int_o^T \left[\Phi_{ij}(t,f) - \overline{\Phi}_{ij}(f)\right]^2 dt} \tag{2}$$

where $\overline{\Phi}_{ij}(f)$ is the mean along the time axis and T is the length of the signals. For any f, $\Phi_{ij}(t,f)$ is a function of time randomly scattered in the range $[0, \pi]$ and its standard deviation $S_{ij}(f)$ is generally not far from the value $\pi/\sqrt{12}$, but if f is a modal frequency the scattering of $\Phi_{ij}(t,f)$ suddenly decreases and its standard deviation falls down to around zero. Consequently, on the $S_{ij}(f)$ plot, modal frequencies are revealed by sharp downward peaks, as exemplified in Fig. 1, which refers to a simulated 3-storey planar shear-type frame having

0.5% damping in every mode, excited by a chirp ground acceleration, the accelerations being measured at the first and second storeys.

Once this preliminary step of frequency localization is accomplished, then the estimators evaluated at the identified modal frequency will supply amplitude and phase relationships as a function of time, and modal shapes estimates, thus completing the modal identification procedure.

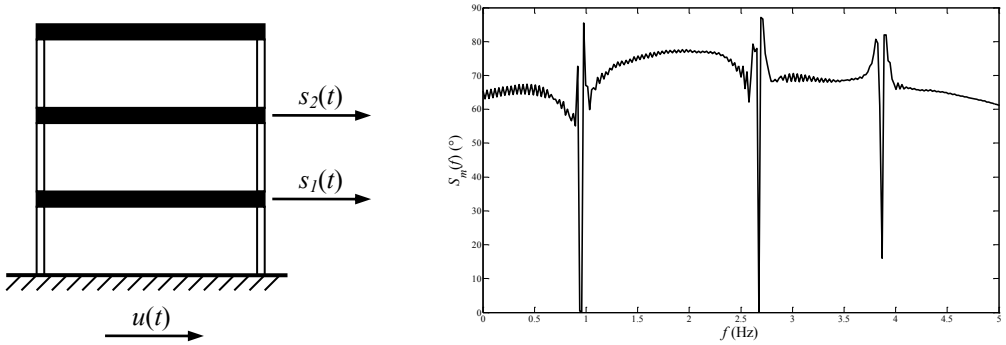

Figure 1 Identification of a simulated 3-storey planar frame, using accelerations measured at the first and second storeys. On the right: the standard deviation of the phase difference instantaneous estimator.

3.2 The instantaneous modal parameters estimation

The methodology adopted to estimate the instantaneous modal parameters follows the optimization procedure proposed in [**2**], based on the instantaneous curve fitting of time-frequency representation of dynamic response signals. The response of a system can be represented in the time frequency plane as a sum of harmonics concentrated at modal frequencies modulated according to the evolution of the modulating waveform.

Given a time-frequency representation of a displacement signal, instantaneous parameters associated with the Frequency Response Function (FRF), H, can be estimated by minimising the following functional at each time t:

$$D(f,t)-|H(f,t)|^2 \tag{3}$$

In this minimisation there is an explicit assumption that the instantaneous energy spectrum $D(t,\omega)$ associated to a general time-frequency transform, approaches a scaled version of the squared modulus of the FRF (the theoretical bases of the method are in

Ceravolo 2001, to be published). In the case of a linear and proportionally damped system one may write:

$$H(f) = \sum_k AR_k \Big/ \left(f_k{}^2 - f^2 + 2j\zeta_k f_k f \right) \tag{4}$$

and instantaneous parameters for optimisation may be chosen among modal amplitudes, AR_k, damping ζ_k, or modal frequency, f_k. A similar relationship could be written for velocity or acceleration signals.

It has been observed that estimation accuracy depends on the relative energetic importance of the modes. In other words, the instantaneous estimator is more accurate in the temporal segments where the mode to be identified is predominant and is not affected by the residuals of the other modes. An important issue is the choice of the TF representation to

be used to estimate the instantaneous energy spectrum $D(\omega,t)$. The square value of the Short Time Fourier Transform (STFT) has been adopted in this paper. Although STFT is affected by the intrinsic limitations in the typical resolution of linear transforms related to the uncertainty principle, the simple structure of this technique provides the computational

advantage which allows to address the problem in a direct manner and to find a reasonably accurate solution. In particular, the type and the length in samples of the window

used in the computation of the STFT seem to influence the damping estimation to a large extent [3]. Setting the window length for the spectrogram depends on the de-correlation

length of the process and requires the availability of a first estimate for damping. In the context of a damage assessment process, a first tentative value for the damping ratio can be obtained in the operational evaluation stage by means of a linear modal estimation.

The short-time Fourier transformation (STFT) and the Continuous Wavelet Transformation (CWT) are two popular ways to compute the time-frequency distribution of a signal. These two algorithms calculate the correlations between the signal and a family of time-frequency functions, thus they cannot achieve an arbitrary fine resolution in both the time and frequency domains simultaneously due to the limitations given by the uncertainty principle.

In addition to these correlation-based approaches, there is another type of time-frequency representation which is motivated by the time-frequency energy density. In contrast to the conventional power spectrum density, the time-frequency energy density function describes the signal's energy distribution in terms of both time and frequency. Compared with the correlation-based methods, the time-frequency energy distribution can yield representations with a better time-frequency resolution which represents a crucial issue for this type of analysis. Among the time-frequency distribution functions of the Cohen class, the Wigner-Ville distribution is obtained by correlating the signal with a time-frequency

shifted version of itself. The main obstacles for the application of Wigner-Ville distribution is the cross-term interference. This cross-term can be removed or reduced by applying a 2D low pass filtering, resulting in what is called the smoothed Wigner-Ville distribution [**3**].

3.3 PCA in identification methods

Applying the TFIE method to a set of N simultaneous measurements provides $N_2 = N!/(2!(N-2)!)$ (i.e. N binomial 2) phase difference estimators $\Phi_{ij}(t,f)$, i.e. one estimator for each pair of signals, and consequently an equal number of phase difference estimator's standard deviations $S_{ij}(f)$.

Apart from the particular case $N = 2$ (hence $N_2 = 1$) corresponding to the only one function $S_{12}(f)$, in the case of $N > 2$ different technique can be devised to extract the modal frequencies from the set of N_2 functions $S_{ij}(f)$, also depending on the degree of *a priori* knowledge the user possesses of the physical system and thus on the correlations he expects between pairs of acquisition channels. One technique which does not require any *a priori* knowledge of that kind merely consists in averaging the N_2 functions before searching for their minima (once again interpreted as the desired modal frequencies), i.e. in evaluating $S_m(f) = 1/N_2 \cdot \Sigma S_{ij}(f)$. This technique has been successfully applied by the authors to the dynamic identification of a number of real scale structures, ranging from historical masonry constructions to concrete and steel frame buildings (Ceravolo et al. 2004, De Stefano et al. 2008, Matta et al. 2009) and can be regarded as a standard approach effectively working in most cases.

However, some cases exist when this approach may prove inadequate. The averaging procedure may in fact fail in recognizing a modal frequency when at least one pair of signals is weakly correlated around it, because the corresponding large standard deviation prevents the average from being small. This is the case when at least one of the two signals has a small energy in that mode, for instance due to that signal being measured close to a modeshape node, or even more likely due to that signal being measured along a direction which is orthogonal to the eigenvector of that mode.

In this paper, a new approach is presented which, keeping the merit of being automatically applicable with no need of *a priori* knowledge, has the further advantage of providing a clearer representation of modal frequency location, thus increasing the identification reliability especially in the critical cases of large damping ratios, close modal frequencies, non-negligible structural non-linearities and input non-stationarity.

The proposed method uses Principal Component Analysis (PCA) to process the N_2 phase difference estimators $\Phi_{ij}(t,f)$. PCA is a well-known statistical technique usually employed to reduce the dimensionality of large data sets. This technique transforms the original set of variables into a substantially smaller set of uncorrelated variables still representing most of the information in the original set [**4**]. This is accomplished through first orthogonalizing the components of the original redundant data vectors (so that they result uncorrelated with each other), then ordering the resulting orthogonal components (principal components) so that those associated with (i.e. explaning) the largest data variances come first, and finally eliminating those components that contribute the least to the variation in the data set. In other words, PCA is commonly used to read the data in a properly rotated reference system, namely in the perspective which exalts data variation.

In the present work, actually, PCA is performed for exactly the opposite purpose, i.e. with the aim to identify (for each frequency) the largest degree of correlation between data vectors (the N_2 phase estimators regarded as sampled functions of time at that frequency), through keeping under observation the value of the smallest among the principal component variances. For each frequency f, the N_2 functions of time $\Phi_{ij}(t,f)$, instead of undergoing a standard deviation evaluation and a subsequent averaging, are subjected to PCA for the sole purpose of evaluating their minimum variance, $\sigma_{min}(f)$. The steadier the estimators at a given frequency, the smaller the minimum variance σ_{min} at that frequency. Since $\sigma_{min}(f)$ will drop to zero at a modal frequency even if only a small subset of the whole measurements result correlated at that mode, the mapping $f \rightarrow \sigma_{min}(f)$ proves more robust than the mapping $f \rightarrow S_m(f)$.

3.4 Numerical example

Let us consider the N_s-storey shear-type linear building structure schematized in Fig. 2, representing a nearly axial-symmetrical modal model, i.e. a structure possessing close modes in the two orthogonal vertical planes. The four identical columns, their centre of stiffness being R, are located at a mutual distance i_x along the x axis and i_y along the y axis. The rectangular rigid floors, identical (and equally spaced) along the height of the building and characterized by a uniform mass density μ, measure l_x and l_y along x and y respectively, and their centre of mass G is eccentric with respect to R by respectively $x_G = e_x \cdot l_x$ = and $y_G = e_y \cdot l_y$. The building is base-excited by two concomitant ground motion horizontal components, either in the shape of two uncorrelated white noise accelerations of equal intensity or by the two components of the 1989 Loma Prieta earthquake accelerograms as recorded in the Natural Sciences' building at UC Santa Cruz (the E-W component being assumed along the x axis). The $N_{dof} = 3N_s$ degrees of freedom resulting from the assumption of rigid floors are measured through 3 accelerometers per storey (the torsional component as if reconstructed from a couple of equally oriented channels), each affected by a certain amount of uncorrelated white noise added as a given percentage (herein 5%) of the true response. All the N_{dof} natural modes are assigned the same value of damping ratio ζ, and the columns rectangular sections are so proportioned as to make the ratio of the second eigenfrequency (either the first flexural mode along y or the first coupled flexural/torsional mode) over the first eigenfrequency (first flexural mode along x) equal to a given value ρ, kept small so as to make the modal model nearly axial-symmetrical. All measured signals consist of 1024 samples digitized at 20 Hz (frequency resolution of approximately 0.02 Hz). When no eccentricity is accounted for, the torsional components are not excited and only 4 out of the whole of the 6 channels are used.

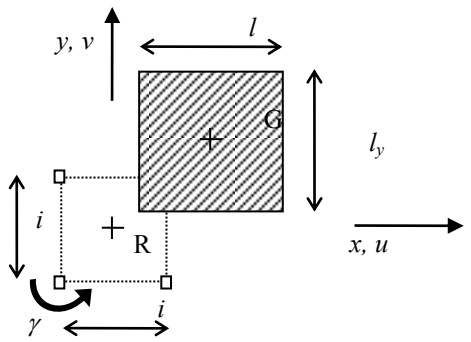

Figure 2 Planar view of the simulated model

In Figs. 3-4 the new approach is compared with the classical one, for the case of a 2-storey concentric building ($N_s = 2$, $e_x = e_y = 0$) having close natural frequencies along the two coordinate axes ($\rho = 1.04$), and for increasing values of the damping ratio ζ, alternatively equal to 0.5%, 2% and 5%. A white noise input is assumed in Fig. 3, the Loma Prieta record is assumed in Fig. 4. Since no eccentricity is considered, the torsional modes are not excited and thus excluded from the acquisition data (only 4 channels are used). The average standard deviation $S_m(f)$ is reported on the left (classical approach), while the minimum variance $\sigma_{min}(f)$ is plotted in lognormal scale on the right (new approach). The true undamped eigenfrequencies are superimposed as dashed vertical lines in the same plots in order to evaluate the identification capabilities of the two methods.

In Fig. 5 the comparison is extended to the case of a 3-storey eccentric building ($N_s = 3$, $e_x = e_y = 0.05$) having close natural frequencies along the two coordinate axes ($\rho \approx 1.06$) and a damping ratio $\zeta = 5\%$. For the sake of clarity, plots are restricted to the first six (out of nine) modes.

From Fig. 3-5 the following observations can be drawn.

In general, frequency localization is more complex as damping gets larger, as the input gets non-stationary, and as torsional modes are activated. Despite such complications, despite the closeness of orthogonal modes, and despite short, noise-contaminated response signals are used here, both approaches appear substantially effective in frequency estimation, thus proving the validity of TFIE as an output-only identification technique.

A closer look at the reported figures, however, reveals that the minimum variance $\sigma_{min}(f)$, approximately as effective as the average standard deviation $S_m(f)$ in the simplest cases, becomes more advantageous in the more complex ones, showing an increased efficacy in frequency separability and correct selection, as is particularly evident from the 5% damping cases, especially when the earthquake excitation is considered.

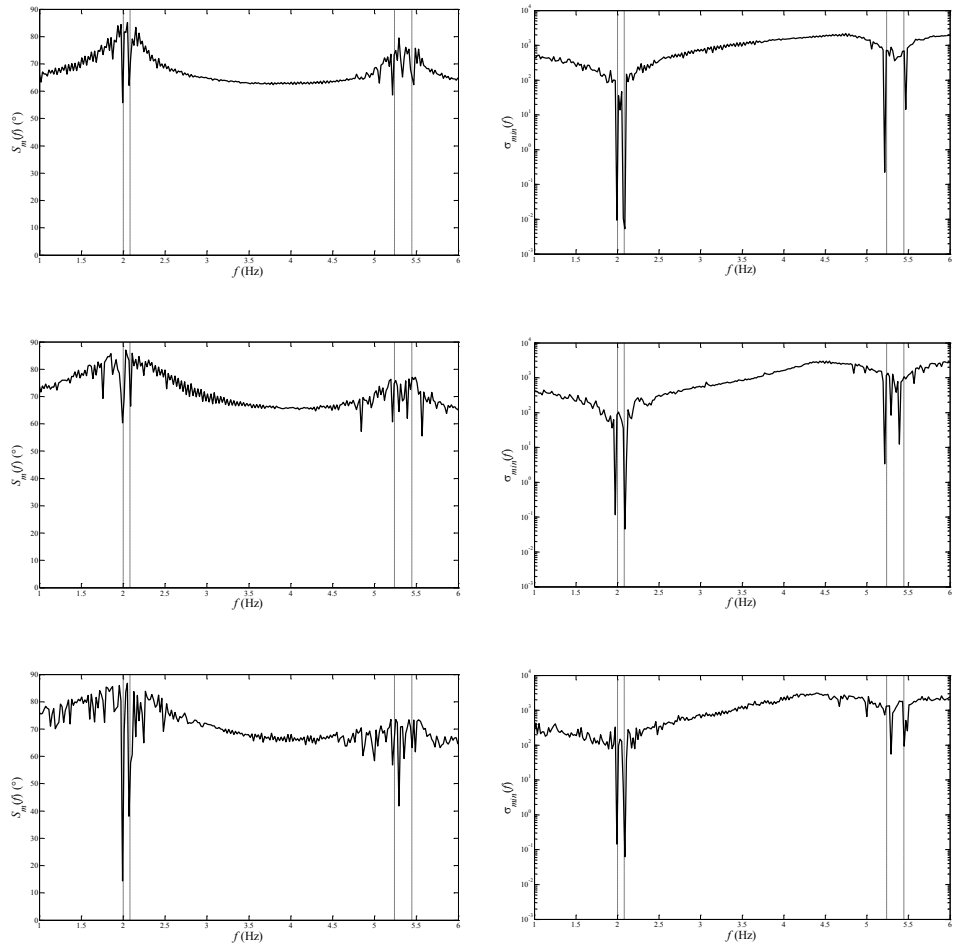

Figure 3 The classical (left) and the new (right) methods under white noise input (Ns = 2, ex = ey = 0).

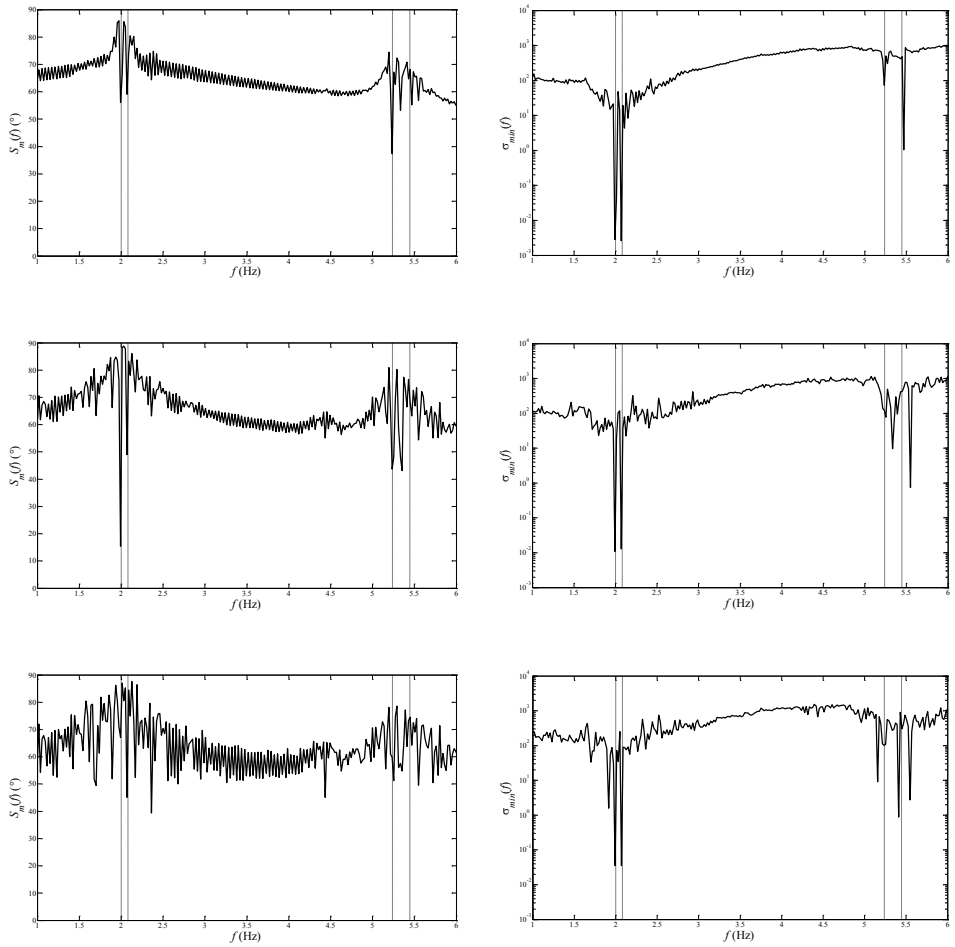

Figure 4 The classical (left) and the new (right) methods under Loma Prieta record (N_s = 2, e_x = e_y = 0).

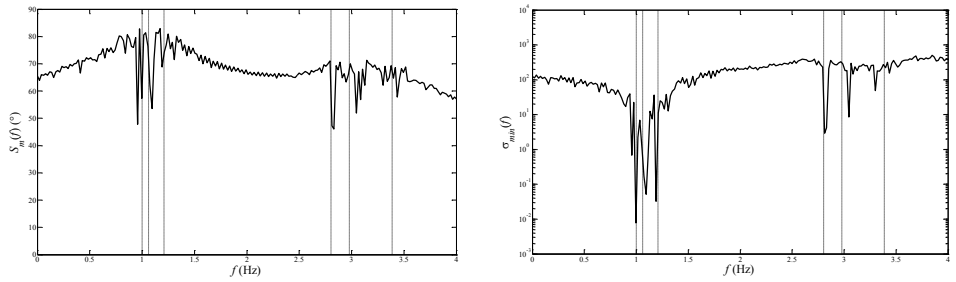

Figure 5 The classical (left) and the new (right) methods under white noise input ($N_s = 3$, $e_x = e_y = 5\%$).

3.5 The Holy Shroud Chapel in Turin: a real-case study

The Holy Shroud Chapel in Turin (Figure 6) is universally recognized as a outstanding example of Italian Baroque architecture. Emanuale Filiberto di Savoia entrusted its design to the famous Italian architect Guarino Guarini, who built the Chapel between 1667 and 1694. Since the very beginning, the monarch's intent was that of housing the precious relic of Christianity in a more prestigious seat. The architectural accomplishments are extraordinary. The whole building conveys Guarini's obsession for architectonic originality and a sense of mystery which are well expressed by the structural complexity and the richness of perfect shapes and theological, astronomic and mathematical symbols. The chapel is composed of a tambour bored by six large windows and surmounted by three big arches which sustain the dome. On the inside, a series of small overlapped arches disposed on six levels creates an hexagonal geometry which diminishes towards the top where it becomes the circular base of a lantern. On the outside, another series of small arches creates a complex plaiting effect and the alternation of black marble and grey stone grants a particular sense of dynamicity.

The recent history of the Holy Shroud Chapel has been marked by a tragic event. A fire broke out in 1997 during some restoration works and it seriously damaged the structure, producing incalculable economic and artistic losses.

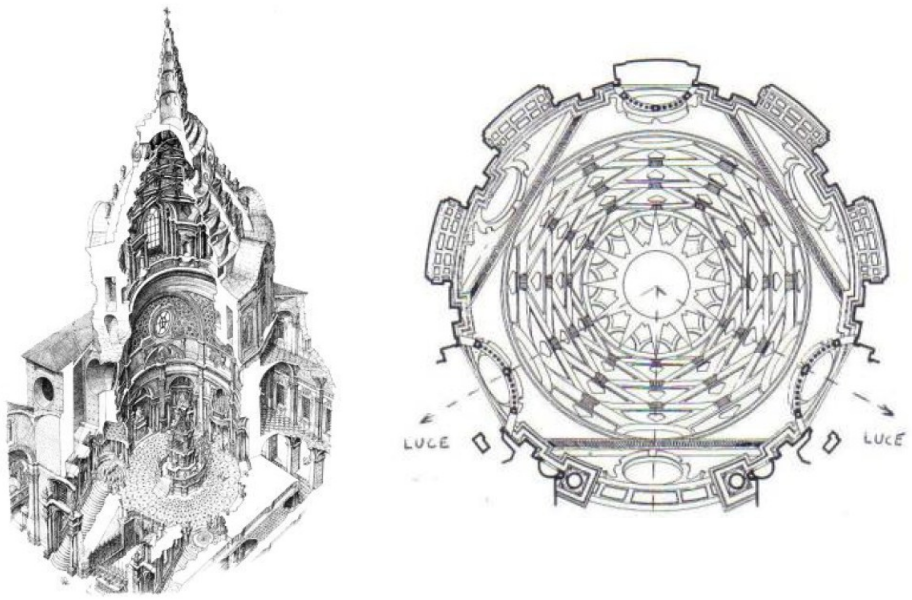

Figure 6 Section and view of the dome of the Holy Shroud Chapel in Turin.

In the following months, the Sovraintendenza dei Beni Architettonici charged the Politecnico di Torino to carry out a general experimental campaign for the purposes of structural assessment. In order to achieve a complete overall image of the Chapel's structural health, the Research Unit to which the authors belong, in association with the University of Kassel, designed a dynamic testing programme, prepared a FE model and adjusted it according to the acquired experimental knowledge. To this aim, 25 accelerometers were deployed on six different levels along three orthogonal directions: radial, tangential and vertical. Dynamic tests were realized adopting four types of excitations: environmental; impulsive through hammering; impulsive through dropping a sphere to the ground near the foot of the building; wind turbulence induced by a Fire-Brigade helicopter flying around the top of the dome.

In previous studies [**5**],TFIE diagrams computed from signals with identical sampling frequencies and lengths were averaged in order to make the downward peaks that mark the modal frequencies clearly visible. Additionally, various time-domain and frequency-domain techniques were employed as well, including ERA [**6**] and FDD [**7**], so as to increase results reliability, until 7 natural frequencies were finally recognized, and eventually utilized for the direct calibration of a FEM numerical model [**8**].

In Figure 7, these very 7 frequencies, drawn as vertical dashed lines, are superimposed on, respectively, the average standard deviation $S_m(f)$, on the left, and the

minimum variance $\sigma_{min}(f)$, on the right, of the set of phase difference instantaneous estimators evaluated from a single fragment of data from the 25 accelerometers (512 samples at 50 Hz).

Mode n°	f [Hz]
1	2.246
2	2.344
3	4.688
4	6.348
5	8.789
6	10.25
7	10.5

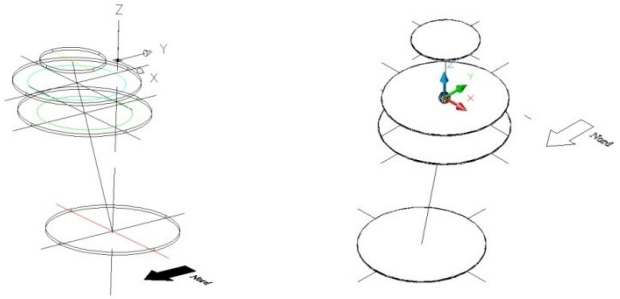

Table 1 Modal frequencies identified (De Stefano, 2008) and first and second modal shapes

Whilst the classical standard deviation can recognize only a few of the 7 previously identified frequencies, the minimum variance appears to correctly catch all of them, with the only exception of the two lower frequencies around 2.3 Hz, which are seen as a single peak instead of two close distinct ones. This is due to poor frequency resolution: increasing the samples analysed, and consequently the frequency resolution, the peak corresponding the second flexural mode appears.

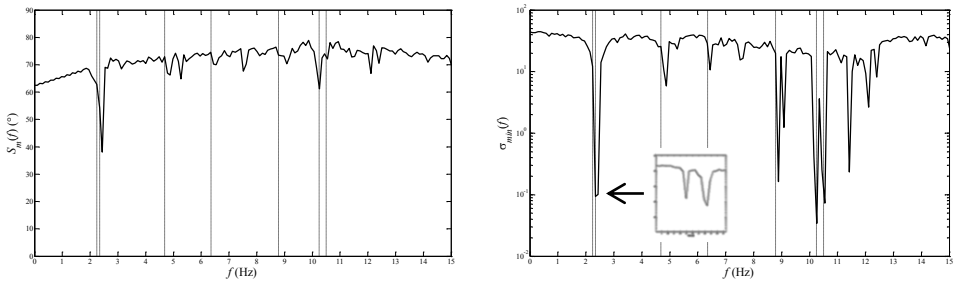

Figure 7 Frequency identification of the Holy Shroud Chapel in Turin: the classical (left) and the new (right) methods applied to 512 samples of ambient vibration measurements digitized at 50 Hz.

Particularly encouraging is also the ability of the new method to locate the two close frequencies around 10 Hz, which the classical approach completely misses.

References

[1] Bonato, P., Ceravolo, R., De Stefano, A., Molinari, F., (2000); *Use of cross time-frequency estimators for the structural identification in non-stationary conditions and under unknown excitation*. J. of Sound and Vib., 237(5), pp. 775-791.

[2] Ceravolo, R., (2004); *Use of instantaneous estimators for the evaluation of structural damping*. J. of Sound and Vib., 274(1-2), pp. 385-401.

[3] Qian, S.E., *Introduction to time-frequency and wavelet transforms*, China Machine Press, 2005.

[4] Jolliffe, I.T., *Principal Component Analysis*, II, Principal Component Analysis, 2002.

[5] De Stefano, A., Enrione, D., Ruocci, G., Bottazzoli, F., (2007); *Robust stochastic model updating to face uncertainties: application to the Holy Shroud Chapel in Turin*. roc. 2nd Int. Conf. on Structural Condition Assessment, Monitoring and Improvement (SCAMI-2).

[6] Juang, J.N., Pappa, R.S.., (1985); *An eigensystem realization algorithm for modal parameter identification and model reduction*. Journal of Guidance, Control, and Dynamics, 8(5).

[7] Brincker, R., Zhang, L., Andersen, P., (2000); *Modal Identification of output-only systems using Frequency Domain Decomposition*. Proc. European COST F3 Conf. On System Identification & Structural Health Monitoring.

[8] De Stefano, A., Enrione, D., Ruocci, G., (2008); *Innovative techniques for structural assessment: the case of the Holy Shroud Chapel in Turin*. Proc. 6th Int. Conf. on Structural Analysis of Historical Con-struction (SAHC 2008).

[9] Bonato, P., Ceravolo, R., De Stefano, A., (1997); *Time-Frequency and ambiguity function approaches in structural identification*. J. of Eng. Mech., 123(12), pp. 1260-1267.

[10] Maia, N.M.N., Silva, J.M.M., *Theoretical and experimental modal analysis*, Research Studies Press, Wiley, 1997.

[11] Matta, E., De Stefano, A., Quattrone, A., (2009); *Reliability issues in vibration-based*

sys-tem identification: lessons from the JETPACS case study. Proc. 4th Int. Conf. on Structural Healt Monitoring on Intelligent Infrastructure (SHMII-4).

[12] Choi, H.I., Williams, W.J., (1989); *Improved time-frequency representation of multicomponent signals using exponential kernels*. IEEE Trans. Acoust. Speech Signal Process, 37(6), pp. 862-871.

[13] Cohen, L., *Time-Frequency Analysis*, Englewood Cliffs, NJ Prentice-Hall Inc., 1995.

[14] Matta, E., De Stefano, A., Quattrone, A., (2009); *Improvement of Time-Frequency domain identification through PCA*. Proceedings IOMAC09, 3rd International Modal Analysis Conference, Ancona (Italy).

[15] De Stefano, A., Actual trends in output only modal identification, in: Baratta, A., Corbi, O., Intelligent structures. An Overview on the Ongoing European Research, Fridericiana Editrice Universitaria, 2003.

Chapter 4

Dynamic approaches to diagnosis: an experimental case

In this chapter some results of a series of experimental test campaigns performed on a masonry arch bridge model built in the laboratory of the Department of Structural and Geotechnical Engineering of the Polytechnic of Turin since 2006 to nowadays are presented. The first part of the chapter concerns the description of the masonry arch bridge model and the criteria adopted in designing and executing the tests campaigns are presented. Furthermore, the results of the experimental modal analysis carried out on the signals acquired from the vibration tests are summarized.

In the second part a proposal for an on-line application of novelty detection technique is formulated and the application based on instantaneous modal parameters identified during the application of pier settlements is presented.

4.1 The Masonry arch bridge model

The 1:2 scaled model of the masonry arch bridge shown in Figure 1 was built in the laboratory of the Department of Structural and Geotechnical Engineering at the Politecnico di Torino. The prototype this model comes from is not a real existing bridge but was designed taking the masonry arch bridges common features, geometric proportions and historical design codes into account.

Figure 1. The scaled masonry bridge: notice the settlement application device under the central pier

The model is a twin-arch bridge with a length of 5.90m, a width of 1.60m and it is 1.75m high. The two arches are segmental arches with a radius of 2.00m and an angular opening of 30°. Each span is 2.00m long between the supports and the thickness of the arch is equal to 0.20m. The model was built with handmade clay bricks also scaled to 130x65x30mm to respect the adopted modelling scale law. Low compressive strength elements were chosen and a mortar with poor mechanical properties was used to bound them in order to reproduce the typical materials of historical constructions.

The mid-span masonry pier, which was cut at a hypothetical middle-height section to allow the insertion of a settlement application system, is imagined to be placed inside the streambed and subjected to the scour of its foundation.

Some hydraulic flume tests were carried out on a further scaled down model of the bridge pier in order to simulate the scour effects in the lab. The foundation settlements and rotations resulting from these investigations were then replicated on the bridge model by means of the four independent screws installed at the extremities of the settlement application system. The spherical plain bearings placed at the head of the screws allow the

rotations of the plate which support the central pier about axes parallel to the longitudinal and transversal directions of the bridge.

In order to simulate the streambed material surrounding the foundation of the central pier, a polystyrene mould was introduced. In this way a polystyrene layer interfaces the pier and the settlement application device and a polystyrene ring surrounds the pier.

More details about the bridge model can be found in [3].

4.1.1 Preliminary studies

The experimental investigations carried out on the masonry arch bridge model were divided in two different sessions. In the first session most of the efforts were addressed to reduce the high uncertainties referred to the material properties and the structural behaviour of this complex structure. Several destructive tests were performed on samples collected during the model construction in order to estimate the mechanical properties of the masonry material. The estimated parameters were then introduced in a numerical model of the bridge to obtain a preliminary calculation of the modal parameters. The information acquired in these initial analyses was helpful to plan the following dynamic tests and to interpret the first results of the modal identification. In this phase also hydraulic tests on a reduced model of the central pier were carried out in order to quantify the settlement to be applied.

Material characterisation tests

Several tests were carried out in order to characterise the mechanical properties of the mortar and of the masonry used to build model.

The characterisations tests on the mortar samples were performed following the prescriptions proposed by the European standard code EN 998-2:2003 adapted to take in account the scaled measure of bricks. The collected samples belong to the M2.5 class of the European standard code EN 998-2:2003 which is one of the poorest in terms of mechanical properties.

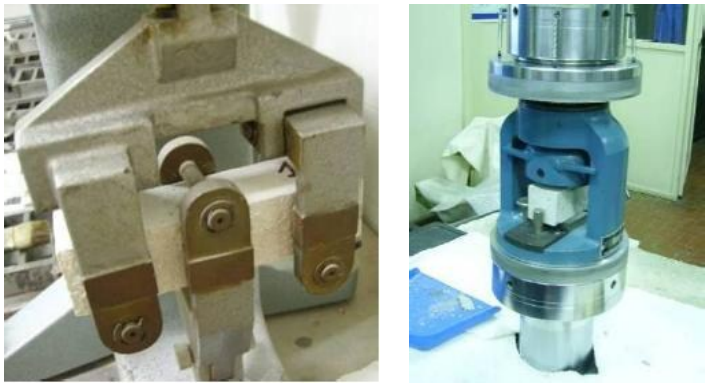

Figure 2. Tests carried out on mortar samples.

The characterisations tests on the masonry samples were performed following the prescriptions proposed by the European standard code UNI EN 1052-1, EN 1052-3:2002 and the American standard code ASTM E 518-02. The masonry samples were adapted in order to resemble the shape of required test specimens while the testing procedures were followed strictly. The destructive tests performed on the masonry samples were:

- axial compression on cubic samples;
- diagonal compression on cubic samples;
- shear test on masonry triplets;
- four points bending test on a segment of arch.

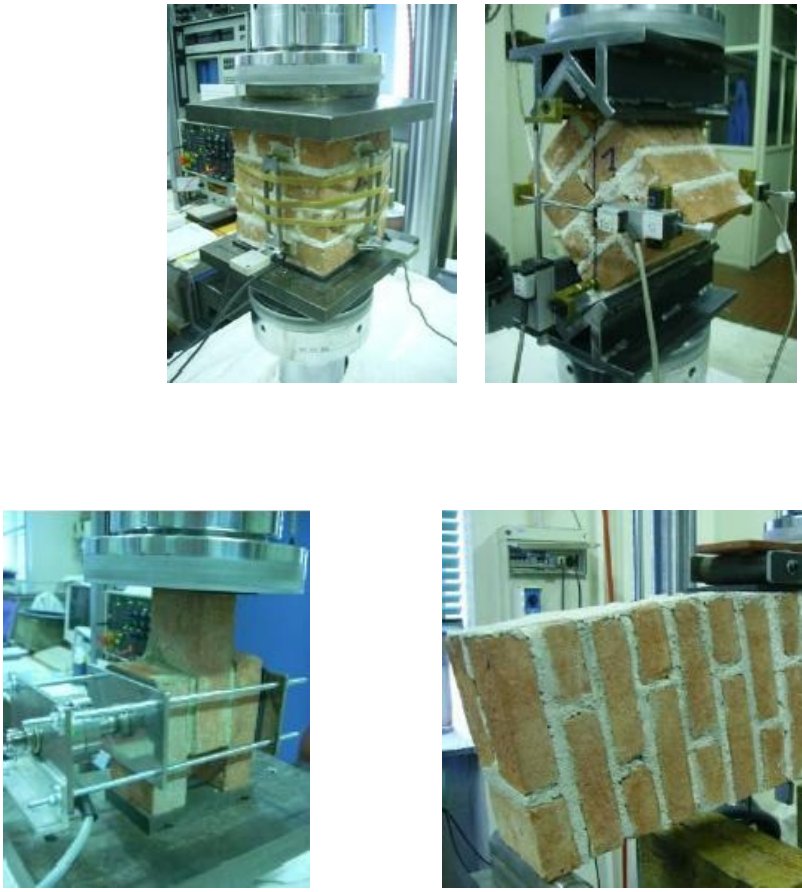

Figure 3 Tests conducted on the masonry samples.

Test	μ [N/mm2]	σ [N/mm2]
Compressive tests: tensile strength	4.278	0.354
Compressive tests: Young modulus E	1451	472
Diagonal tests: tensile strength	0.304	0.088
Diagonal tests: shear strength	0.430	0.125
Diagonal tests: shear Young modulus G	940	436
Shear tests (0.1 kN pre-compression): shear strength	0.794	0.301
Shear tests (0.5 kN pre-compression): shear strength	1.013	0.188
Four points bending tests: R modulus of rupture	0.22	//

Table 1 Results from the compressive tests, diagonal tests, shear tests and four point bending tests.

Flume tests

The hydraulic model was designed scaling the pier dimensions down so that the ratio between the length of the bridge and the width of the pier was maintained. The bottom section of the pier scaled model was connected with a hypothetic foundation base. The rectangular foundation was dipped into the bed material, whose uniform mean diameter was 0.80 mm, while the pier was hung up but not allowed to move during the flume tests.

The evolution of the soil profile produced by the induced scour was periodically monitored through a laser scanner acquired by a digital camera. The images taken during the tests were then automatically processed to define the portion of the foundation lateral face not covered by the bed material at each time step. The corresponding portion on the arch bridge model was freed from the polystyrene ring surrounding the bottom part of the pier to simulate the reduction of the lateral restrain at the foundation base.

Also the undermining effects were experienced in the flume tests, especially when the foundation base was not excessively dipped in the bed material. The erosion of the soil underneath the foundation, and consequently the loss of its bearing action, is simulated in the experimental model through the settlements application device previously described.

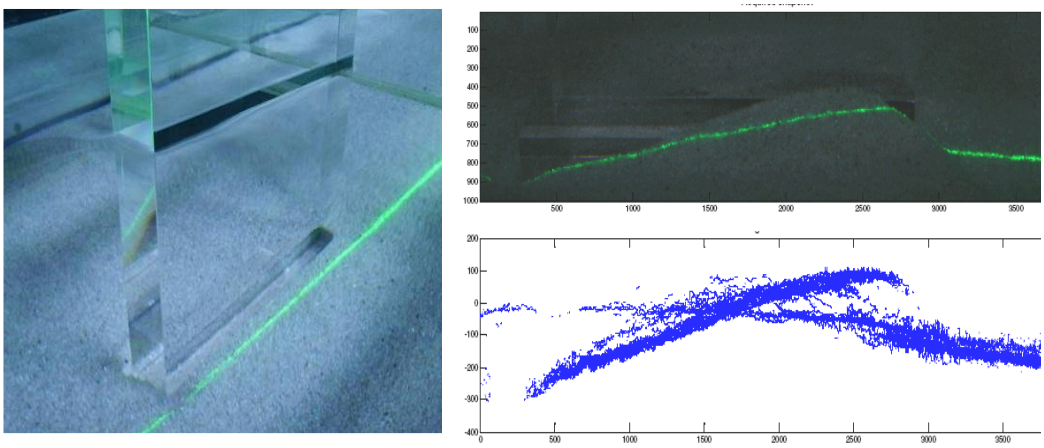

Figure 4 Hydraulic flume tests and scour profile

Numerical models

A 3D numerical model of the arch bridge was realised in the ADINA Finite Element package to estimate and assimilate modal parameters. The purpose was to better understand the dynamic behaviour of the structure and to plan accurately the following vibration analyses. In fact, the selection of the sensors location must be assessed carefully in order to allow a suitable resolution in the mode shapes for the highest number of identified modes.

The model consists mainly in solid elements and spring elements able to simulate the polystyrene layer and the settlement application device. The mechanical properties have been inherited from the material characterisation tests. The model is subdivided into a series of elements groups, where each group includes all those finite elements which share common mechanical features or structural functions.

In order to predict cracks locations, a numerical model of the masonry arch bridge [**1**] was built in the DIANA FE package which was able to simulate the non-linear behaviour of masonry. The FE package implemented a smeared cracking model which incorporates a tension cut-off, tension softening and shear retention. After the results of non-linear analysis, it was decided to add masses at the top of the central pier so as to take in account the weight of the missing part of the pier and to partially compensate the arch effect developed by massive abutments.

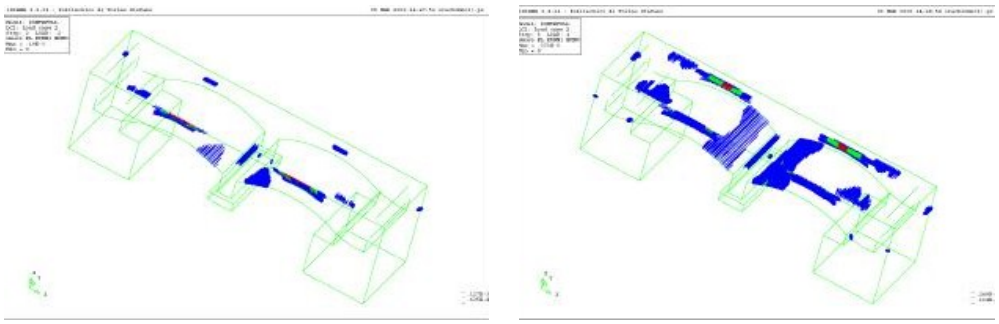

Figure 5. Non-linear model: smeared crack pattern with an applied settlement of 2 mm and 14 mm

4.2 The experimental test campaigns

4.2.1 Experimental test program

As previously stated, the main objective of the experimental test was to determine the capability of a structural health monitoring system, based mainly on dynamic measures, to detect the occurring of damage (such as scour at the bridge pier foundation). In this framework, dynamic testing ensures to identify a set of parameters to be monitored. A sensitivity analysis has been carried out on the parameters to choose the most reliable to detect the damage. Several damage steps have been applied to the structure in accordance with hydraulic flume tests as shown in Table 2.

Experimental campaign	Damage steps	Settlement [mm]	Rotation [rad]	Polystyrene
1st campaign	Healthy State (HS)	0	0	0%
2nd campaign	DS1	0	0	18%
	DS2	0.25	0	25%
	DS3	1	4.21E-04	37.5%
	DS4	2.25	1.01E-03	47%
3rd campaign	DS5	2.25	1.23E-03	56%
	DS6	2.8	1.23E-03	72%
	DS7	3.6	1.27E-03	81%
	DS8	4.7	1.30E-03	91%
	DS9	7.6	1.28E-03	100%

Table 2 Damage steps, middle pier settlement, pier rotation, polystyrene removed

	Time	Step	Excitation	Measurements
1st campaign	October 2008	HS	AV, IH	ACC, SG, T, OPT
	November 2008	HS	AV, IH	ACC, SG, T, OPT
	January 2009	HS	AV, IH	ACC, SG, T, OPT
	February 2009	HS	AV, IH	ACC, SG, T, OPT
	March 2009	HS	AV, IH	ACC, SG, T, OPT
2nd campaign	April 2009	HS (applied masses)	AV, IH	ACC, SG, T, OPT
		DS1	AV, IH, S	ACC, SG, T, OPT
		DS2	AV, IH, S	ACC, SG, T, OPT
		DS3	AV, IH, S	ACC, SG, T, OPT
		DS4	AV, IH, S	ACC, SG, T, OPT
3rd campaign	September 2010	HS (post-relaxation)	AV, IH, S	ACC, SG, T, OPT
		DS5	AV, IH, S	ACC, SG, T, OPT
	October 2010	DS6	AV, IH, S	ACC, SG, T, OPT
		DS7	AV, IH, S	ACC, SG, T, OPT
		DS8	AV, IH, S	ACC, SG, T, OPT
		DS9	AV, IH, S	ACC, SG, T, OPT

Table 3 Experimental tests timeline

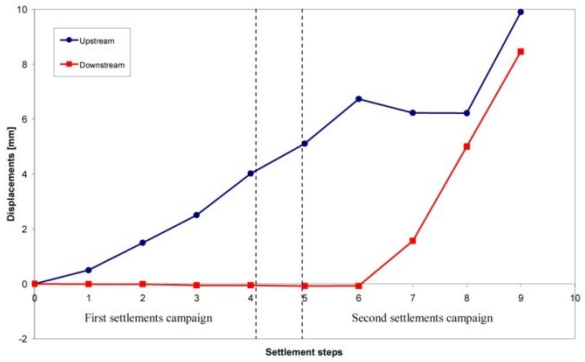

Figure 6 The settlements evolution trough the tests

Table 3 shows the timeline of the experimental tests. Different excitation sources were applied to the bridge model: ambient vibrations (AV), impact hammer (IH) and a shaker (S). Several physical quantities were monitored under the different excitations: acceleration measurements (ACC), strain deformation (SG and OPT) and temperature (T).

Several differential settlements steps were introduced by lowering the plate at the top of the mechanical device according to the results of specific hydraulic flume tests carried out on a further scaled model of the pier. Two settlements application campaigns were arranged into different lapses of time. In the former, four steps of settlement were carried out acting only on the two screws at the front-side of the model, this leading to increasing differential settlements coherent with the first stages of the streambed erosion localised at the upstream section of the bridge's pier. The displacements realized at the front-side were equal to 0.5, 1.5, 2.5 and 4.0mm, respectively. Slight cracks opening were observed at the edge between the arch barrels and the longitudinal spandrel walls after the third step application. At the conclusion of the forth step a partial detachment between the bottom of the pier and the top of the plate was noticed, meaning that the pier was suspended and further settlements application would have resulted ineffective.

The settlements campaign was resumed at the ending of the relaxation phenomena which restored the contact between the pier and the plate. Since the evolution of scour involves larger and larger portions of foundation soil underneath the pier, in the final stages the undermining effect produces a compensation of the previous differential settlements which lead to a quasi-uniform configuration. Therefore, the steps of the second campaign were applied acting also on the back-side screws of the settlement application system. The resulting evolution of the prescribed displacements throughout the whole destructive tests campaign is presented in the plot of Figure 6. In the last five steps of the settlements application the opening of new cracks in the arch barrels and the propagation of the former ones were observed.

Figure 7 Crack pattern after damage step 9

The application of the prescribed displacements was coupled with the removal of larger and larger portions of the polystyrene ring surrounding the pier base in order to simulate the concomitant erosion of the streambed around the foundation.

4.2.2 Experimental setups

Dynamical vibration tests require a careful identification of an optimal sensor location. In order to achieve a good mode shapes resolution, a heuristic approach was employed. The arch barrels were subdivided in 11 segments whose ends were assumed as measuring points for both the edge and the middle lines. Other 6 positions at the springing sections of the pier were materialised to capture the longitudinal displacements. The 4 mid-span sections of the arch barrels lateral faces and the 2 pier frontal faces were considered for the lateral and torsional modes. Finally, the 2 positions on the longitudinal spandrel walls at the middle section of the deck were added to identify the vertical modes.

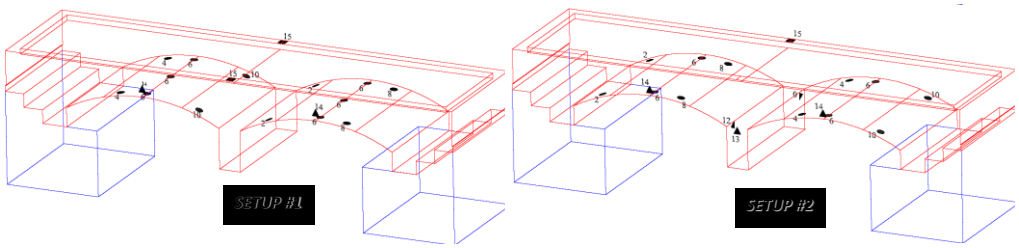

Figure 8. Experimental setups for vibration tests.

The sampling frequency was fixed to a value of 400 Hz to acquire the signals produced by both ambient noise and impact hammer excitations, using an instrumented hammer. A 180 seconds time laps was adopted for the ambient noise acquisitions. Several impacts were acquired in a 60 seconds time, even if only one impact per acquisition was used in the dynamic identification. The hammer impacts were applied in the same sensors positions along the longitudinal, transversal and vertical directions of the bridge model in order to excite properly all the modes estimated by the numerical modal analysis. Two setups were used for each vibration tests in order to capture the higher number of natural modes. Each setup consisted of 18 channels leading to 36 instrumented positions.

Forced vibration tests were performed by using a shaker TIRA TV 51220, capable to supply a rated peak force of 200 N. The force applied was acquired by using a mechanical impedance sensor PCB Piezotronics 288D01 (measurement range ±222.4 N pk). Five type of excitation tests were carried out:

- random: random excitation in a 10-100 Hz band,
- sweep sine: linear chirp from 10 to 100 Hz,
- shock: impulsive excitation,
- resonance: sine excitation at resonance frequencies,
- sine: sine excitation from 10 to 100 Hz, with 1 Hz resolution.

4.2.3 Experimental modal analysis results

The results of the experimental modal analysis performed on data acquired in the vibration tests carried out on each damaging step of the bridge model are here summarized. It was decided to employ two techniques working in the time domain due to the great spectral resolution they offer and their modal uncoupling capability. The Eigenvalue Realization

Algorithm (ERA) was used to analyse the free decay responses, whilst ambient vibration signals called for a Stochastic Subspace Identification (SSI).

The estimation of both natural frequencies and damping ratios did not show a monotonic trend during the different campaigns. Figure 9 shows the trend of the first four natural frequencies. It is noteworthy that, whilst in second campaign the trend of the first frequency is almost monotonic and highlights stiffness degradation (mainly related to the boundary conditions of the pier); in the third campaign the interpretation of the curve is more complex. Firstly, the first frequency increased up to 19.23 Hz, this meaning that relaxation made pier settle, increasing the boundary condition stiffness. In fact, after DS 4, the pier was almost completely suspended. Secondly, this phenomenon governs mainly the first modal shape, as it can be seen from 2nd and 4th natural frequencies which retain their values almost equal between the 2nd and the 3rd campaign.

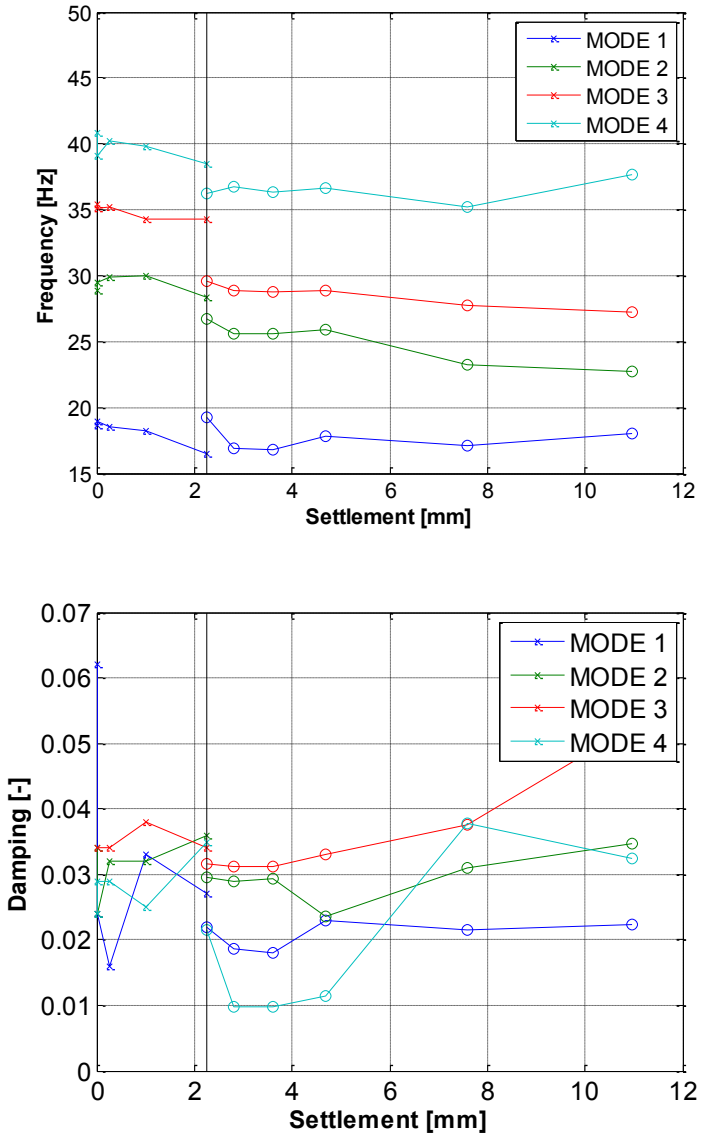

Figure 9. Natural frequencies and damping ratios of the first 4 modes through the various damage steps (damage step 0 corresponds to the healthy state of the bridge). Left side: 2nd campaign. Right side: 3rd campaign.

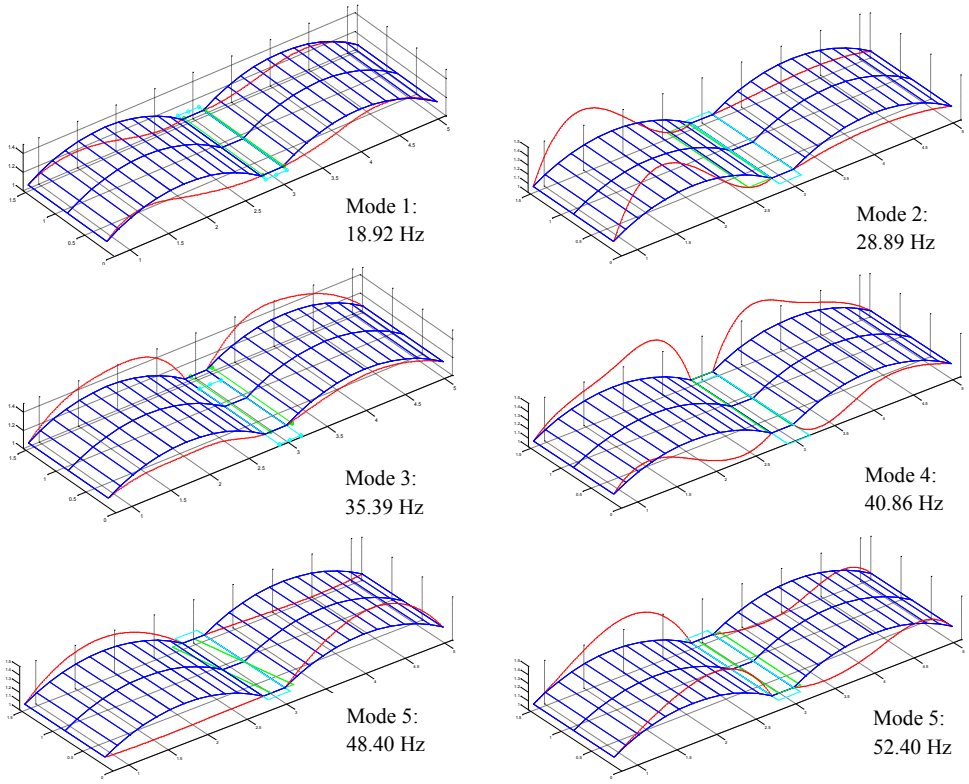

Figure 10. Modal shapes of the first 6 modes of the reference state

4.3 On-line outlier analysis

The main aim of test campaign carried out on the bridge model was to develop and assess a dynamic monitoring procedure suitable for the protection of this typology of structures from scour and undermining effects. A SHM methodology was developed using Outlier analysis [**2**]; in order to exploit its limited computational effort, the damage sensitivity and the results accuracy. The choice of a data-driven approach to the damage detection was forced by the complexity and uncertainties of the structure which prevented to define a reliable numerical model and the difficulties to incorporate the noise effects which are unavoidable in the vibration measurements. Several outlier analyses were carried out

both in the time and in the frequency domain [**3**]. An on-line Outlier analysis procedure was also developed and the flow-chart of its algorithm is presented in .

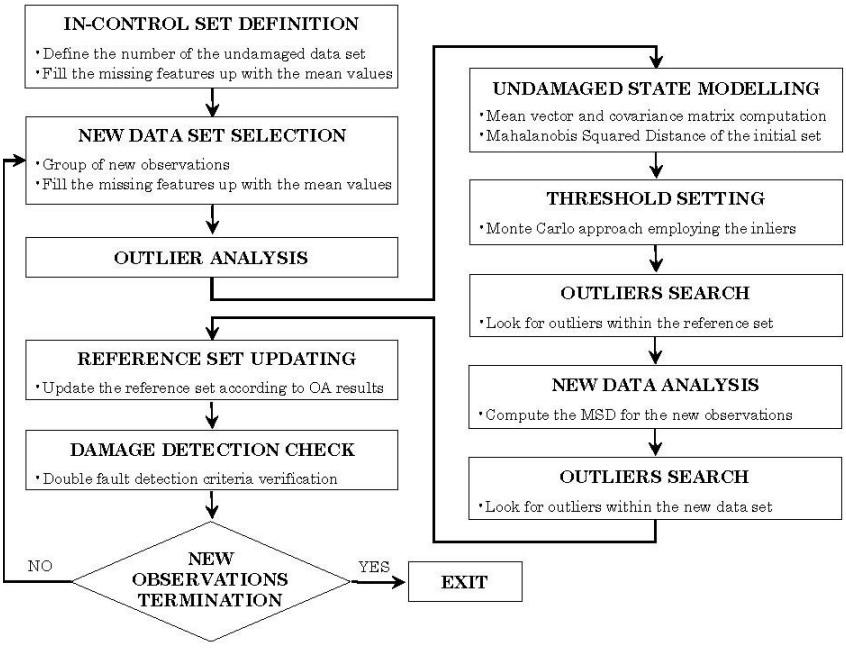

Figure 11 On-line Outlier Analysis methodology pursued

By way of example, Figure 12 shows the result for the Outlier analysis carried out on the measurements of the second campaign. The acquired signals were analysed in the frequency domain in terms of transmissibility functions. Small portions of the spectra were selected by means of a genetic algorithm and used as inputs to compute the statistical distance assumed as damage index. All the sets concerning the measurements acquired after the introduction of the settlement steps are above the threshold which defines the in-control field. This result proves the accuracy of the damage detection method and the sensibility of the selected features.

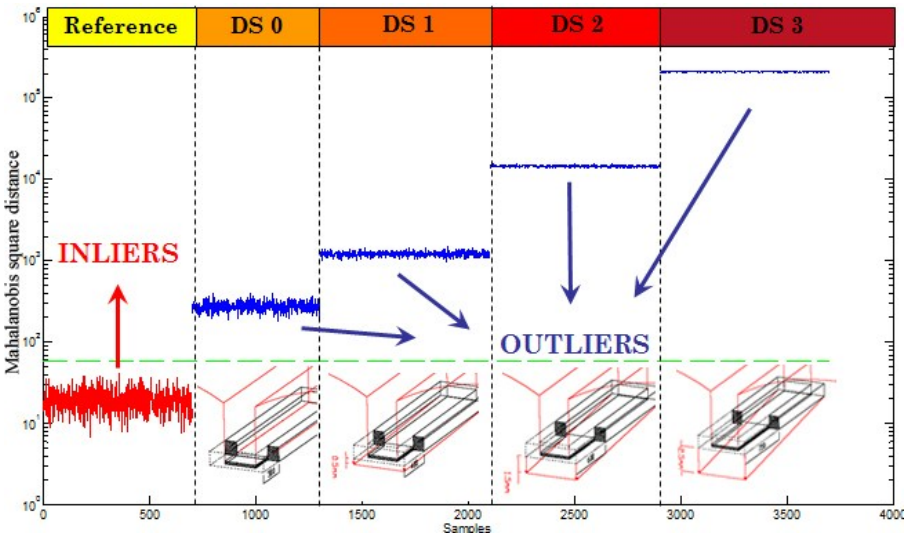

Figure 12. Results of Outlier Analysis.

In this thesis, the above on-line outlier analysis is proposed adopting the instantaneous estimation of modal parameters as symptoms.

4.3.1 The pursued methodology

The recent achievements in the sensing and information technologies are pushing towards the development of on-line monitoring systems capable to provide as fast as possible assessment of structural health state. In particular, the detection of a fault in the structural system, which is the main goal of monitoring, is progressively evolving in a real-time evaluation of the damage occurrence. "Real-time" is to be understood as the continuous analysis of monitored data aimed at assessing the state of the structure and the identification of anomalies in its behaviour in the shorter lapse of time from its occurrence. The concrete possibilities offered by this enhancement of the damage detection are mainly related to the investigation of sudden events threatening the constructions. The selection of reliable features, able to capture the occurrence of damages and to follow their evolution in time is a main issue to investigate.

The vibration-based SHM process is commonly described as a sequence of four steps [**4**] ,

- the operational evaluation
- the data acquisition

- the feature selection
- the statistical model development.

The last point consists in the development of algorithms to identify damage in a unambiguous and statistically significant manner. The methodology here adopted to deal with the instantaneous detection of damage follows this general subdivision of tasks but disregards the strict temporal sequence whit whom the operations are accomplished.

The approach which is here pursued conceives the last three steps of the list above as a whole damage assessment framework, where the three actions are iteratively repeated and the passage to the next is performed without the completion of the previous. More precisely, each action entails the processing of a limited bank of data in order to provide its evaluation immediately. The obvious reason which justifies this strategy is the goal to minimize the time lapse between the conclusion of the previous action, i.e. the extraction of the selected features from the data, and the detection of damage.

The operational evaluation is excluded from the aforementioned cycle since it refers to a preliminary step although of vital importance. At this stage the system and the operational environment it functions in are characterised and the reference state of the structure (also referred as baseline) is evaluated. This phase involves the monitoring of the structure over a period of time which should be enough to fully observe all the different states the system undertakes without the occurrence of damage. The following damage detection process is anticipated by the definition of the most sensitive features with reference to the postulated damage.

Once that the measurements settings are arranged and the best features are identified, the assessment of the system can be initiated in a repetitive and automatic manner. The data sets are periodically acquired at an appropriate frequency rate and for opportune time intervals and then the measurements are transmitted to a processing unit which performs the features extraction. The core of the damage detection framework is finally reached. This couples the instantaneous estimation of modal parameters, here assumed as damage features, with the capabilities of a novelty detection algorithm carried out in real-time.

The instantaneous modal parameters estimation

The methodology adopted to estimate the instantaneous modal parameters follows the optimization procedure proposed by Ceravolo [**5**] (detail in Chapter 2), based on the instantaneous curve fitting of time-frequency representation of dynamic response signals.

The response of a system can be represented in the time – frequency plane as a sum of harmonics concentrated at modal frequencies modulated according to the evolution of the modulating waveform.

Assuming the dynamic response of the system locally stationary, the instantaneous energy spectrum $D(\omega,t)$ approaches a scaled version of the squared modulus of the

Frequency Response Function (FRF). The instantaneous estimation of the modal parameters can be carried out through the minimization of the functional (1) at each time t:

$$D(\omega, t) - |H(\omega, t)|^2 = 0 \qquad (1)$$

Under the assumption of a linear and proportionally damped structure the FRF is defined as function of modal amplitudes, AR_k, damping, ζ_k, and modal frequency, ω:

$$H(\omega) = \sum_k \frac{AR_k}{(\omega_k^2 - \omega^2 + 2j\zeta_k\omega\omega_k)}$$

A similar relationship could be written for mobility and accelerance form.

An important issue is the choice of the TF representation to be used to estimate the instantaneous energy spectrum $D(\omega,t)$. The square value of the Short - Time Fourier Transform (STFT) has been adopted in this paper. Although STFT is affected by the intrinsic limitations in resolution typical of linear transforms related to the uncertainty principle, the simple structure of this technique provides the computational advantage which allows to address the problem in a direct manner and to find a reasonable solution. In particular, the length and the type of the window in samples used in the calculus of the STFT seems to influence the damping estimation to a large extent. Setting the window length for the spectrogram depends on the de-correlation length of the process and requires the availability of a first estimate for damping.

The on-line novelty detection

According to the statistical pattern recognition interpretation of the damage assessment, the damage detection is conceived as a novelty detection problem. This type of problem entails only the availability of the data from the undamaged state of the structure, while no *a priori* information about the damaged states are required. The indication of the damage occurrence is provided as a measure of the discordance of a candidate observation from the data set which represents the normal condition of the system. An observation which appears inconsistent with the data used to represent the baseline is considered as generated by a different state of the system and thus labelled as an outlier, i.e. a novelty. This process of outliers recognition is named Outlier Analysis.

Different metrics can be adopted to quantify this measure of discrepancy between two sets of data. The observations derived from the measurements are generally expressed in terms of multivariate features, those which have proved to offer the best discrimination among the processed candidates. The statistical distance commonly employed in the outlier analysis is the Mahalanobis squared distance because it suitably copes with the comparison

of multivariate observations. The mapping between a candidate observation $\{x_\zeta\}$ defined in a multidimensional space, whose dimension equals the number of damage sensitive features, and the scalar damage index D_ζ is provided by equation (2):

$$D_\zeta = \left(\{x_\zeta\} - \{\bar{x}\}\right)^T [S]^{-1} \left(\{x_\zeta\} - \{\bar{x}\}\right) \tag{2}$$

where $\{\bar{x}\}$ and $[S]$ are the mean vector and the covariance matrix of the reference data set, respectively. A Monte Carlo approach based on extreme value statistics is used to compute the threshold value which discriminates the candidate observations as inliers or outliers. The threshold value is extracted from a uniformly-distributed population with the same dimensions of the data set assumed as reference, i.e. the number of features and the number of observations. A confidence limit percentage usually varying between 1% and 5% is set to define the exceeding threshold over a large number of trials.

In the case of an off-line application of the novelty detection the observations of the reference set are limited to a well-defined data set which is assumed as representative of the baseline of the system. The limits of the reference set are subjectively established and a single threshold value is set depending on the size of the normal data. All the new observations are then processed as candidate outliers using in equation (x) the mean vector and the covariance matrix of the unfaulted data set.

In a more realistic SHM system the vibration measurements are continuously acquired and no limit is established to define the baseline response of the structure. As soon as a new set of data is acquired the damage sensitive features are extracted and immediately processed in order to label the patterns according to the results of the damage assessment. When a new observation exceeds the threshold a novelty is detected and damage is inferred. Otherwise the pattern is supposed to be generated from the undamaged state of the system and thus added to the reference set. Consequently, the mean vector and the covariance matrix of the unfaulted data set used to classify the new observations are updated.

This real-time approach to the novelty detection is certainly more appealing because it does not require the *a priori* and subjective definition of the reference set. On the contrary, the reference set is progressively updated to introduce new observations derived from states of the system which are not necessarily related to damage. This characteristic enhances significantly the robustness of the damage assessment. However, the pursued goal is much more challenging because the damage identification is particularly affected by the erroneous classifications of the new patterns. A false-positive damage detection may occur because the undamaged states of the system are not exhaustively embodied in the reference set acquired so far. On the contrary, the large variability of the features may cover trends or changes actually related to the development of damaging phenomena and thus leading to missed alarms which could have serious consequences. Therefore, a reliable real-time novelty detection should be capable to cope with the noise affecting the data and possible misclassifications in order to provide a credible warning in the shortest lapse of time. Some

criteria aimed at the fast and accurate distinction between inliers and outliers must be established to respond to the aforementioned requirements.

The main differences between the in-line outlier analysis implemented in this study and the traditional off-line version refer to the treatment of the reference data set and the definition of reliability criteria for the damage detection. For the former issue a limited portion of the reference set is assumed to be composed by observations produced by the undamaged state of the structure. This assumption is unavoidable to initiate the damage assessment process. However, all the observations following this in-control set are considered as candidate outliers supposing their membership unknown. The new observations are grouped together in small sets which are analysed one by one. The gathering of the observations into small groups reproduces the periodic acquisition of data from a realistic monitoring system. The outlier analysis of each new set is carried out by means of equation (2) and their Mahalanobis squared distance value is calculated.

The results are compared with the threshold obtained using the same Monte Carlo approach based on extreme value statistics adopted in the off-line novelty detection. Differently, further requirements beyond the simple exceeding of the threshold are introduced in the on-line procedure to assure the reliability of the damage detection. Two conditions must be satisfied at the same time to classify an outlier as actually representative of a faulted condition of the system. The first condition refers to the detection of the same outlier in two successive steps of the analysis. The second implemented criterion is related to the consecutiveness of the detected outliers within a single step. A certain number of consecutive observations belonging to the same set must be classified as outliers to assure the detection of a "real" novelty.

The motivation for the introduction of these requirements derives from the erroneous detections of outliers due to the lack in the exhaustiveness of the reference set. The noise in the measurements or the occurrence of new states of the system not necessary related to a faulted condition are the reasons for the detection of false outliers. The reliability of the damage detection can be guaranteed only through the discrimination between accidental and systematic outliers. Indeed, the false-positive detections are generally isolated and not correlated with the other observations because of their accidental origin. Moreover, the detection of a deviation from the normal condition due to the occurrence of a new state of the structure not observed yet or a faulty measurement is not generally repeated if the corresponding data set is included in the reference. In this case we should correctly distinguish the reason of the detected novelty between an anomaly in the data, rather than an anomaly in the system.

In order to prevent the eventuality of a false detection, the contemporary satisfaction of both the criteria is required to finally detect the damage occurrence. At each introduction of a new set of candidate observations the reference set is re-defined according to the results of the previous analysis step. The observations previously classified as inliers are added to the reference set in order to introduce the contribution of potential new states of the structure not affected by damage which otherwise could lead to incorrect novelty detections. The previously identified outliers are included in the new reference set but they are discarded

from the updating of its mean vector and covariance matrix in order to prevent a bias of the detection. The satisfaction of the two reliability criteria implies the repetition of the outlier analysis for all the observations acquired so far, apart from those belonging to the in-control set which are assumed unfaulted. Because of this continuous re-calculation, the search for the outliers is extended to both the previously processed and the new observations.

The confirmation of the systematic deviation from the normal condition produces an unavoidable delay in the damage detection because a further analysis step is required to verify the accidental or systematic origin of the outliers. Moreover, the second requirement raises a problem of arbitrariness in the number of repeated consecutive detections. The suitable number of consecutive detected outliers is not an easy identifiable parameter. A value too small may lead to the possible identification of false-positive outliers. On the contrary, the definition of a too large value may delay the damage detection. A 20% of the number of new observations added at each analysis step is a reasonable compromise for the number of consecutive outliers.

4.3.2 Validation of the proposed method

The methodology presented in this study is validated on the detection of the damage effects produced by applying the settlements to the pier on the masonry arch bridge model.

The features extraction and the statistical model development are carried out on the vibration measurements acquired during the settlements application by means of the instantaneous modal parameters estimation and the real-time novelty detection described in the next.

The extraction of instantaneous modal features

The instantaneous damage assessment was carried out on the signals acquired throughout the introduction of the third damage step, as reported in Table 2. By way of example, the effects of the settlements application on the first vertical bending mode are depicted in Figure 2.

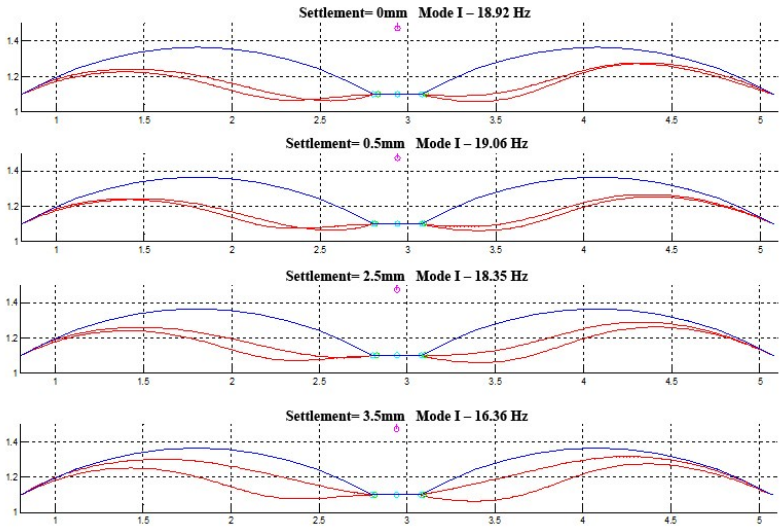

Figure 13 1st Mode shape variation (step 0 to step3)

The variation of the modal parameters can be ascribed to the change in the boundary conditions of the central pier, followed by the consequent opening of cracks between the arch barrels and spandrels walls which developed with the settlements applications and were visibly observed at the end of the third damage step.

Several trials were accomplished in order to define a suitable choice for the type and length of the analyzing window. A Hanning-type window with length of 80 samples provided an optimal STFT representation for the estimate of the FRF. A set of tentative values for the three variables was defined to start the optimisation. The values of the natural frequency (18Hz) and the damping ratio (3%), estimated before the application of the third settlement step were assumed at this scope. The initial modal amplitude was obtained as the value of the instantaneous response estimation evaluated at the modal frequency. The minimisation of equation xxx was repeated at each time instant and the initial values of the modal parameters were updated every time with the results of the previous calibration. A moving average was finally applied to smooth the instantaneous evolution from spurious peaks.

Figure 14 shows the averaged results obtained from the analysis of the selected signals. The modal frequency estimates turned out to be satisfactory and confirmed the considerations derived from the previous analysis of the instantaneous response estimation.

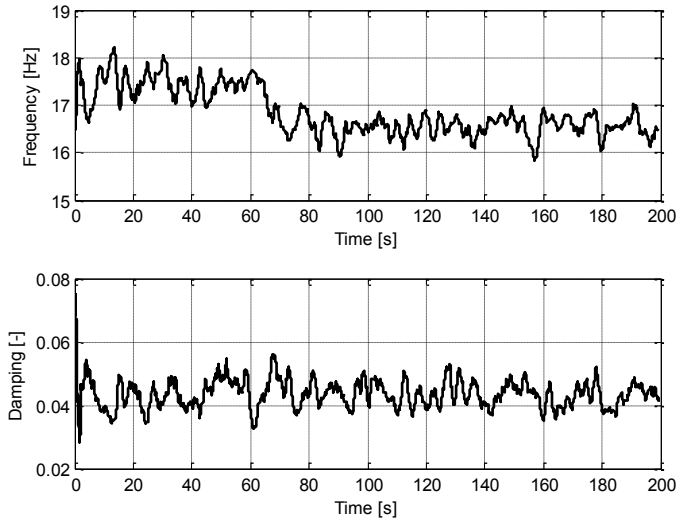

Figure 14 Evolution of the instantaneously estimated modal parameters averaged among all the selected signals: natural frequency (top) and damping ratio (bottom).

4.3.3 The results of the on-line damage detection

The instantaneously identified modal parameters were then adopted as input features to perform the outlier analysis and validate its real-time application on the simulated damage scenario. For the sake of brevity, only the results obtained for the third damage step are presented in this study. The reference set used for the comparison with the candidate observations (2) was composed with the features extracted from the measurements acquired in the lapse of time immediately before the introduction of the settlement step. This approach was pursued to verify the actual capability of the method to detect the slightest deviations produced by the damage occurrence and thus indentify its triggering instant. Moreover, the lack of significant damage effects detected in the previous settlement steps justifies the assumption of integrity for the reference set defined above. As already mentioned, the online outlier analysis requires the initial selection of a set of sound observations to initiate the damage assessment process. This in-control set was created with 5000 samples, corresponding to the first 50s acquired at the beginning of the third vibration measurements set when the settlement step had not been applied yet. The following observations were collected in sets of 50 samples and their features were processed by means of equation (2) on the basis of a reference set progressively expanded. The threshold value for the Mahalanobis

square distance was computed adopting the Monte Carlo technique and a confidence limit percentage of 1%.

The observations below the threshold were labelled as inliers and added to the reference set in order to take new undamaged states of the system into account. The samples exceeding the threshold were marked as "false" outliers until one of them was detected in two successive analyses and followed by at least other 10 consecutive outliers. The satisfaction of both these requirements marked the detection of an outlier actually related to a change in the state of the structure.

The accuracy of the proposed method is evaluated on the basis of the capability to identify the instant of the change of the structural response in the most rapid and reliable way. The features obtained in the previous stage, i.e. the instantaneous frequency and the damping ratio of the first bending mode, are initially adopted separately in order to evaluate their sensitivity in conjunction with the novelty detection.

Finally, they are considered together to investigate the advantages of the fusion between data of different nature. In each case the responses acquired at the 6 sensors locations already considered in the instantaneous estimation of the modal parameters are analysed simultaneously. The result of the on-line outlier analysis employing the instantaneous estimates of the natural frequency of the first mode is shown in Figure 15. The health state of the bridge model is expressed by means of the Mahalanobis square distance computed for each acquired sample. The damage index is compared with the threshold value, represented by the horizontal line in the plot, to label each observation as inliers or outliers. The inliers in the figure are depicted by a solid line and count the 5000 samples of the in-control set and the following 1412 observations.

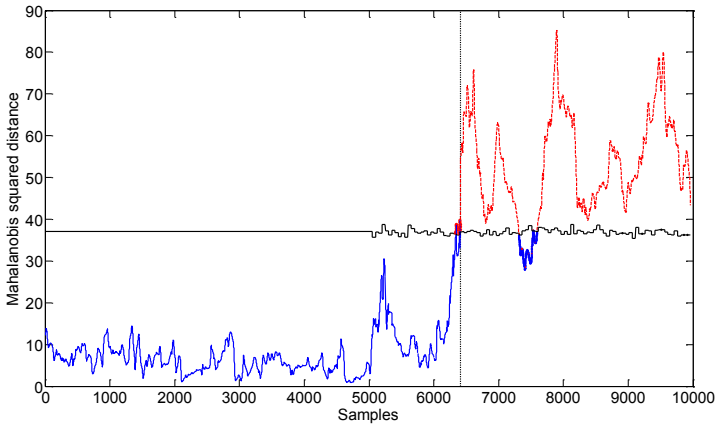

Figure 15 Result of the on-line outlier analysis carried out on the instantaneous estimates of the natural frequency.

The detected time instant corresponds to the drop of the identified frequency which is visible at t=70s in Figure 14.The detection of the change in the response of the system is marked in the figure by a dashed vertical line which splits the plot into two sides. The right-hand side is characterised by the presence of the outliers linked by a dashed line and exceeding the threshold. A small group of sample is recognised as inliers even beyond the detection of the damage occurrence and, due to the irreversibility of damage, it may be easily classified as a set of false-negative observations. Few samples are labelled as false-positive detections just before the instant of time marked as turning-point of the structural response. The recognition of this change has required the processing of only one set of samples after its occurrence because of the satisfaction of the criteria assumed to prevent the false-positive detections. The profile of the threshold line resembling the blade of a saw is due to the re-calculation of this value after the adding of a new piece of information in the reference set.

The capability to detect in real-time the evolution of the modal parameters means the possibility of providing early warnings which could be decisive for the preservation of the structure and the safety of its occupants.

The introduction of the criterion of the consecutiveness of outliers detection allows to enhance the exhaustiveness of the training data.

References

[1] Invernizzi, S., Lacidogna, G., Manuello, A., Carpinteri, A., (2009); *Damage assessment of a two-span model masonry arch bridge*. Proceedings of the SEM Annual Conference, Albuquerque, USA.

[2] Worden, K., Manson, G., Fieller, N.R.J., (2000); *Damage detection using outlier analysis*. Journal of Sound and Vibration, 229(3), pp. 647-667.

[3] Ruocci, G., (2010); *Application of the SHM methodologies to the protection of masonry arch bridges from scour*. Politecnico di Torino PhD Thesis.

[4] Doebling, S.W., Farrar, C.R., Prime, M.B., Shevitz, D.W., (1996); *Damage Identification and Health Monitoring of Structural and Mechanical Systems from Changes in Their Vibration Characteristics: A Literature Review*. Technical Report LA-13070-MS , Los Alamos National Laboratory, Los Alamos, NM.

[5] Ceravolo, R., (2004); *Use of instantaneous estimators for the evaluation of structural damping*. J. of Sound and Vib., 274(1-2), pp. 385-401.

[6] Ruocci, G. et al., (2011); *Experimental testing of a masonry arch bridge model subject to increasing level of damage*. 4th International Conference on Advances in Experimental Structural Engineering, Ispra, Italy.

[7] Van Overschee, P., De Moor, B., *Subspace Identification for Linear Systems: Theory and Implementation - Applications*, Kluwer Academic Press Dordrecht, 1996.

[8] Qian, S.E., *Introduction to time-frequency and wavelet transforms*, China Machine Press, 2005.

[9] Maia, N.M.N., Silva, J.M.M., *Theoretical and experimental modal analysis*, Research Studies Press, Wiley, 1997.

[10] Farrar, C.R., Worden, K., (2007); *An introduction to structural health monitoring*. Phil. Trans. R. Soc. A, 15(265), pp. 303-315.

[11] Ewins, D.J., *Modal testing*, Research Studies Press Ltd, 2000.

Chapter 5

Dynamic tests and reliability analysis of five dismounted bridge beams

This chapter aims at describing the tests campaign carried out on five precast bonded post-tensioned concrete bridge beams, recently dismounted after a service life of 50 years. The girders were part of the deck of a recently dismounted viaduct of an Italian motorway. The beams showed different deterioration levels, mainly due to the different exposure to corrosive agents. The test campaign were designed for evaluating the residual load bearing capacity of the members. The static tests were performed up to ultimate load adopting a four-point bending test configuration, applying the load by means of four hydraulic jacks and controlling the level of the applied forces. Dynamic measurements were acquired before and after the static tests by using different excitation sources. Experimental modal analysis were performed and the results are presented and compared.

The tests highlight the connection among residual strength and dynamic characteristics, as periods. The residual resistance of the of the beams has been expressed as a function of measured symptoms and the evolution in time is estimated. Nevertheless the reliability of the beams has been also estimated.

5.1 Introduction

The management of a complex structural system, such as a bridge, requires to cope with several issues: to check the actual serviceability conditions, to assess the safety margins and to analyze its vulnerability to natural phenomena hazards, acting to mitigate the related risk. Several factors, as aggressive environmental conditions, corrosion and cracking propagation due to cyclic loads, may bring to a substantial reduction of the safety margins. Moreover the demand for extending the service life of the existing structures and the increase of the service loads and volumes entail the need for assessing the structural safety over the years. The implementation of an effective monitoring system may allow to get a thorough knowledge of the actual operational conditions, and hence to plan a rational scheduling of maintenance, optimizing the employment of the economic resources.

Structural diagnostics is often associated to the analysis of vibration measurements, since the dynamic behavior is strictly connected to the global characteristics of the monitored object. The variation of these quantities can be used as indicator of occurring damages. Nowadays, one of the most challenging issues is represented by the effective integration between the knowledge gained by monitoring (diagnosis) and the structural safety formulations (prognosis). At this purpose, performing experimental tests on structures during their lifetime, or at the end of the service life, constitute an important source of data to be used in developing predictive models and calibrating health monitoring techniques.

The reduction of structural safety during the service life is a widely debated issue. Several factors, such as corrosion, rheological effects, increasing of service loads, cracking propagation due to cyclic loads, may act simultaneously on a structure over its lifetime and lead to a substantial reduction in its capability to meet the required performances.

In this chapter, the results of experimental tests on bridge beams are presented. An extensive tests campaign was carried out to evaluate the residual load-bearing capacity and the dynamic characteristics of a set of precast bridge girders, recently dismounted after 50 years of service life. The different levels of deterioration, expressed in terms of flexural strength, and the identified modal periods have been then used to the evaluate the reliability of the beams

5.2 Description of the tested structures

The experimental testing campaign was commissioned by the Italian motorway company *ATS autostrada TO-SV S.p.A.*, at the aim of evaluating the residual strength of a set of bridge beams removed from *Pesio* viaduct after fifty years of service life during the modernization works of *A6 Torino-Savona* motorway.

The tested beams had all the same geometrical characteristics and presented different degradation levels. Each deck of the viaduct was constituted by five 35 m long simply supported beams. The section of the beams had a trapezoidal shape with linearly varying height from 1.55 m at the supports to 2.95 m at the midspan. The beams were constituted by a bottom precast part completed by a 0.1 m thick, cast-in-place slab. The post-tensioning reinforcement consisted of 5+5 six-strand tendons, placed in the two sloping lateral walls. The design characteristics of the employed materials were:

- Post-tensioning tendons steel - ultimate tensile strength: 1600 MPa;
- Concrete – cube compressive strength: 45 MPa;

Beam	Date	Tests
B01	12/05/2011	Static
B02	20/05/2011	Static+Dynamic
B03	27/05/2011	Static+Dynamic
B04	16/06/2011	Static+Dynamic
B05	27/06/2011	Static+Dynamic
B06	06/07/2011	Static
B07	13/07/2011	Static+Dynamic
B08	22/07/2011	Static
B09	29/07/2011	Static

Table 1 Tests planning

Figure 1 Views of the Pesio viaduct and a phase of the demolition of the decks

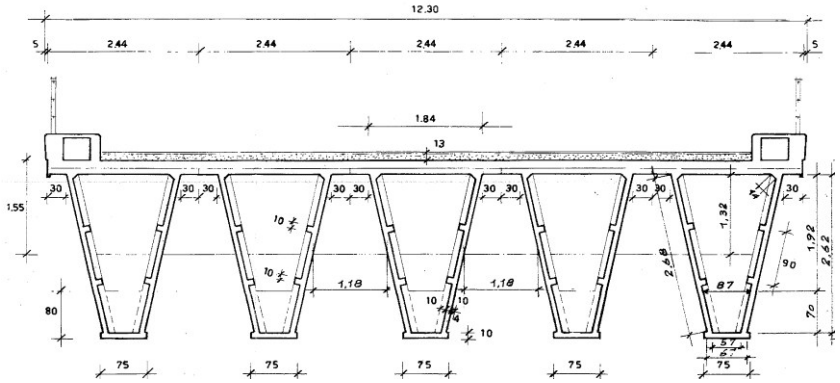

Figure 2 Midspan cross section of the Pesio Viaduct deck (from original documentation)

The tested beams present different deterioration levels. The different evolution of the deterioration process can be mainly attributed to their position in the deck. The edge beams are usually more exposed to weather, chemical attacks, chlorides constituents de-icing salts and pollutants emitted by vehicle traffic. Moreover they undergo higher stress levels, resulting in the years in a wider opening of cracks and then in an increased deterioration rate.

The health state of the tested beams were classified into three categories (good, intermediate and bad condition) on the basis of a visual inspection (Table 2).

Beam	Condition Rating	Midspan ultimate moment M_u [kNm]
B01	Bad	11172
B02	Intermediate	22581
B03	Good	20142
B04	Good	18336
B05	Intermediate	19321
B06	Bad	12087
B07	Bad	11242
B08	Good	14960
B09	Good	14924

Table 2 Visual inspection rating and static test ultimate load

5.3 Static tests sessions

A four-point static bending test was chosen to determine the ultimate load capacity. The forces, applied by means of four hydraulic jacks, were progressively incremented performing loading and unloading cycles until reaching the ultimate load. The static tests have been designed in order to investigate the whole behavior of the post-tensioned beams, determining both the decompression moments and the ultimate bending strengths. Table 2 lists the condition rating of the beams and their ultimate bending moments, Figure 3 shows the test configuration. The Figure 3 shows the test bench and the bending moments induced by the self-weight and the contrast system.

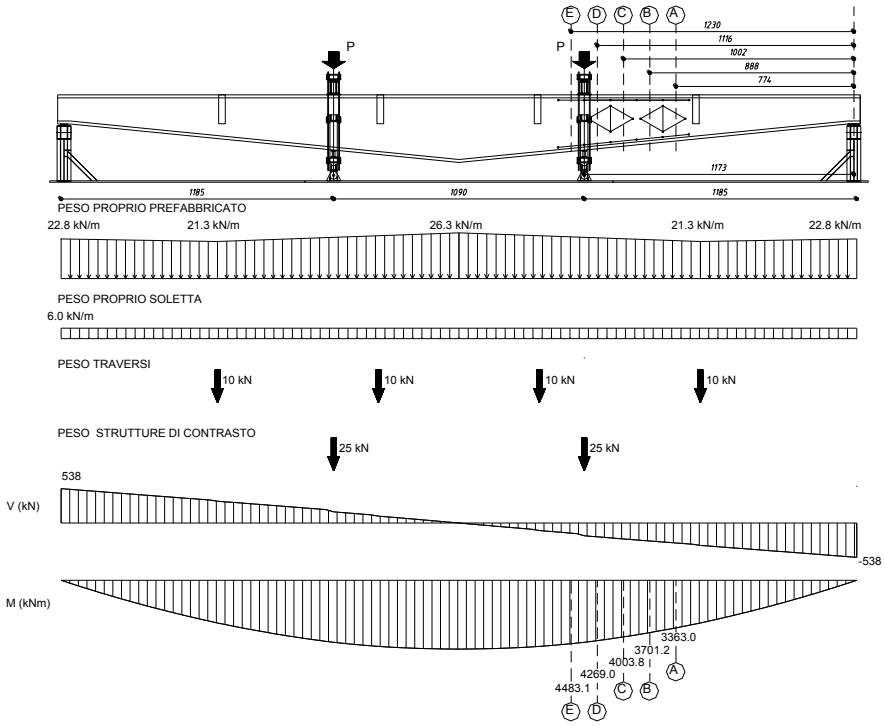

Figure 3 Test bench and bending moments induced by self-weigh and contrast systems

Figure 4 A beam placed on the test bench

5.4 Vibration tests planning

The beams were tested after the dismantlement and, in three cases, after the execution of the static tests (Table 3).

Different excitation sources have been employed: ambient vibration, impulsive loads applied using a sledge hammer and, on the beams B04, B05 e B07, sweep sine excitation an electro mechanical vibrodyne was also used to apply a sweep sine excitation. The Table 3 reports the summary of tests performed.

Beam	Before static test (BST)	After static test (AST)
B02	Hammer, Ambient vibr.	-
B03	-	Hammer, Ambient vibr.
B04	Hammer, Ambient vibr., vibrodyne	Hammer, Ambient vibr., vibrodyne (*)
B05	Hammer, Ambient vibr., vibrodyne	Hammer, Ambient vibr., vibrodyne
B07	Hammer, Ambient vibr., vibrodyne	-

(*) Test performed after the application of a static load of P=0.88 P_u

Table 3 Dynamic tests – experimental setups

The characteristics of the employed dynamic acquisition system are here reported:

- 18 monoaxial accelerometer PCB Piezotronics mod. 3701G3FA3G (Fig. 5)
  - Sensitivity: 1 V/g;
  - Measurement Range: ±3g;
  - Broadband resolution: 30 μg
- Multichannel data acquisition LMS Difa – SCADAS III
- External stabilized power supply
- Notebook with acquisition software
- Low noise coaxial cable
- Digital thermohygrometer
- Sledge hammer
- Vibrodyna Losenhausenwerk tipo 2000/4-20

The placement of the sensors on the structure represents one of the most important issue in the design of a monitoring system. The accuracy of the modal identification is highly influenced by the measuring positions. An appropriate sensor deployment must fulfil the following requirements:

- the achievement of a good modal shape resolution
- the identification of an adequate number of natural modes
- the ease in the distinction among all identified modes
- the capacity to catch the three-dimensional structural response.

Given the simplicity of the structures examined, the most important requirements to keep into account were to obtain a good spatial mode shape resolution and the identification of an adequate numbers of natural modes. The accelerometers have been placed along the longitudinal axis of the beam on the slab (Fig. 10), with a closer spacing in the middle part of the span. Three accelerometers were placed along transversal axis to discriminate among

torsional and transversal bending modes. The configuration have been changed between the first two test campaigns and the following three: the first preliminary results suggested to employ more sensors and a different spacing to optimize the spatial resolution of the modes.

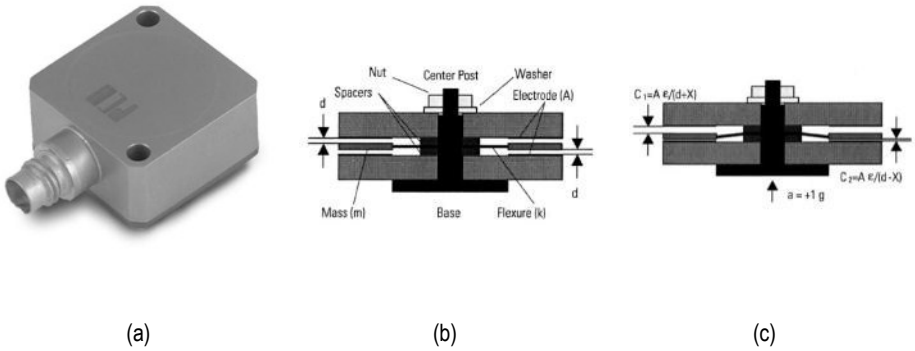

(a) (b) (c)

Figure 5 PCB 3701G3FA3G capacitive accelerometer employed (a) and cross section in the "0g" condition (b) and"1g" condition (c)

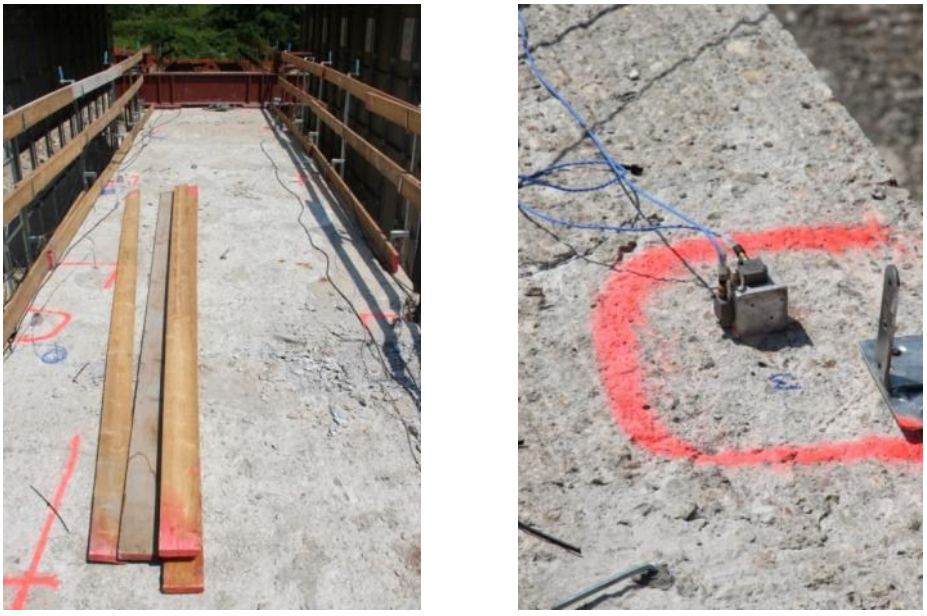

Figure 6 An accelerometer placed on the slab

5.4.1 Methodology of testing

The dynamic tests have been performed on five beams before the static tests (BST), namely in the condition they were after the dismantlement, and in three cases after the execution of static tests (AST) (Table 3). As mentioned above, different sources of excitation were used, at the aim to apply different modal identification methods and obtain more reliable results.

All the measurements have been acquired at using a sampling frequency of 400 Hz. The impact tests (Figure 7) were carried out by hitting the beams along the slab with a sledge hammer both in vertical and transversal directions. In each position several impacts were applied, spaced each other appropriately in time to run out the effect of previous stroke. The details of the test configurations are shown in the paragraphs referring to the individual acquisition campaigns.

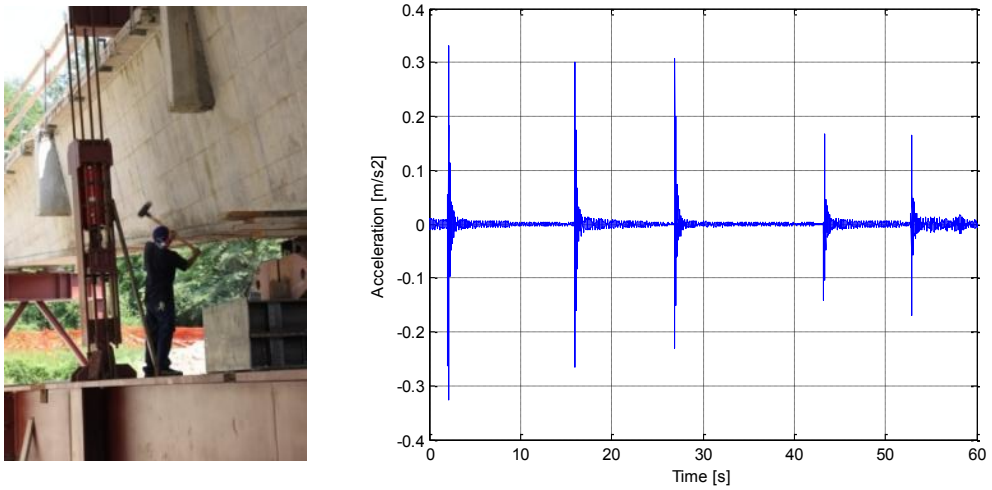

Figure 7 A phase of execution of the impact test and an example of the acquired signal

The forced tests were designed in order to apply an almost constant amplitude force in the chosen frequency range. The vibrodyne is constituted by two masses mounted eccentrically on two disks rotating in opposite directions with the same phase and frequency.

The force applied can be modulated varying both the angle α between the eccentric masses, from 0° (no force applied) up to 132°, and the angular velocity. The characteristics of employed vibrodyne are:

- Range: 2-20 Hz
- Maximum force amplitude: 20 kN

Basing the decision on the FE model and the preliminary results of the previous tests on the beams B02 and B03, the vibrodyne has been positioned to maximize the number of excitable modes in its operative range (Figure 10).Thus it was possible to excite a range of frequencies including the first two flexural modes and the first torsional mode of the beams. The vibrodyne and the engine were tied to the beam through a double set of steel profiles UPN 200 placed on intrados and extrados, connected by Diwidag ∅ 26mm bars.

Figure 8 View of the vibrodyne anchorage system

Due to the issues regarding the accuracy of manual control of the engine and to guarantee the safety of workers on the beams during the execution of the tests, it was decided to apply only the minimum amplitude level, keeping the phase angle between masses at minimum value, 2°. The spectral analysis was performed and the identified frequencies used as references.

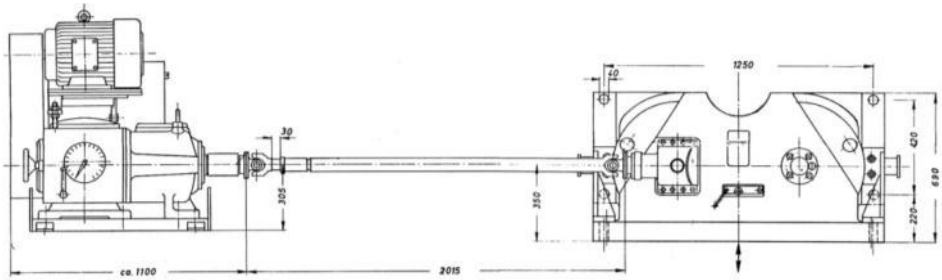

Figure 9 Scheme of vibrodyne Losenhausenwerk employed

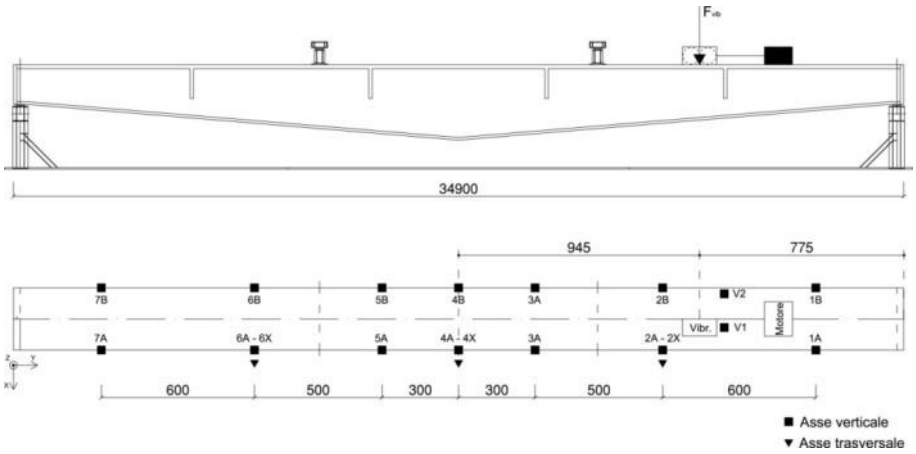

Figure 10 Vibrodyne test setup

5.5 Experimental tests

The results of the experimental modal analysis performed are here summarised. Both the free decay and the ambient vibration responses were analysed, the former by the ERA method and the latter using the CVA technique. Also the spectral analysis results of vibrodyne-tests responses are summarized.

For each beam a brief description the visual inspection rating and static tests results are provided. The test configurations are also depicted and modal analysis results presented. The results of the experimental modal analyses performed on the data collected from the ambient excitation and the hammer impact tests are compared. The averages of the modal characteristics are also reported and modal shapes identified are plotted.

5.5.1 Data processing

After a preliminary analysis of the spectral content, the signals acquired were pretreated by filtering out of the bandwidth [0 - 50 Hz], removing the trends and reducing sampling frequency to 200 Hz. Several modal identification sessions were performed.

Among all the available methods which can be employed to identify the modal parameters, it was decided to adopt two techniques working in the time domain due to the great spectral resolution they offer and their modal uncoupling capability. The Eigenvalue Realization Algorithm (ERA) was used to analyse the free decay responses, whilst ambient vibration signals called for a Stochastic Subspace Identification (SSI). A brief theoretical explanation of the selected methods has been provided in the Chapter 2.

Some tolerance criteria were adopted to discard computational modes, based on modal shape assurance coherence criterion (MAC) and fixing a maximum value of damping ratio. The chosen parameters are:

- MAC > 85%
- $0 \leq \zeta \leq 10\%$

A data cleansing process was further introduced in order to neglect those results which differed from the mean frequencies more than the computed standard deviation.

5.5.2 Beam B02

The state of the beam was healthy and there were not any evidences of damage or reinforcement corrosion. The same good state was observed on the slab. The test was executed on May 20th, 2011, measuring the beam vibration in its condition before the static load test.

Figure 11 Beam B02 placed on the test bench

Static test result

An initial loading - unloading cycle was performed up to 500 kN, then the load was increased until the ultimate state, reached at 1500 kN, when the beam collapsed. The failure was due to the overcoming of compressive strength of upper slab, in the span zone between the loads.

Sensors setup

Vibration tests were carried out using 12 uniaxial accelerometers, placed along the longitudinal axis of the beam, on the upper slab (Figure 12). The acquisition directions are:

- X direction: transversal direction
- Z direction: vertical direction

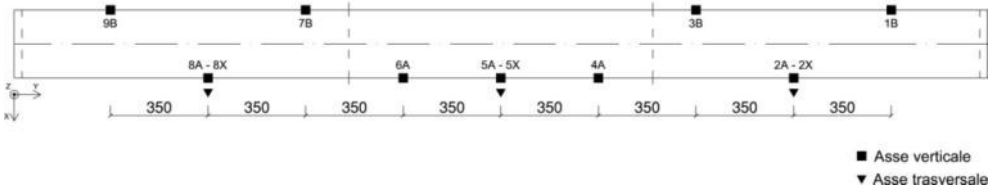

Figure 12 B02 vibration test setup

Figure 13 The beam collapsed after static test

Experimental modal analysis results

The following tables show the mean values and the standard deviations of the nine natural frequencies and damping ratios identified applying ERA and SSI methods. A qualitative description of the associated mode shapes, reported in Figure 15, is also furnished.

	f_i [Hz]		ζ [-]	
Mode	**μ**	**σ**	**μ**	**σ**
1 *(I flex or)*	2.839	0.023	0.021	0.008
2 *(I flex vert)*	4.234	0.018	0.014	0.002
3 *(II flex or)*	9.599	0.014	0.011	0.002
4 *(I torc)*	10.237	0.022	0.007	0.002
5 *(II flex vert)*	13.625	0.034	0.010	0.002
6 *(III flex or)*	17.662	0.062	0.018	0.005
7 *(III flex vert)*	28.044	0.110	0.022	0.003
8 *(I torc)*	33.432	0.050	0.016	0.002
9 *(IV flex vert)*	40.736	0.065	0.021	0.004

Table 4 B02: Experimental modal parameters (mean value and standard deviation) – SSI

	f_i [Hz]		ζ [-]	
Mode	**μ**	**σ**	**μ**	**σ**
1 *(I flex or)*	2.829	0.004	0.010	0.002
2 *(I flex vert)*	4.107	0.036	0.011	0.004
3 *(II flex or)*	9.264	0.110	0.015	0.011
4 *(I torc)*	10.131	0.034	0.015	0.004
5 *(II flex vert)*	13.516	0.019	0.010	0.001
6 *(III flex or)*	17.591	0.052	0.021	0.002
7 *(III flex vert)*	28.602	0.666	0.013	0.011
8 *(I torc)*	33.338	0.042	0.011	0.001
9 *(IV flex vert)*	41.369	0.510	0.007	0.005

Table 5 B02: Experimental modal parameters (mean value and standard deviation) - ERA

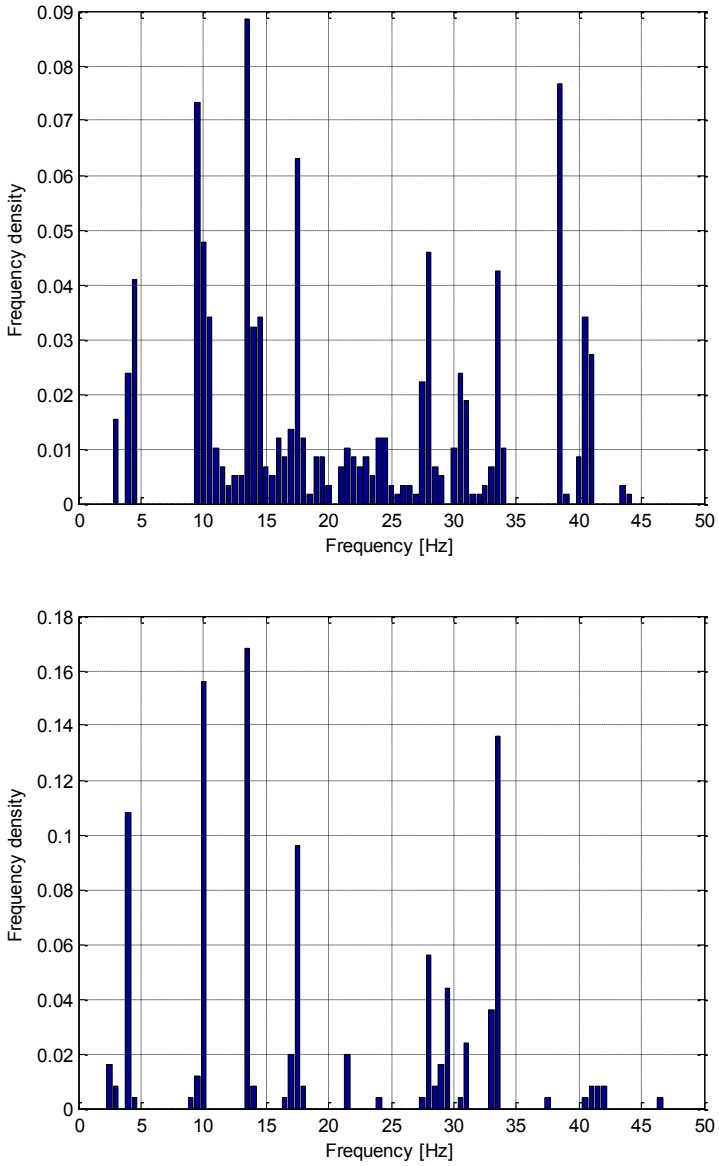

Figure 14 B02: Identified frequencies distribution: ambient vibration (a) and hammer impacts (b)

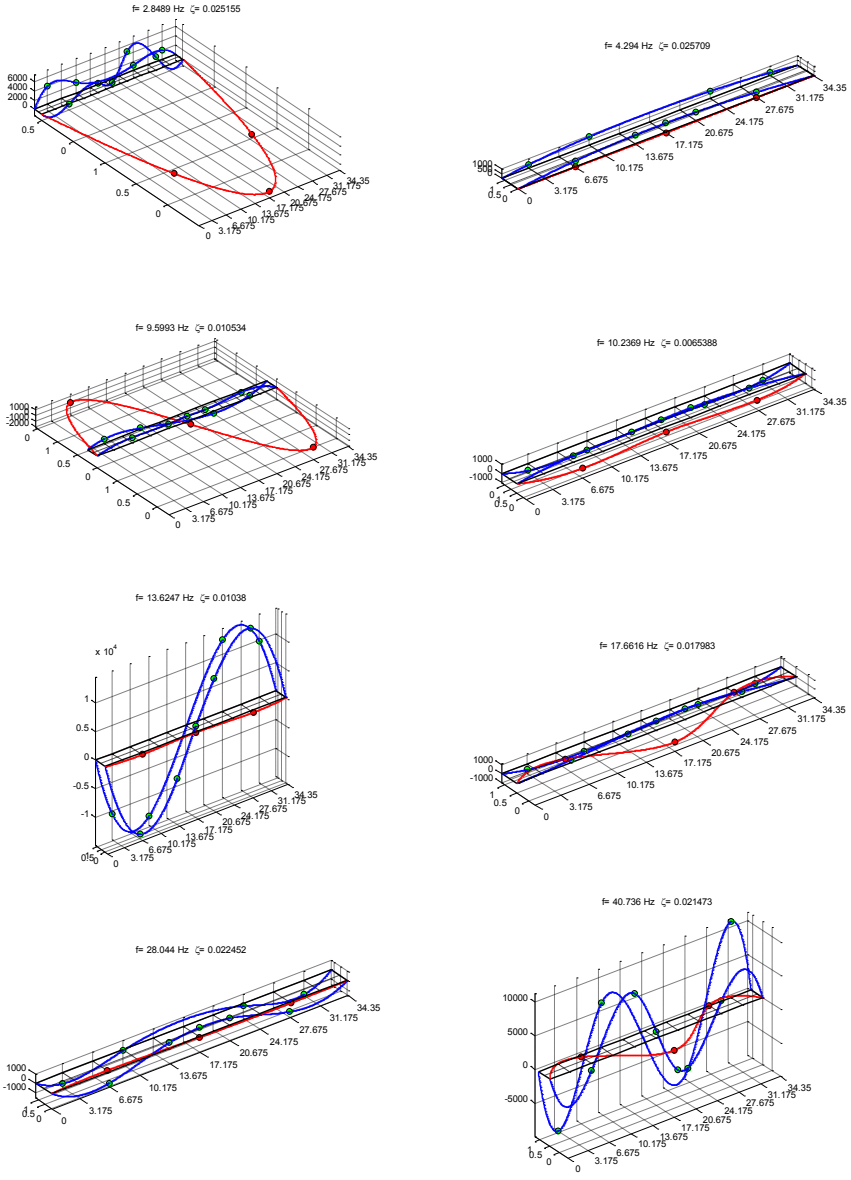

Figure 15 B02: experimental modal shape (ambient vibration)

5.5.3 Beam B03

The state of the beam was healthy and there were not any evidences of damage or reinforcement corrosion. The same good state was observed on the slab. The test was executed on May 27th 2011, measuring the beam vibrations respectively in its initial condition and immediately after the application of the maximum static load (corresponding to the beam ultimate limit state). In the former case, the collected data weren't acquired properly and then discarded. In the following only the experimental measurements on the beam in its ultimate limit state are analysed.

Figure 16 Beam B03 placed on the test bench

Static test result

A first loading - unloading cycle was performed up to 610 kN, than the load was increased until reaching the ultimate load, at 1560 kN. The failure was due to the overcoming of compressive strength of the upper slab, in the midspan. The quick release of the load

prevented to spread the failure to the rest of compress section of the slab, avoiding the full collapse of the beam.

Figure 17 View of the failure section on the upper slab

Sensors setup

Vibration tests were carried out using 13 uniaxial accelerometers, placed along the longitudinal axis of the beam, on the upper slab. The acquisition directions are:

- X direction: transversal direction
- Z direction: vertical direction

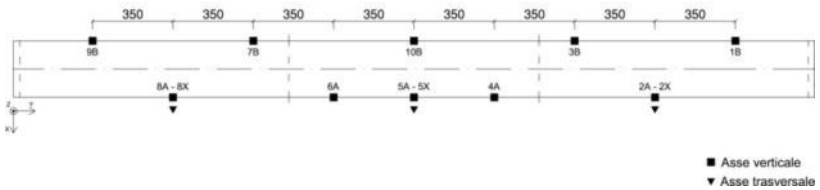

Figure 18 B03 vibration test setup

Experimental modal analysis results

The following tables show the mean values and the standard deviations of the nine natural frequencies and damping ratios identified applying ERA and SSI methods. A qualitative description of the associated mode shapes, reported in Figure 20, are also furnished. In the following the experimental measurements on the beam in its ultimate limit state are presented. The test have been performed only in AST configuration.

	f_i [Hz]		ζ [-]	
Mode	**μ**	**σ**	**μ**	**σ**
1 *(I flex or)*	2.578	0.002	0.013	0.005
2 *(I flex vert)*	3.729	0.057	0.046	0.005
3 *(I torc)*	6.391	0.082	0.021	0.008
4 *(II flex or)*	9.031	0.063	0.020	0.004
5 *(II flex vert)*	12.472	0.063	0.011	0.003
6 *(III flex or)*	16.585	0.112	0.013	0.001
7 *(III flex vert)*	24.226	0.073	0.018	0.005
8 (IV flex vert)	38.416	0.030	0.002	0.002
9 *(II torc)*	41.495	0.085	0.012	0.002

Table 6 B03: Experimental modal parameters (mean value and standard deviation) – SSI

	f_i [Hz]		ζ [-]	
Mode	**μ**	**σ**	**μ**	**σ**
1 *(I flex or)*	2.543	0.124	0.036	0.024
2 *(I flex vert)*	3.603	0.069	0.041	0.010
3 *(I torc)*	5.755	0.044	0.028	0.005
4 *(II flex or)*	8.985	0.110	0.013	0.005
5 *(II flex vert)*	12.461	0.036	0.012	0.003
6 *(III flex or)*	16.648	0.038	0.027	0.004
7 *(III flex vert)*	24.364	0.053	0.030	0.002
8 *(II torc)*	29.779	0.064	0.016	0.002
9 (IV flex vert)	36.005	0.131	0.027	0.003

Table 7 B03: Experimental modal parameters (mean value and standard deviation) - ERA

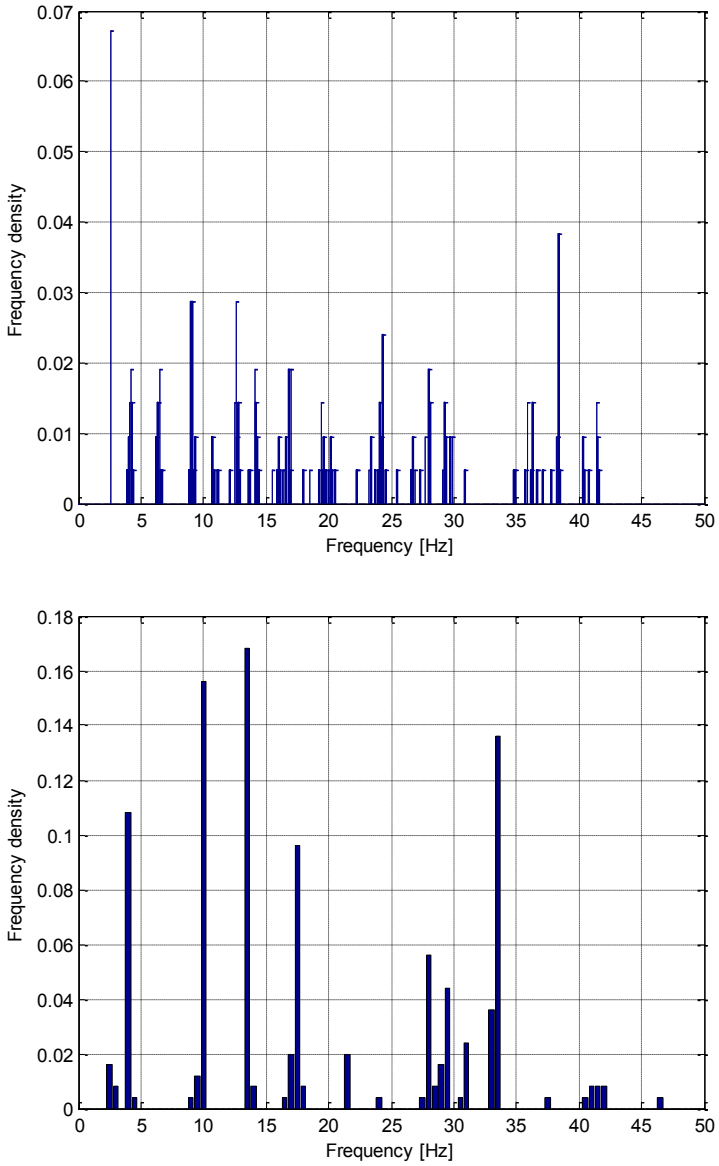

Figure 19 B03: Identified frequencies distribution: ambient vibration (a) and hammer impacts (b)

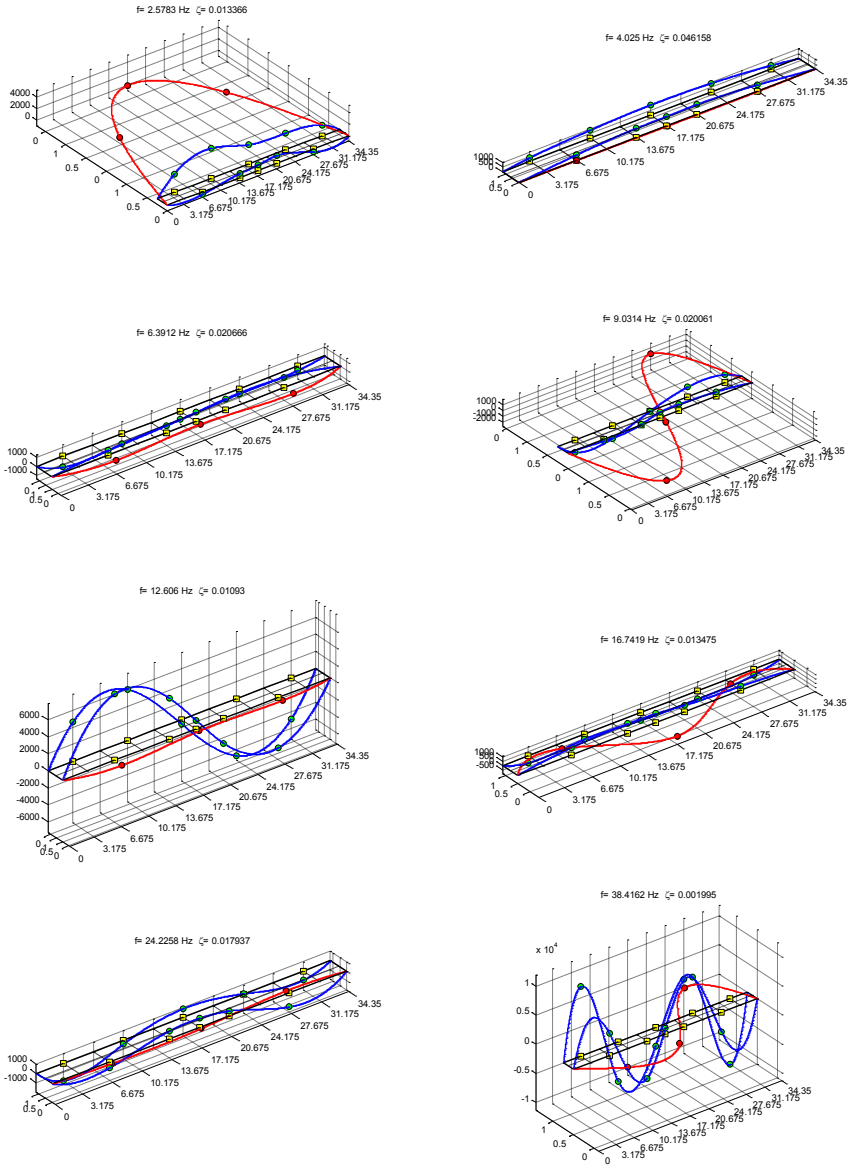

Figure 20 B03: experimental modal shape (ambient vibration)

5.5.4 Beam B04

The state of the beam was healthy and there were not any evidences of damage or reinforcement corrosion. The same good state was observed on the slab. The test was executed on June 16th, 2011, measuring the beam vibration respectively in its initial condition and after the application of a static cyclic load equal to 1000 kN, value corresponding to the 88% of the ultimate bearing capacity afterwards measured.

Figure 21 Beam B04 placed on the test bench

Static test result

An initial loading - unloading cycle was performed up to load of 1000 kN, than the load was increased until the ultimate state, reached at 1141 kN when the beam collapsed. The failure was due to the overcoming of compressive strength of upper slab, in the span zone between loads.

Figure 22 B04: views of collapsed beam

Sensors setup

Vibration tests were carried out using 19 uniaxial accelerometers, placed along the longitudinal axis of the beam, on the upper slab. The acquisition direction are:

- X direction: transversal direction
- Z direction: vertical direction

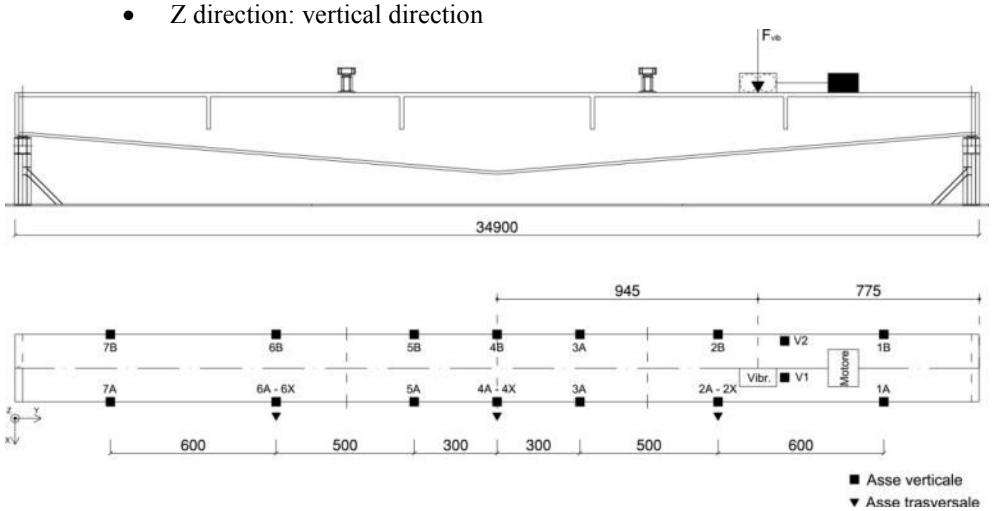

Figure 23 B04 vibration test setup

Experimental modal analysis results

BST campaign

The following tables show the mean values and the standard deviations of the nine natural frequencies and damping ratios identified applying ERA and SSI methods. A qualitative description of the associated mode shapes, reported in Figure 25, is also furnished. In the following, the experimental results of BST campaign are presented.

	f_i [Hz]		ζ [-]	
Mode	**μ**	**σ**	**μ**	**σ**
1 *(I flex or)*	2.786	0.010	0.007	0.003
2 *(I flex vert)*	4.015	0.008	0.005	0.001
3 *(I torc)*	8.903	0.013	0.009	0.000
4 *(II flex or)*	9.458	0.078	0.010	0.004
5 *(II flex vert)*	13.343	0.034	0.009	0.002
6 *(III flex or)*	16.860	0.041	0.011	0.002
7 *(III flex vert)*	28.921	0.140	0.018	0.004
8 *(II torc)*	-	-	-	-
9 *(IV flex vert)*	40.548	0.046	0.006	0.001

Table 8 B04: Experimental modal parameters (mean value and standard deviation) – SSI

	f_i [Hz]		ζ [-]	
Mode	**μ**	**σ**	**μ**	**σ**
1 *(I flex or)*	2.816	0.125	0.027	0.021
2 *(I flex vert)* (*)	5.893	0.037	0.076	0.005
3 *(I torc)*	8.899	0.252	0.031	0.006
4 *(II flex or)*	9.706	0.083	0.018	0.012
5 *(II flex vert)*	14.007	0.035	0.018	0.004
6 *(III flex or)*	17.074	0.055	0.024	0.004
7 *(III flex vert)*	28.701	0.092	0.026	0.002
8 *(II torc)*	-	-	-	-
9 (IV flex vert)	40.551	0.677	0.022	0.018
(*) Frequency not used in next analysis				

Table 9 B04: Experimental modal parameters (mean value and standard deviation) – ERA

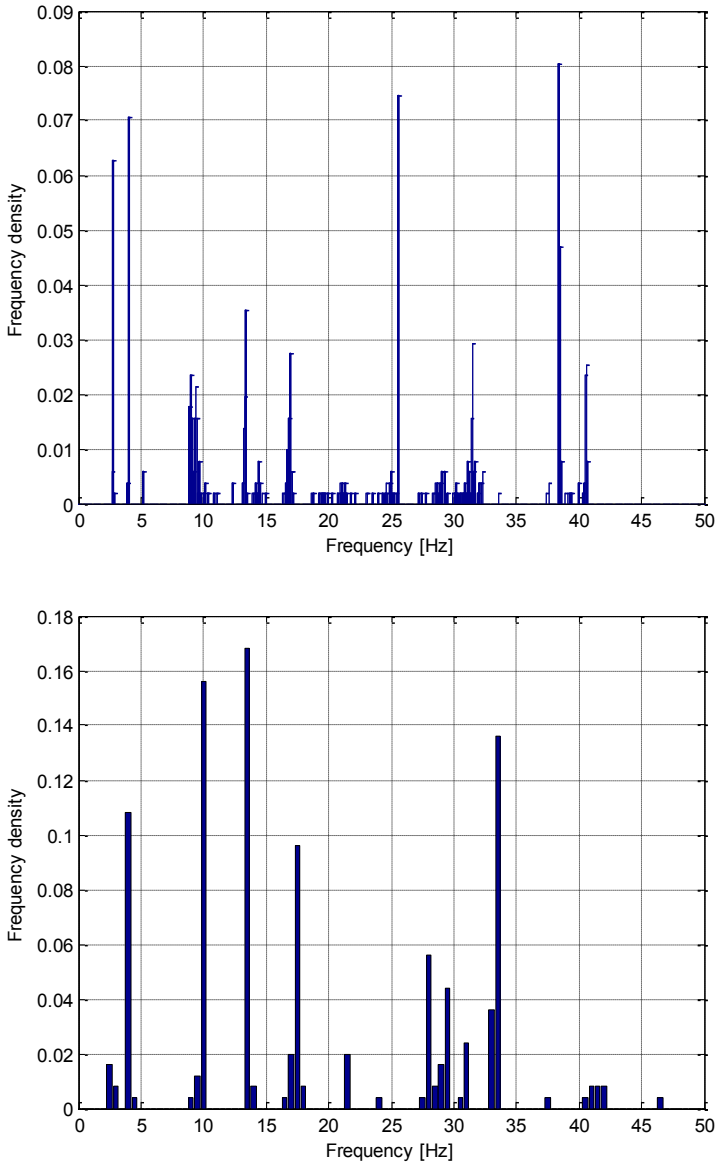

Figure 24 B04: Identified frequencies distribution: ambient vibration (a) and hammer impacts (b)

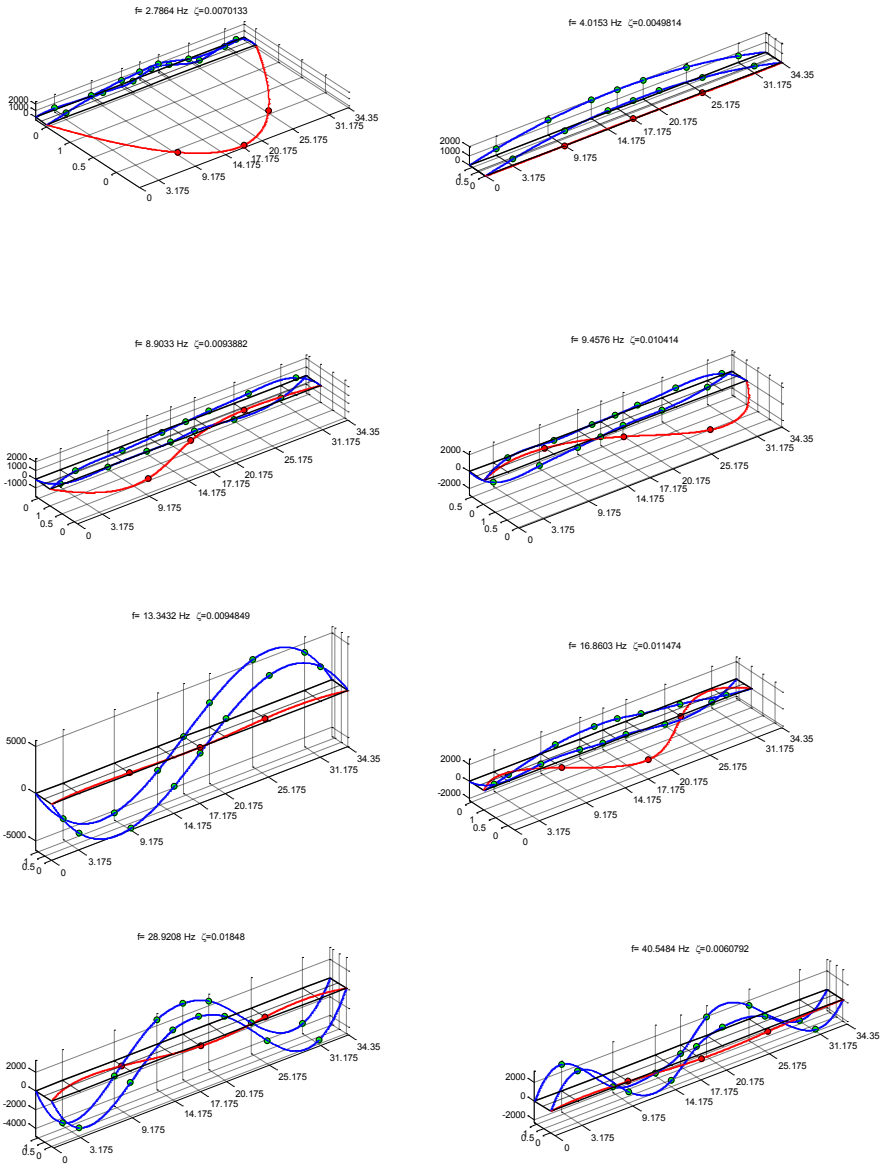

Figure 25 B04: experimental modal shape (ambient vibration)

AST campaign

The following tables and figures report the results of modal analysis performed on the vibration measurements acquired on the beam after the first loading – unloading cycle (P_{max}= 1000 kN, 88% of the ultimate load reached).

	f_i [Hz]		ζ [-]	
Mode	**μ**	**σ**	**μ**	**σ**
1 *(I flex or)*	2.746	0.022	0.004	0.000
2 *(I flex vert)*	3.853	0.001	0.019	0.002
4 *(II flex or)*	9.109	0.018	0.018	0.003
3 *(I torc)*	9.922	0.090	0.028	0.009
5 *(II flex vert)*	12.962	0.054	0.012	0.002
6 *(III flec or)*	16.890	0.064	0.016	0.002
7 *(III flex vert)*	24.613	0.312	0.017	0.004
7b *(III flex vert)*	29.272	0.078	0.011	0.002
8 *(I torc)*	32.422	0.194	0.014	0.003
9 (IV flex vert)	38.715	0.041	0.014	0.005

Table 10 B04: Experimental modal parameters (mean value and standard deviation) – SSI

	f_i [Hz]		ζ [-]	
Mode	**μ**	**σ**	**μ**	**σ**
1 *(I flex or)*	2.709	0.127	0.029	0.036
2 *(I flex vert)*	3.886	0.028	0.033	0.009
4 *(II flex or)*	8.800	0.063	0.024	0.007
3 *(I torc)*	9.611	0.071	0.018	0.008
5 *(II flex vert)*	12.859	0.040	0.012	0.002
6 *(III flec or)*	16.950	0.077	0.020	0.004
7 *(III flex vert)*	24.702	0.110	0.013	0.005
7b *(III flex vert)*	28.623	0.134	0.019	0.002
8 *(I torc)*	32.145	0.055	0.018	0.001
9 (IV flex vert)	39.143	0.171	0.027	0.005

Table 11 B04: Experimental modal parameters (mean value and standard deviation) – ERA

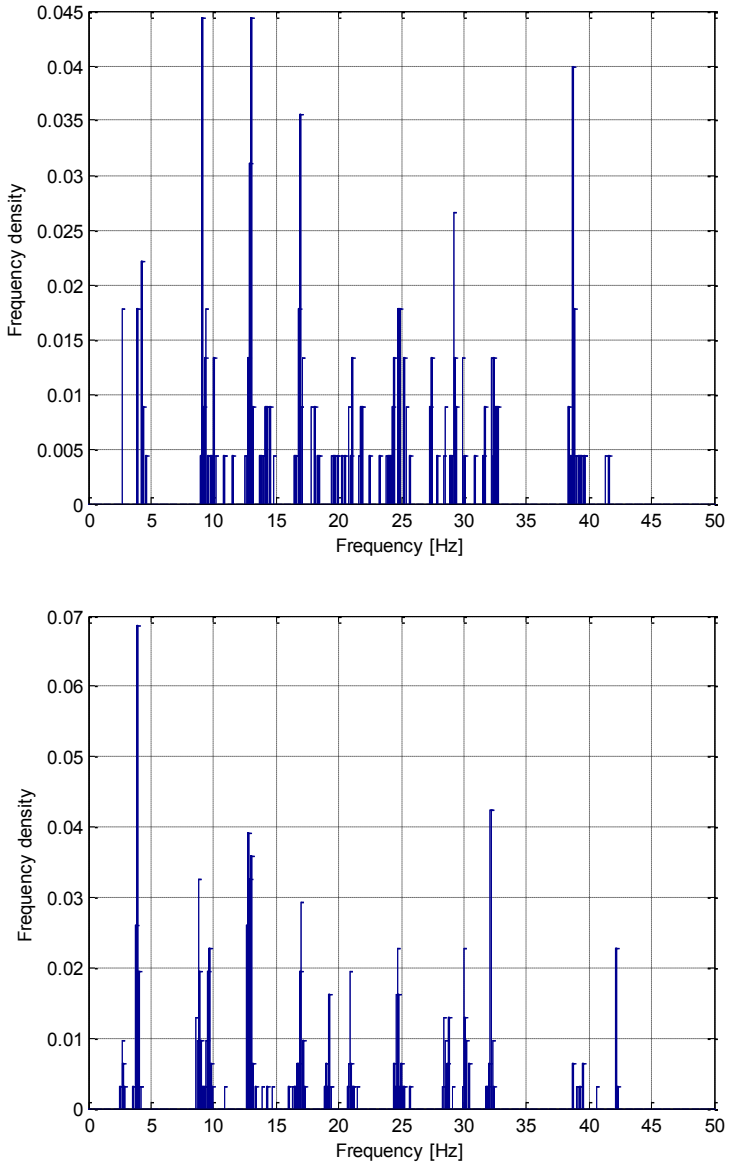

Figure 26 B04: Identified frequencies distribution: ambient vibration (a) and hammer impacts (b)

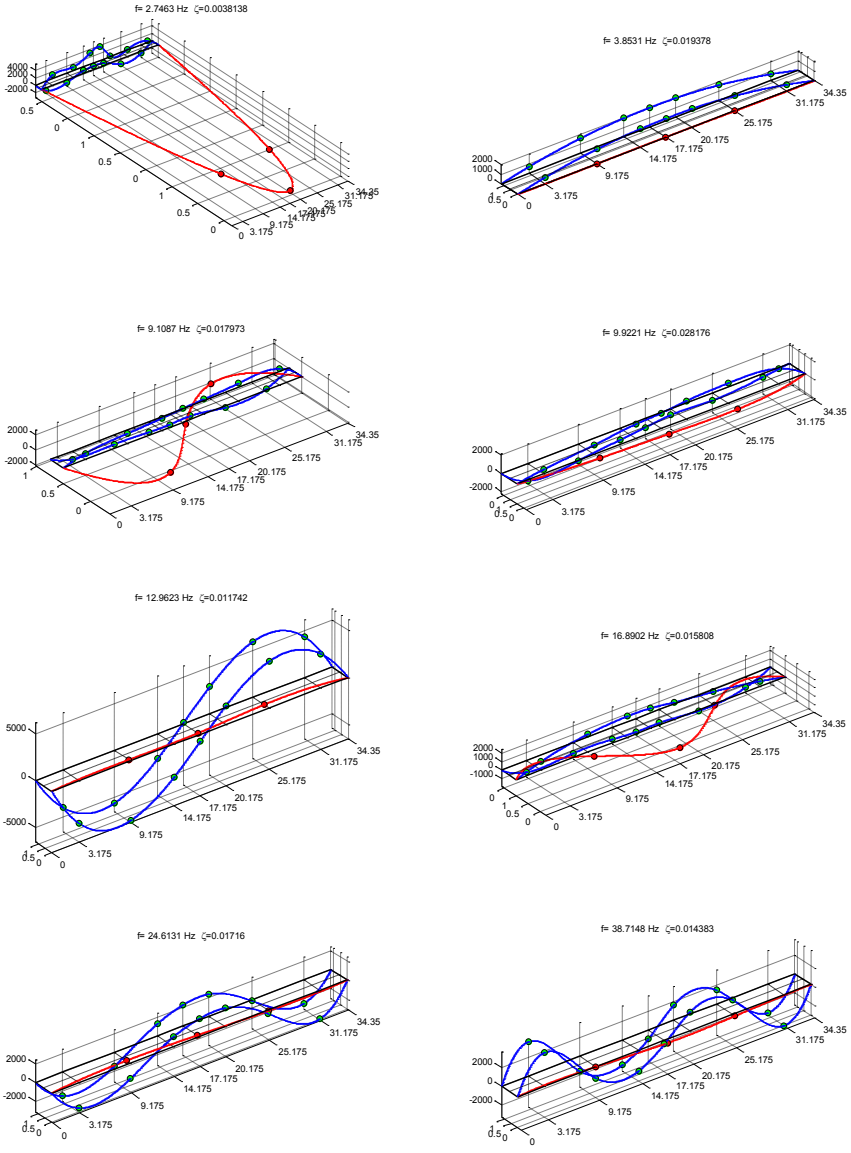

Figure 27 B04: experimental modal shape (ambient vibration)

5.5.5 Beam B05

The state of the beam was medium degraded and there were not evidences of important damage or reinforcement corrosion. A good state was observed on the slab. The tests were executed on June 23th and 26th, 2011, measuring the beam vibration respectively in its initial condition and immediately after the application of the ultimate static load equal to 1320 kN.

Figure 28 Beam B05: view of the beam on the bench test

Figure 29 Beam B05: the vibrodyne placed on the slab

Static test result

An initial loading - unloading cycle was performed up to 610 kN. A second loading cycle was performed up to 1150 kN. In the third cycle, the load increased up to 1320 kN. The failure was due to the overcoming of compressive strength of upper slab in the midspan (Figure 30).

Figure 30 B04: view of the slab in the failure section

Sensors setup

Vibration tests were carried out using 19 uniaxial accelerometers, placed along the longitudinal axis of the beam, on the upper slab. The acquisition direction are:

- X direction: transversal direction
- Z direction: vertical direction

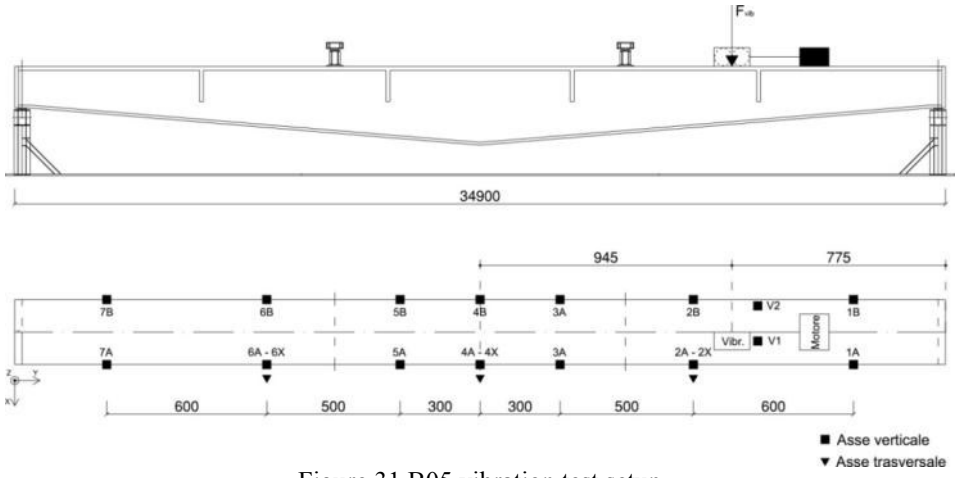

Figure 31 B05 vibration test setup

Experimental modal analysis results

BST campaign

The following tables show the mean values and the standard deviations of the nine natural frequencies and damping ratios identified applying ERA and SSI methods. A qualitative descriptions of the associated mode shapes, reported in Figure 32, is also furnished. In the following, the experimental results of BST campaign are presented.

	f_i [Hz]		ζ [-]	
Mode	**μ**	**σ**	**μ**	**σ**
1 *(I flex or)*	2.851	0.002	0.008	0.007
2 *(I flex vert)* (*)	4.955	0.035	0.032	0.009
4 *(II flex or)*	9.232	0.033	0.011	0.003
3 *(I torc)*	9.743	0.032	0.013	0.002
5 *(II flex vert)*	13.646	0.017	0.014	0.004
6 *(III flex or)*	17.125	0.082	0.014	0.003
7 *(III flex vert)*	27.689	0.085	0.015	0.002
8 *(II torc)*	34.216	0.125	0.010	0.002
9 (IV flex vert)	40.349	0.085	0.028	0.004
(*) Corrupted frequency. Not used in next analysis				

Table 12 B05: Experimental modal parameters (mean value and standard deviation) – SSI

	f_i [Hz]		ζ [-]	
Mode	**μ**	**σ**	**μ**	**σ**
1 *(I flex or)*	2.857	0.216	0.028	0.025
2 *(I flex vert)*	4.191	0.0122	0.018	0.005
4 *(II flex or)*	8.916	0.081	0.020	0.009
3 *(I torc)*	9.517	0.074	0.019	0.008
5 *(II flex vert)*	13.621	0.012	0.017	0.001
6 *(III flex or)*	16.712	0.152	0.018	0.007
7 *(III flex vert)*	28.612	0.045	0.009	0.001
8 *(II torc)*	33.971	0.038	0.016	0.001
9 (IV flex vert)	40.714	1.029	0.015	0.004

Table 13 B05: Experimental modal parameters (mean value and standard deviation) – ERA

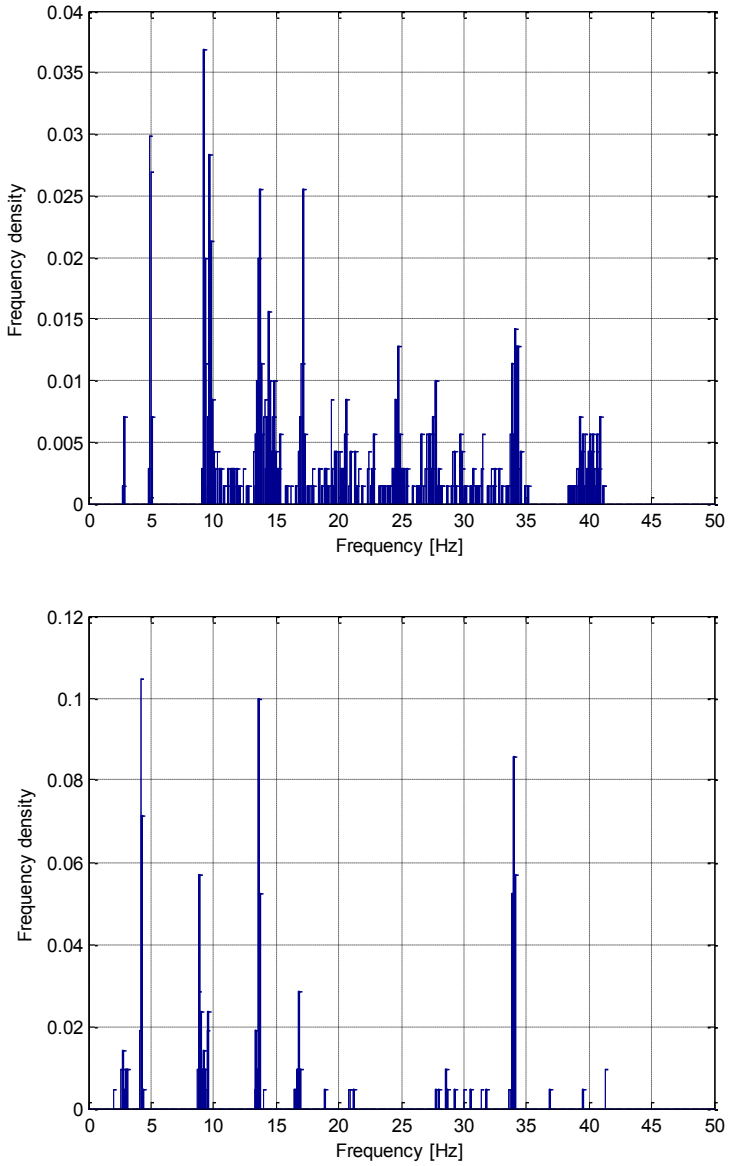

Figure 32 B05: Identified frequencies distribution: ambient vibration (a) and hammer impacts (b)

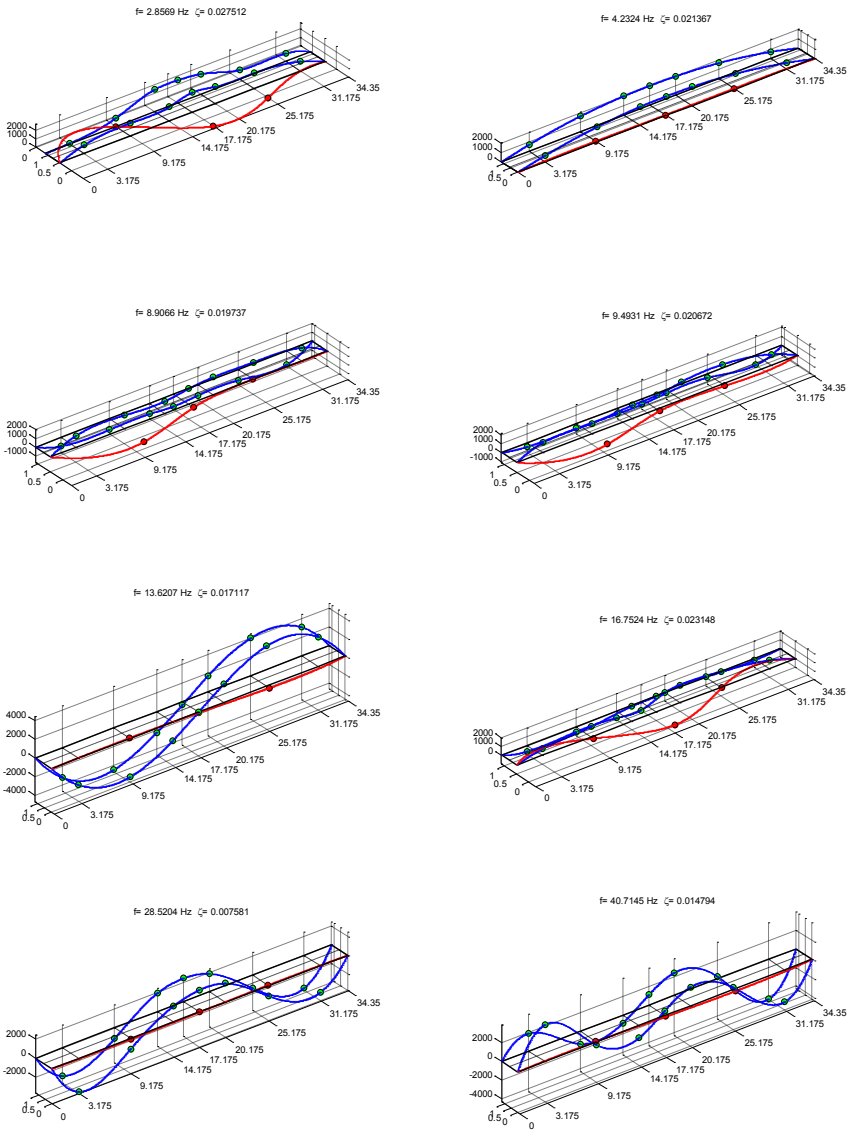

Figure 33 B05: experimental modal shape (free decay vibration)

AST campaign

The following tables and figures report the results of modal analysis performed on the vibration measurements acquired on the beam after the last loading – unloading cycle (P_u= 1320 kN, ultimate load reached).

	f_i [Hz]		ζ [-]	
Mode	**μ**	**σ**	**μ**	**σ**
1 *(I flex or)*	2.721	0.022	0.020	0.016
2 *(I flex vert)* (*)	4.768	0.054	0.031	0.007
4 *(II flex or)*	9.107	0.067	0.013	0.004
3 *(I torc)*	9.705	0.034	0.019	0.003
5 *(II flex vert)*	12.969	0.037	0.011	0.002
6 *(III flex or)*	16.815	0.207	0.017	0.006
7 *(III flex vert)*	24.454	0.054	0.017	0.003
8 *(II torc)*	31.985	0.219	0.020	0.004
9 (IV flex vert)	39.484	0.167	0.021	0.003
(*) Corrupted frequency. Not used in next analysis				

Table 14 B05: Experimental modal parameters (mean value and standard deviation) – SSI

	f_i [Hz]		ζ [-]	
Mode	**μ**	**σ**	**μ**	**σ**
1 *(I flex or)*	2.399	0.326	0.020	0.021
2 *(I flex vert)*	4.006	0.037	0.037	0.005
4 *(II flex or)*	8.769	0.103	0.016	0.006
3 *(I torc)*	9.077	0.094	0.016	0.008
5 *(II flex vert)*	12.882	0.015	0.011	0.001
6 *(III flex or)*	17.545	0.096	0.030	0.004
7 *(III flex vert)*	24.496	0.051	0.017	0.002
8 *(I torc)*	32.080	0.029	0.014	0.001
9 (IV flex vert)	38.871	0.628	0.023	0.007

Table 15 B05: Experimental modal parameters (mean value and standard deviation) – ERA

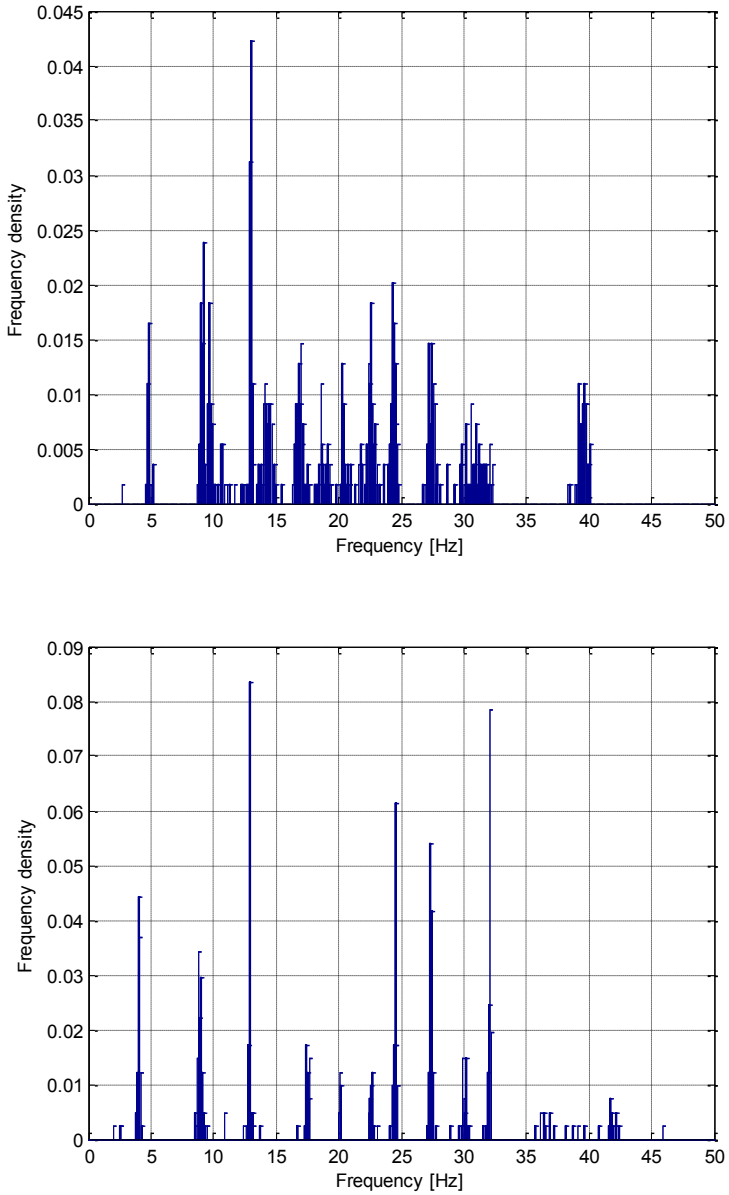

Figure 34 B05: Identified frequencies distribution: ambient vibration (a) and hammer impacts (b)

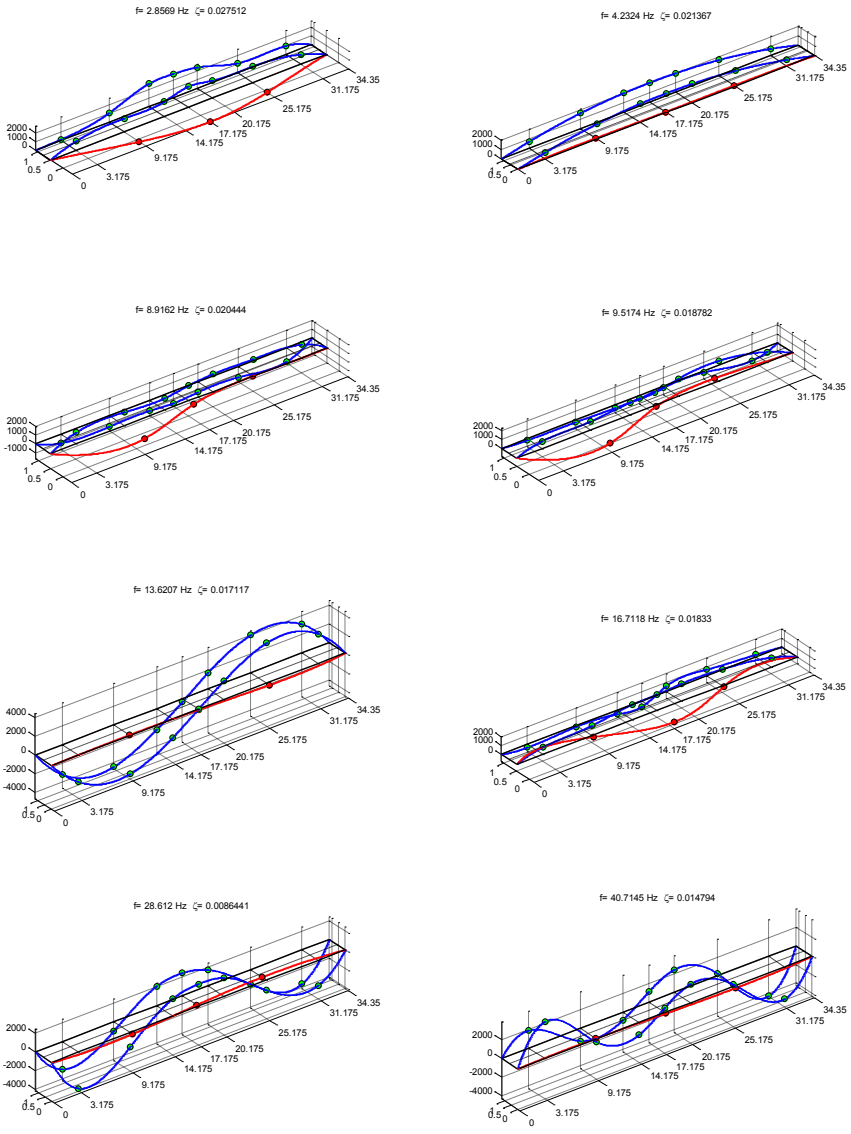

Figure 35 B05: experimental modal shape (ambient vibration)

5.5.6 Beam B07

The beam was in bad conditions, caused by a widespread corrosion in the longitudinal and transversal ordinary reinforcement, particularly near the surface in the east side of the beam, and marked corrosion of tendons in the lower flange. The deterioration was located near the point of application of the loads and it was more extended in east side of the beam. Here some strands sections were partially reduced by the corrosion and the surrounding concrete showed deep longitudinal cracks (Figure 36, Figure 37). Some relevant damage were observed on the slab (Figure 39).

The beam was originally placed on external side of the deck, and the most damage occurred on the side most exposed to the deteriorating factors. Furthermore, important damages have been observed in the sections next to the drainpipes (Figure 38): it clearly demonstrate how errors in the design and the lack of care in details can affect the durability of a structure.

Figure 36 Beam B07: view of the beam on the bench test (east side, the most degraded)

Figure 37 East side of B07: corroded ordinary reinforcement and tendons

Figure 38 B07: post-tensioned and ordinary reinforcements corroded (east side)

Figure 39 B07: localized damages on the slab and a view of the failure section

Static test result

An initial loading - unloading cycle was performed up to 370 kN, than the load was increased until the ultimate state, reached at 537 kN. due to the progressive failure of prestressed and ordinary transverse reinforcement placed in the most corroded area, with the formation of a large vertical crack and some cracks parallel to the cables in the failure area.

Sensors setup

Vibration tests were carried out using 17 uniaxial accelerometers, placed along the longitudinal axis of the beam, on the upper slab. The acquisition direction are:

- X direction: transversal direction
- Z direction: vertical direction

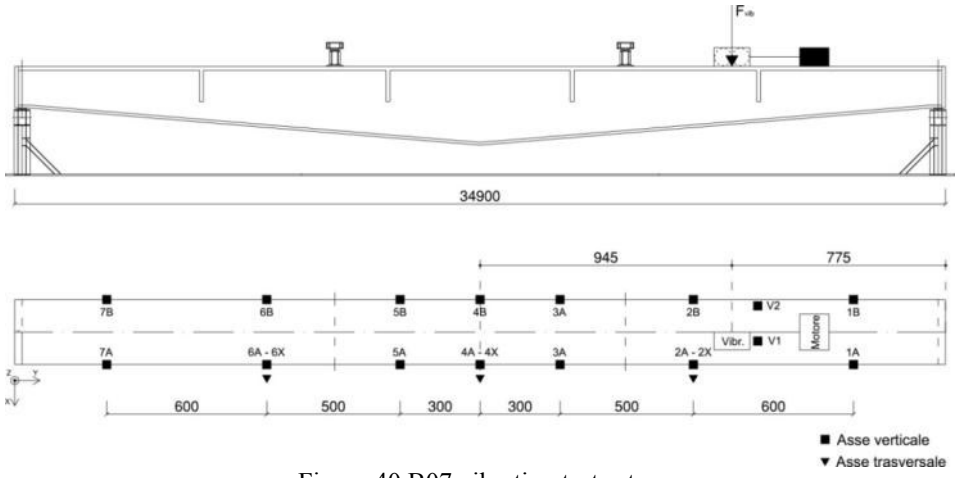

Figure 40 B07 vibration test setup

Experimental modal analysis results

BST campaign

The following tables show the mean values and the standard deviations of the nine natural frequencies and damping ratios identified applying ERA and SSI methods. A qualitative description of the associated mode shapes, reported in **Errore. L'origine riferimento non è stata trovata.**, is also furnished. In the following, the experimental results of BST campaign are presented.

	f_i [Hz]		ζ [-]	
Mode	**μ**	**σ**	**μ**	**σ**
1 *(I flex or)*	2.747	0.024	0.042	0.021
2 *(I flex vert)* (*)	3.960	0.007	0.010	0.003
4 *(II flex or)*	9.175	0.042	0.015	0.001
3 *(I torc)*	9.794	0.032	0.007	0.002
5 *(II flex vert)*	12.933	0.045	0.017	0.002
6 *(III flex or)*	17.032	0.095	0.018	0.003
7 *(III flex vert)*	26.264	0.127	0.018	0.002
8 *(II torc)*	33.634	0.346	0.020	0.004
9 (IV flex vert)	40.277	0.052	0.020	0.002

Table 16 B07: Experimental modal parameters (mean value and standard deviation) – SSI

	f_i [Hz]		ζ [-]	
Mode	**μ**	**σ**	**μ**	**σ**
1 *(I flex or)*	2.716	0.107	0.031	0.020
2 *(I flex vert)*	4.008	0.029	0.008	0.004
4 *(II flex or)*	8.865	0.021	0.021	0.002
3 *(I torc)*	9.767	0.041	0.011	0.002
5 *(II flex vert)*	13.155	0.038	0.019	0.002
6 *(III flex or)*	17.050	0.044	0.032	0.004
7 *(III flex vert)*	26.096	0.042	0.023	0.001
8 *(II torc)*	32.929	0.069	0.021	0.004
9 (IV flex vert)	40.385	0.263	0.020	0.003

Table 17 B07: Experimental modal parameters (mean value and standard deviation) – ERA

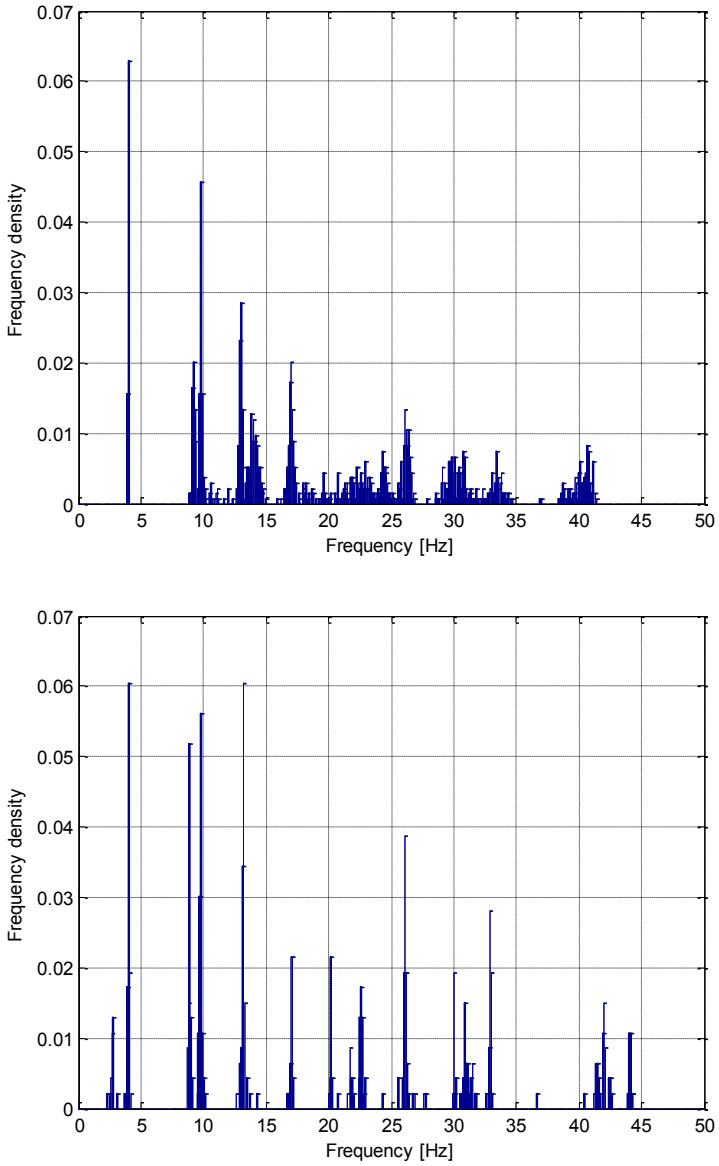

Figure 41 B07: Identified frequencies distribution: ambient vibration (a) and hammer impacts (b)

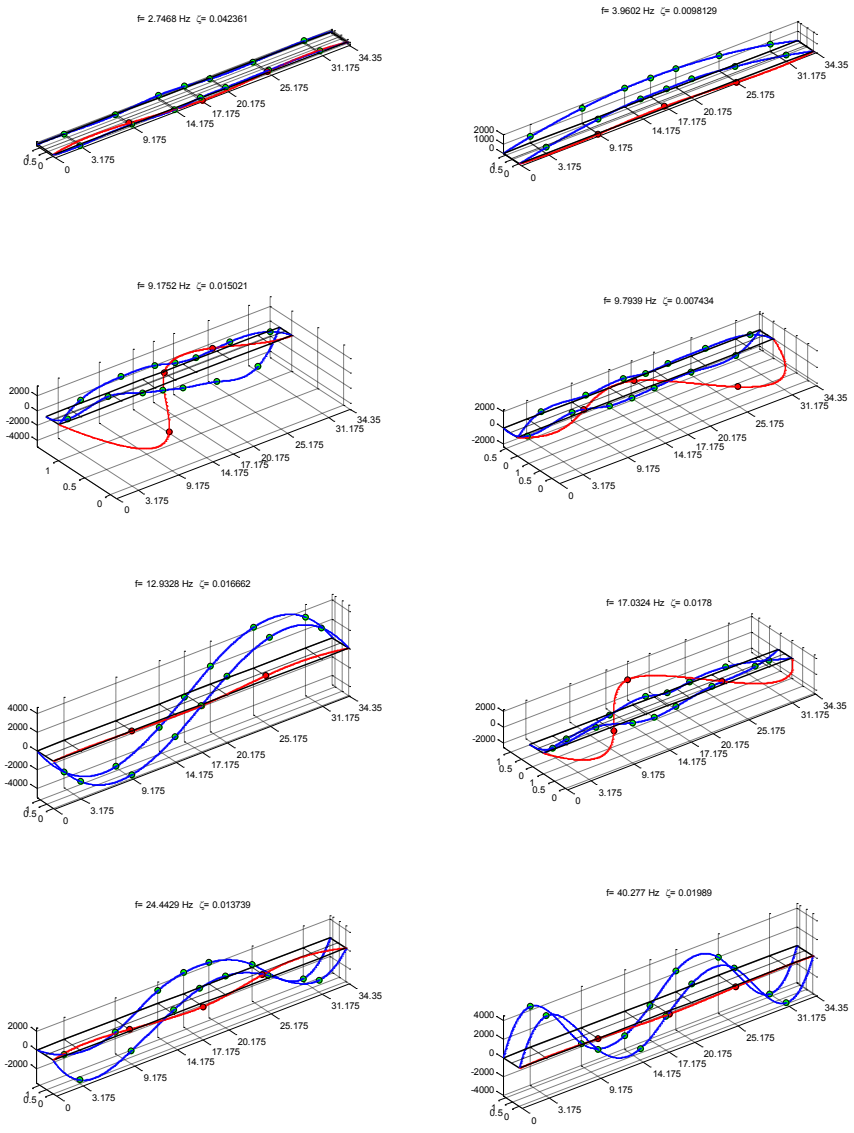

Figure 42 B07: experimental modal shape (free decay vibration)

5.6 Discussion of the experimental results

The variation of the modal parameters is one of the most clear indicator of occurring variations in the structural behaviour and it's widely used in damage detection techniques and structural health monitoring, as described in Ch. 2. In facts, the modal parameters describe the dynamic response of a structure and, since they are directly connected to its physical characteristics (mass, stiffness, damping), they are directly influenced by their variations. In particular, the easiness of extraction along with the physically tangible relation between their changes and the changes in the stiffness and mass of a structure, natural frequencies have been mainly used as damage detectors [1], [2], [3].

In the next paragraphs, the comparison of modal parameters identified from vibration measurements acquired before and after the static tests is reported. Furthermore, the connection between the deterioration levels (expressed in terms of ultimate bearing moment) and the identified modal parameters is highlighted.

5.6.1 Changes in modal parameters due to the application of the ultimate load

In Figure 43 the comparisons between the values of modal frequencies of the four bending modes identified in the initial conditions and post-rupture (beam B05) and in the intermediate state (beam B04) are depicted. The measured percentage change varies between 3% and 14%

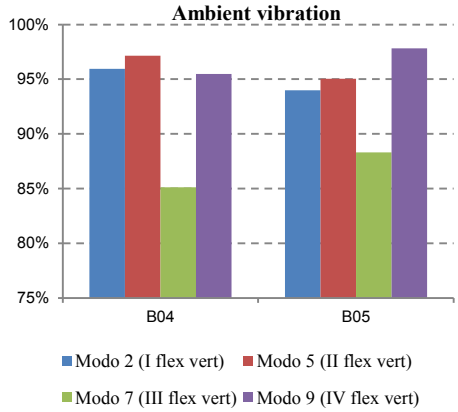

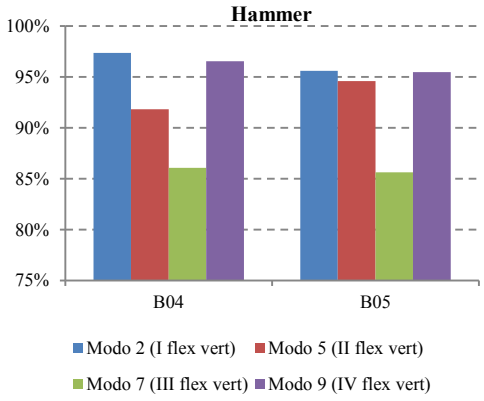

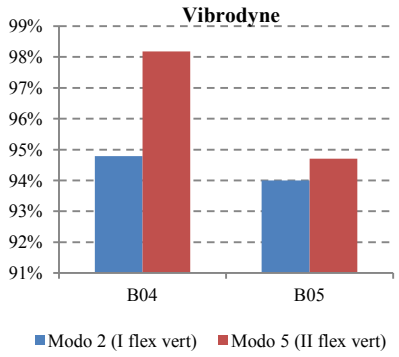

	B04 (*)			B05		
	SSI	***ERA***	***VIB.***	***SSI***	***ERA***	***VIBR.***
I flex	0.96	0.97	0.95	0.94	0.96	0.94
II flex	0.97	0.92	-	0.95	0.95	-
III flex	0.85	0.86	-	0.88	0.86	-
IV flex	0.95	0.97	0.98	0.98	0.95	0.95

B04 (*) tests performed after a maximum load P=0.88 P_u

Figure 43 Comparison between bending modal frequencies identified in vibration test performed before and after ultimate load application

As reported in the former paragraphs, all the tested beams showed a fragile failure mechanism. The beams B02, B04 and B05 showed mostly brittle failure due to the crushing

of the upper slabs whereas in the case of the beam B07, failure has been caused by the rupture of the corroded reinforcement.

The magnitude of the observed changes in modal frequencies may be related to the type of failure mechanism exhibited during the static tests. In facts, a fragile failure mechanism requires a low ductility demand to ordinary and post-tensioning reinforcement and, consequently, small permanent deformations.

The dynamic tests have been performed after the unloading of the structure. We can reasonably imagine that the residual prestressing forces re-closed the most of the concrete cracks propagating during the loading phase, raising in small variation of the stiffness and, consequently, of the modal frequencies.

Beam	Classification	Pu [kN]	Midspan Mu [kNm]
B02	Intermediate	1503	21683
B03	Good	1295	19244
B04	Good	1141	17439
B05	Intermediate	1225	18423
B07	Bad	536	10345

Table 18 Classification and ultimate loads and bending moments in midspan section

5.6.2 Influence of deterioration on the modal parameters

The following graphs show the variation of the first four bending modes as a function of the ultimate bending moments in the midspan section.

Figure 45 and Figure 46 highlight a correlation between the dynamic characteristics of the beams and the ultimate bending strengths. Both static and dynamic tests showed the different evolution in time of the beams after 50 years in service, the former in terms of residual load-bearing capacity, the latter in terms of changes in modal frequencies.

The following figures show the variation of the first four bending modes as a function of the ultimate bending strength in the midspan section, used as a global symptom of deterioration level. The results of the analysis, reported, indicate a correlation between the dynamic characteristics of the beams and the ultimate bending strength. The ultimate bending strength and the dynamic behaviour of the beams are both influenced by the evolution of deterioration developed during the years in service. The velocity of deterioration in the bridge beams is strongly influenced by the position occupied in the deck. The edge beams are more exposed to aggressive corrosive stressors and to higher cyclical loads than the central beams. Both static and dynamic tests showed the different evolution in time of the beams after 50 years in service, the former in terms of residual load-bearing capacity, the

latter in terms of changes in modal frequencies. The following diagrams show the frequencies as a function of residual load-bearing capacity.

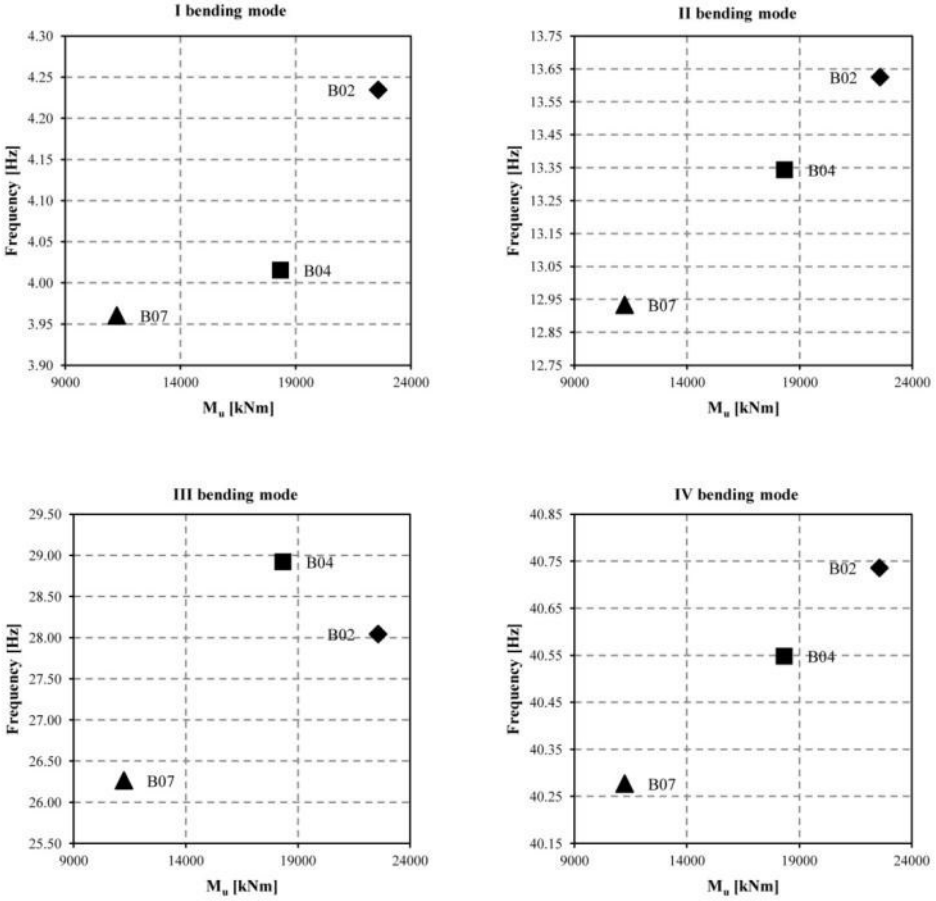

Figure 44 Identified bending modal frequencies identified - ambient vibration test performed in BST condition

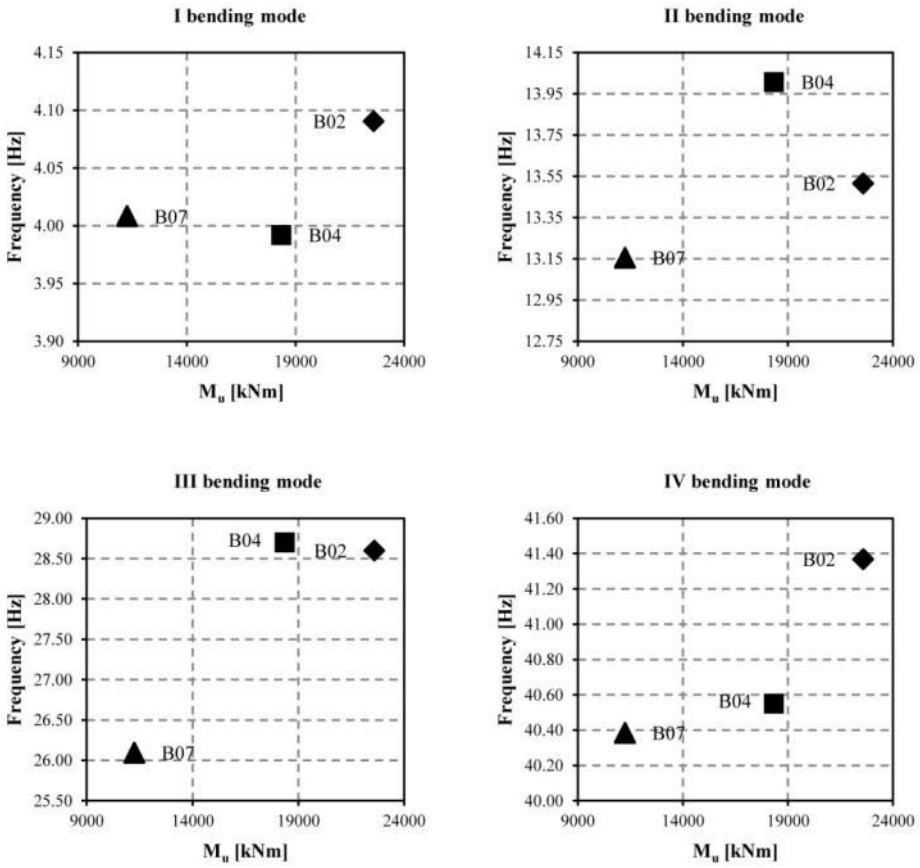

Figure 45 Identified bending modal frequencies identified - impact vibration test performed BST condition

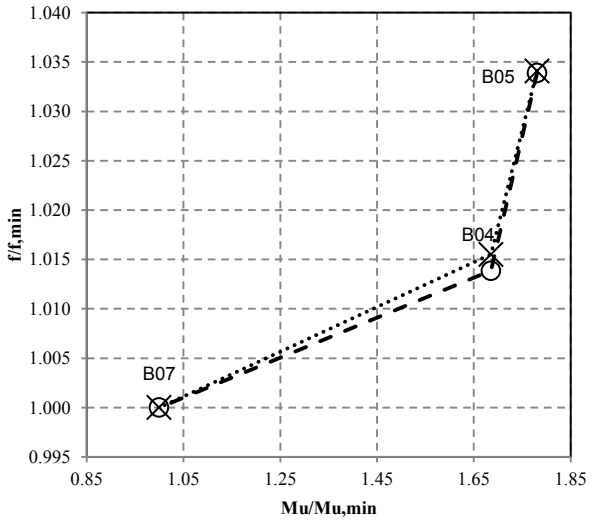

Figure 46 Normalized 1st (circle) and 2nd (cross) modal frequencies vs normalized ultimate bending strength in forced sinusoidal vibration tests

The ultimate bending strength and the modal parameters are both influenced by the different levels of deterioration of the beams. These differences can be mainly attributed to the different position occupied in the deck. Indeed, the edge beams usually undergo higher stress levels and are more exposed to deterioration factors, as weather, chemical attacks of chlorides contained in de-icing salts and pollutants emitted by vehicle traffic. An important role was also played by the lack of care in the design of the non-structural details. This phenomenon is pointed out by the behavior of beam B07 (Fig. 46). The residual bending strength has been possibly affected by the localized damage induced in the section next to the drainpipes, as indicating by the different failure behavior. The beams B02, B04 and B05 showed mostly brittle failure due to the crushing of the upper slabs whereas in the case of the beam B07, failure has been caused by the rupture of the corroded reinforcement.

The changes in the modal parameters after the application of the maximum static load show how the failure mechanism affects the dynamic behavior of the structure. In facts, the beams that had a moderate and reliable damage condition due to an uniform deterioration attack, resulting in an higher flexural strength, showed a higher decrease of flexural frequencies, as resulting in Fig. 48. It could be explained by the increasing of permanent strains in the prestressing reinforcement due to the higher ultimate load. The wider residual cracks pattern and the reduction of the stiffness caused the greater lowering of modal frequencies than in the case of beams having local damages.

Figure 47 Beam B07: corrosion of the post-tensioned tendons and ordinary reinforcement. The deterioration is particularly advanced in the sections next to the drainpipes

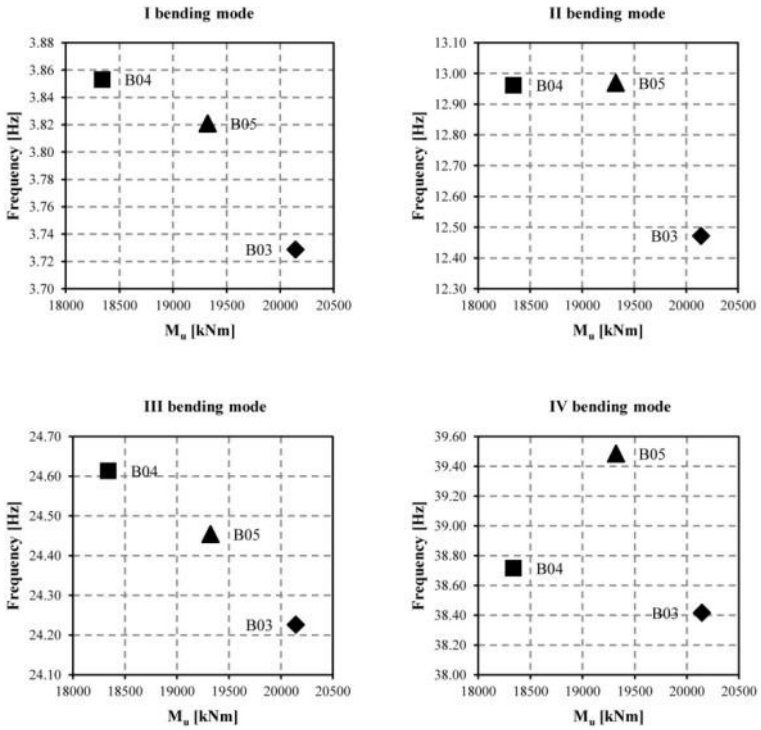

Figure 48 Bending modal frequencies identified in hammer vibration tests performed after static tests

5.7 Assessment of load bearing capacity evolution

5.7.1 Time-variant resistance

In this work, the simplified resistance degradation function proposed by Enright and Frangopol [5] for concrete bridge beams under corrosion is adopted. The time-variant resistance of a structural member with respect to a given failure mode can be expressed as the product of the initial resistance and a resistance degradation function:

$$R(t) = R_0 \cdot g(t), \tag{1}$$

where R(t) is the resistance at the generic time t, R_0 is the resistance at t = 0 and g(t) is a resistance degradation function (i.e. fraction of initial resistance of member remaining at time t).

Figure 49 shows the four mean profiles associated with different failure modes and degradation rate. Degradation cases "a" and "b" are associated with the assumptions of medium and high moment resistance degradation, respectively, and cases "c" and "d" are associated with the assumptions of medium and high shear resistance degradation.

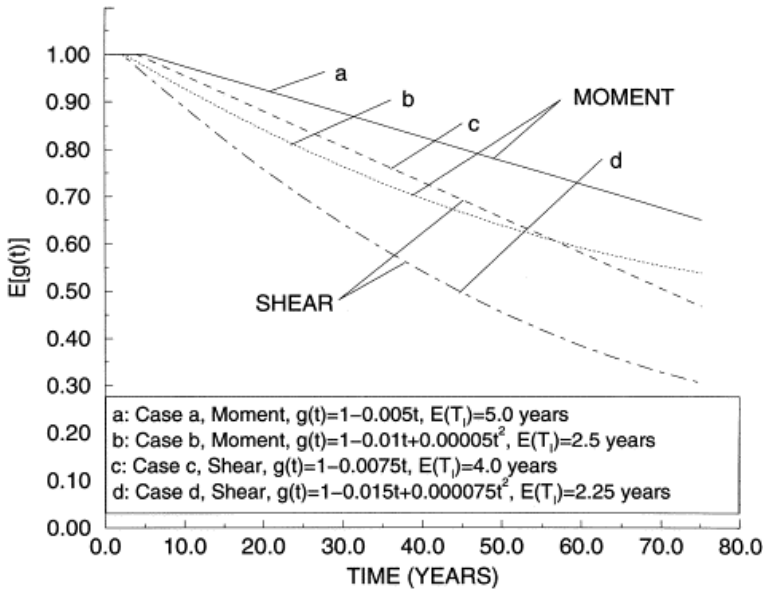

Figure 49 Mean resistance degradation function for cases a –d [5]

Assuming a bi-linear profile (case "a") due to a bending moment failure type as the test under consideration, the degradation profiles of tested beams can be estimated. They are based on the parameters suggested in literature [5]; they become the base for the assumptions for the experimental test data. In fact in Eq. 2, t_I is the time of damage initiation, assumed equal to 5 years for each beam, and k is the degradation rate, evaluated by means of the experimental tests results.

$$\begin{cases} 1 & t \le t_I \\ g(t) = 1 - k \cdot t & t > t_I \end{cases} \qquad t_I = 5 \text{ years}, \qquad k = \frac{1 - M_{R,50} / M_{Rm}}{50 - t_I} . \quad (2)$$

Beam	k
B01	0.0119
B02	0.0013
B03	0.0035
B04	0.0052
B05	0.0043
B06	0.0110
B07	0.0118
B08	0.0083
B09	0.0084

Table 19 Resistance degradation rates k

Table 19 shows the estimated resistance degradation rates of the tested beams. As stressed before, the failure modes of beams B02, B03, B04 and B05 were equal, and therefore their structural responses can be considered as representative of beams showing a moderate and reliable damage condition due to an uniform deterioration attack. On the contrary, the more deteriorated beams B01, B06 and B07 showed a failure mode highly influenced by local damages, reflecting in the corresponding degradation rates.

5.7.2 Symptom-variant resistance

Each deck of the viaduct was built by five beams having the geometrical and mechanical characteristics nominally equals. Therefore, the identified modal parameters can be attributed to beams, which although have been in service for the same number of years, they show different deterioration levels, expressed in terms of ultimate flexural strength. Under these assumptions, the identified modal periods can be used as symptoms [4, 5, 6] to describe the evolution of the structural conditions of a beam, having the same characteristics of the investigated structures, affected to deterioration.

Figure 50 shows the experimental bending moments at collapse, as a function of the first flexural periods of the tested beams, normalized by the corresponding values estimated for the undamaged conditions. Both the scaling factors have been estimated through a FE model, assuming the mean values of the material properties and the geometrical dimensions reported in the original design documents.

Adopting a Weibull distribution, that is widely used in lifetime distribution models [32], the evolution of the damage as a function of the symptoms can be expressed as:

$$g(S) = \exp\left\{-\left[\left(S / S_{(t=0)} - 1\right)\cdot \alpha\right]^{\gamma}\right\}, \qquad (3)$$

where $\alpha = 14.52$ and $\gamma = 2.38$ have been estimated fitting the experimental data through the least-square method. Equation 3 supplies an estimation of the evolution of the flexural resistance in terms of the selected symptom *S*.

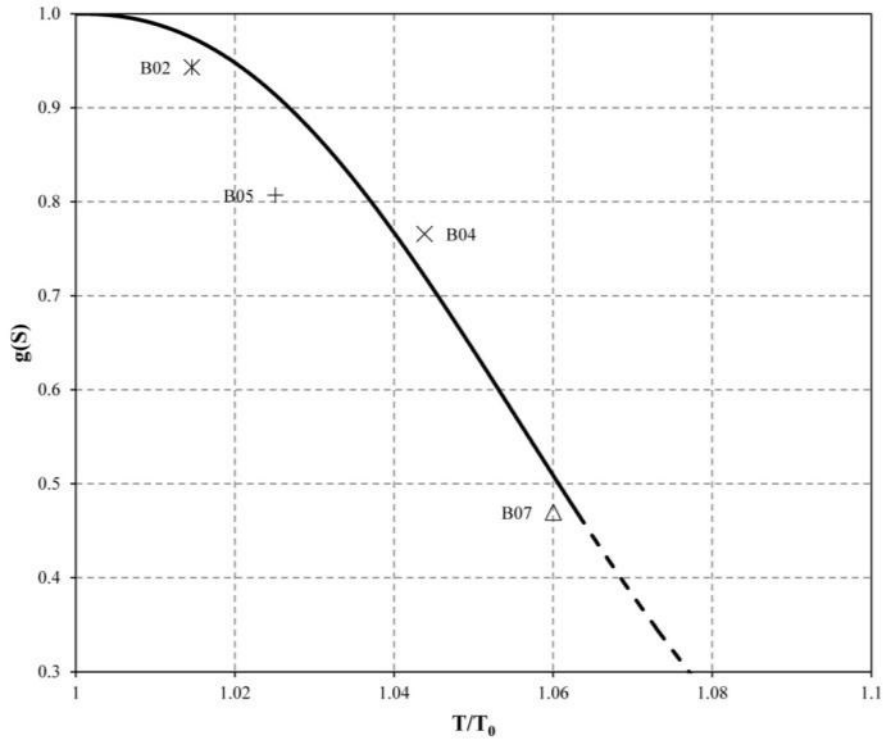

Figure 50 Normalized symptom-variant flexural resistance. The dashed part of the curve indicates the part of the diagram not directly investigated by the experimental tests, but only extrapolated by data fitting

The diagram in Fig.50 shows the variation of the resistance in function of the ratio between the measured period T, the symptom, and the period T_0, of a beam of the same type.

5.8 Assessment of structural reliability

The assessment of structural reliability of the tested beams has been performed. The reliability index, β, is defined as a function of probability of failure, P_F,

$$\beta = -\Phi^{-1}(P_F) \qquad (4)$$

Where $-\Phi^{-1}(P_F)$ is the inverse standard normal distribution function.

The statistical models of the actions and resistances are based on existing literature [32] and on the experimental data collected. In particular, the ULS design moment has been calculated according to the European standard EC1 UNI EN 1991-2:2005, adopting the Courbon's method to evaluate the design load acting on an edge beam (Load Model 1) [33]. The reliability index has been estimated assuming the statistical parameters for resistance and loads reported in Table 20. The reliability index at t = 0 is $\beta_0 = 4.01$. The flexural resistance of each beam has been modeled adopting a lognormal statistical distribution, which has the mean equal to the experimental ultimate bending moment value and the coefficient of variation CoV 0.1.

Model	Distribution	CoV
Resistance	lognormal	0.1
Permanent Load	lognormal	0.1
Accidental Load	lognormal	0.2

Table 20 Statistical parameters for loads and resistance at t = 0 [31]

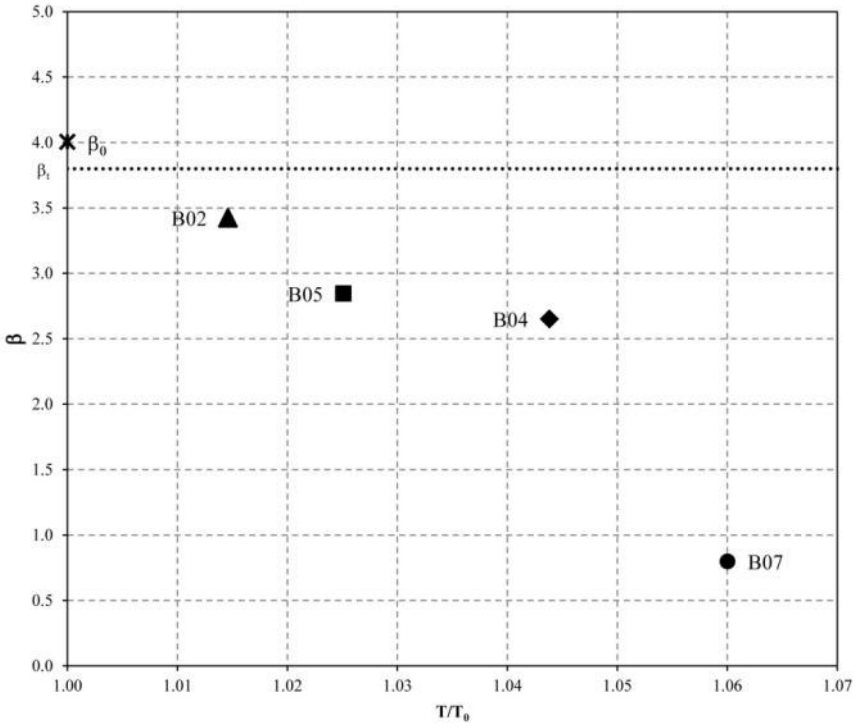

Figure 51 Reliability index β of beams B02, B04, B05 and B07 as a function of normalized symptom

5.8.1 Time-varying reliability index

The reliability profile is defined as the variation of the reliability index with time. Assuming a bi-linear profile [5], from the experimental data is possible to estimate the deterioration rates (Eq. 5).

$$\begin{cases} \beta(t) = \beta_0 & 0 \le t \le t_I \\ \beta(t) = \beta_0 - \alpha \cdot (t - t_I) & t > t_I \end{cases} \qquad t_I = 5 \text{ years.} \tag{5}$$

In Fig. 51 and Fig. 52, the dotted horizontal line indicates the recommended minimum value of reliability index β_t =3.8 at ultimate limit states for structures belonging to the class RC2 for a 50 years reference period, according to the European standard EC0 [34].

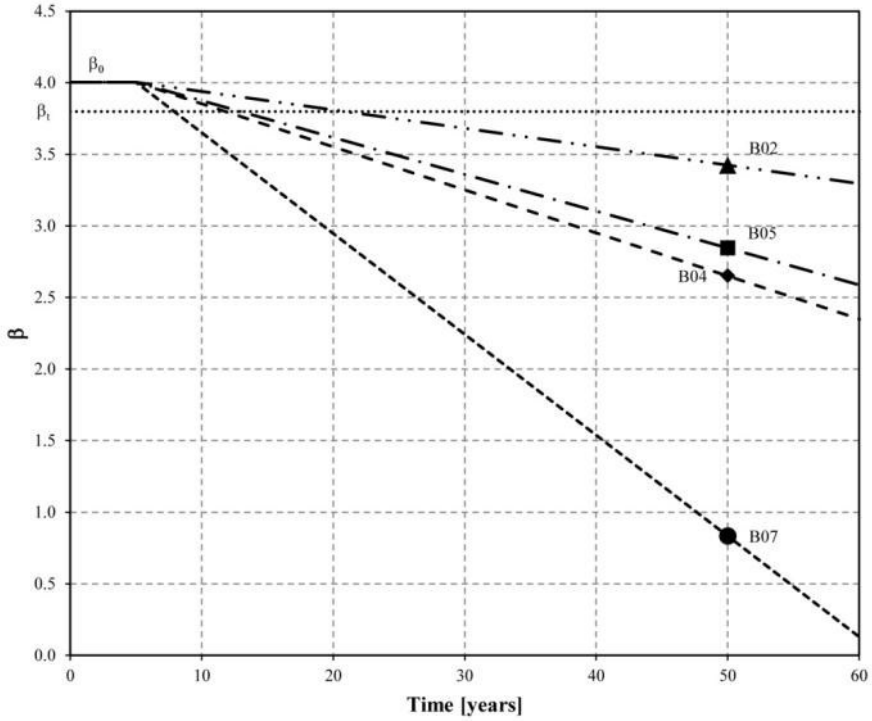

Figure 52 Estimated time-variant reliability index profile of beams B02, B04, B05 and B07

References

[1] Brincker, R., Andersen, P., Kirkegaard, P.H., Ulfkjaer, J.P., (1995); *Damage Detection in Laboratory Concrete Beams*. Proceedings of the 13th International Modal Analysis Conference, 668-674.

[2] Doebling, S.W., Farrar, C.R., Prime, M.B., Shevitz, D.W., (1996); *Damage Identification and Health Monitoring of Structural and Mechanical Systems from Changes in Their Vibration Characteristics: A Literature Review*. Technical Report LA-13070-MS , Los Alamos National Laboratory, Los Alamos, NM..

[3] Friswell, M.I., (2007); *Damage identification using inverse methods*. Philosophical Transaction of the Royal Society A, 365, pp. 393-410

[4] Cempel, C., Natke, H.G., Yao, J.T.P., (2000); *Symptom reliability and hazard for systems condition monitoring*. Mechanical Systems and Signal Processing, 14(3), pp. 495 – 505.

[5] Ceravolo, R., Pescatore, M., De Stefano, A., (2009); *Symptom based reliability and generalized repairing cost in monitored bridges*. RELIABILITY ENGINEERING & SYSTEM SAFETY, 94(8), pp. 1331-1339.

[6] Enright M.P., Frangopol D.M. (1998), *Probabilistic analysis of resistance degradation of reinforced concrete bridge beams under corrosion*, Engineering Structures, 20 (1998), 960-971.

[7] Enright, M.P., Frangopol, D.M., (1998); *Service-life prediction of deteriorating concrete bridges*. Journal of Structural Engineering ASCE, 3(124), pp. 309-317.

[8] Larimore, W.E., (1990); *Canonical Variate Analysis*. Proceedings of the 29th IEEE Conference on Decision and Control, Honolulu, Hawaii, 635-639.

[9] Juang, J.N., Pappa, R.S., (1984); *An eigensystem realisation algorithm (ERA) for modal parameter identification and modal reduction*. NASA/JPL Workshop on identification and control of flexible space structures.

[10] Van Overschee, P., De Moor, B., *Subspace Identification for Linear Systems: Theory and Implementation - Applications*, Kluwer Academic Press Dordrecht, 1996.

[11] Ewins, D.J., *Modal testing*, Research Studies Press Ltd, 2000.

[12] Farrar, C.R., Worden, K., (2007); *An introduction to structural health monitoring*. Phil. Trans. R. Soc. A, 15(265), pp. 303-315.

[13] Peeters, B., DeRoeck, G., (1999); *Reference-based stochastic subspace identification for output-only modal analysis*. Mechanical Systems and Signal Processing, 13, pp. 855-878

[14] Lawless, J.F., *Statistical models and methods for lifetime data*, New York J. Wiley & Sons, 1982.

[15] Natke, H.G., Cempel, C., *Model – Aided Diagnosis of Mechanical Systems*, Germany Springer, 1997.

[16] Thoft-Christensen, P., Jensen FM, F.M., Middleton , C.R., Blackmore, A., Assessment of the reliability of concrete slab bridges, in: Frangopol D.M., C.R.B..R.R., Reliability and Optimization of Structural Systems, 1997, pp. 321-329.

[17] Enright, M.P., Frangopol, D.M., Hearn, G., (1996); *Degradation of reinforced concrete bridges under aggressive conditions*. Materials for the New Millennium - ASCE, Vol. 2, pp. 978 - 987.

[18] Mori, Y., Ellingwood, B., *Methodology for reliability-based condition assessment: application to concrete structures in nuclear plants*, Washington, DC Nuclear Regulatory Commission, 1993.

[19] ISO, (2010); *Bases for design of structures - Assessment of existing structures*. International standard ISO 13822

[20] Bonato, P., Ceravolo, R., De Stefano, A., (1997); *Time-Frequency and ambiguity function approaches in structural identification*. J. of Eng. Mech., 123(12), pp. 1260-1267.

[21] Brownjohn, J.M.W., Lee, J., Cheong, B., (1999); *Dynamic performance of a curved cable-stayed bridge*. Engineering structures,(21), pp. 1015-1027.

[22] De Stefano, A., Actual trends in output only modal identification, in: Baratta, A., Corbi, O., Intelligent structures. An Overview on the Ongoing European Research, Fridericiana Editrice Universitaria, 2003.

[23] Diamantidis, D., *Probabilistic Assessment of Existing Structures.*, Diamantidis, Joint Committee on Structural Safety, RILEM Publications S.A.R.L., 2001.

[24] Felber, A.J., Ventura, C.E., (1996); *Frequency Domain Analysis of the Ambient Vibration Data of the Queensborough Bridge Main Span*. Proceedings of the 14th International Modal Analysis Conference, Dearborn.

[25] Fox, R.L., Kapoor, M.P., (1968); *Rates of Change of Eigenvalues and Eigenvectors*. AIAA Journal, 6(12), p. 2426.

[26] Gladwell, G.M.L., *Inverse Problems in Vibration*, Dordrecht Springer, 1986.

[27] Rucker, W., Hille, F., Rohrmann, r., (2006); *Guideline for Structural Health Monitoring*. Samco.

[28] Thoft-Christensen, P., (1998); *Assessment of the reliability profiles for concrete bridges*. Engineering Structures, 20(11), pp. 1004-1009.

[29] Stewart, M.G., Rosowsky, D.V., (1998); *Time-dependent reliability of deteriorating reinforced concrete bridge decks*. Structural Safety,(20), pp. 91-109.

[30] Stewart, M.G., Rosowsky, D.V., (1998); *Structural safety and serviceability of concrete bridges subject to corrosion*. ASCE Journal of Infrastructure Systems,(4), pp. 146-155.

[31] Susoy, M., Catbas , F.N., Frangopol, D.M., *Evaluation of Time-Variant Bridge Reliability Using Structural Health Monitoring*. IMAC-XXVI Conference & Exposition on Structural Dynamics - Technologies for Civil Structures.

[32] Nowak A.S., Collins K.R., *Reliability of Structures.* Mc Graw Hill International Editions, 2000

[33] UNI EN 1991-2:2005 Eurocode 1 - Actions On Structures - Part 2: Traffic Loads On Bridges

[34] UNI EN 1990: 2002 Eurocode 0 – Basis of structural design

Chapter 6

Conclusions

The thesis deals with the application of the health monitoring strategies to the assessment of the structural reliability. This can be considered as a function of some measurable quantities, to be intended as symptoms, which reflect the state of damage.

The main focus of the research is on the vibration based techniques. Monitoring the modal quantities is, in fact, nowadays widely used in different fields of engineering, because it can provide a more thorough knowledge of the global structural behaviour. Moreover, periodic or continuous monitoring can track the structural changes and help to characterize the eventual state of damage and its evolution.

The work has been divided in three parts: features extraction, damage detection and safety assessment.

Relating to the feature extraction, an improved version of the time-frequency identification technique has been proposed and validated through numerical and experimental studies. In particular the TF approach has been used because it proved in the past to be very effective for use in non-stationary condition and under unknown excitation. Moreover, the frequency estimation based on instantaneous phase difference seems to be little affected by influence of damping, this improving the capability to differentiate the coupled modes. However the standard identification procedure, based on searching the minima of the mean of standard deviation functions of the instantaneous phase difference estimators, may fail in presence of weakly correlated signals.

Such a difficulty has been overcome applying the Principal Component Analysis, In particular, by substituting the average of standard deviation whit the smallest principal component variance, extracted from the set of instantaneous estimators. The proposed method has been validated trough numerical examples and then successfully applied to a real complex case study, the Holy Shroud Chapel in Turin. This structure is particularly challenging due to his geometrical configuration and the presence of damages caused by a destructive fire broke out in 1997.

In the second part, an on-line novelty detection technique has been implemented in conjunction of instantaneous modal identification, in order to detect and characterize the damage. In this contest, the instantaneous modal frequencies are considered as a symptom. Therefore, the application of outlier analysis is devoted to detect the important structural changes and to reduce the time lapse between the occurrence of damage and its detection.

The proposed technique has been applied to a laboratory case study, a masonry arch bridge scaled model, built on the Department of Structural and Geotechnical Engineering of Politecnico di Torino. The structure has been subjected to extensive experimental test campaigns since 2008. A brief description of the tests performed has been reported and a synthesis of main results depicted.

The third part regards the assessment of existing structures on the basis of the monitored parameters. The integration of the health monitoring strategies with the safety assessment is a promising tool to be used in management of complex structural systems and into the evaluation of the structural behavior of existing elements. Experimental tests on damaged structures can provide important information to be used in developing SHM techniques and calibrating predicting models.

The results of experimental tests on bridge beams dismounted after 50 years of service life are presented. The tests highlight the connection among residual strength and dynamic characteristics, as periods. The residual resistance of the of the beams has been expressed as a function of measured symptoms and the evolution in time is estimated. Nevertheless the reliability of the beams has been also estimated. Finally, the results obtained indicate that the knowledge coming from monitoring systems and the classical structural safety formulations lend themselves to be usefully combined together for improving the reliability assessment of existing structures.

References

[1] Allemang, R.J., (2002); *The Modal Assurance Criterion (MAC): twenty years of use and abuse*. IMAC.

[2] Bonato, P., Ceravolo, R., De Stefano, A., Molinari, F., (2000); *Use of cross time-frequency estimators for the structural identification in non-stationary conditions and under unknown excitation*. J. of Sound and Vib., 237(5), pp. 775-791.

[3] Bonato, P., Ceravolo, R., De Stefano, A., (1997); *Time-Frequency and ambiguity function approaches in structural identification*. J. of Eng. Mech., 123(12), pp. 1260-1267.

[4] Brincker, R., Andersen, P., Kirkegaard, P.H., Ulfkjaer, J.P., (1995); *Damage Detection in Laboratory Concrete Beams*. Proceedings of the 13th International Modal Analysis Conference, 668-674.

[5] Brincker, R., Zhang, L., Andersen, P., (2000); *Modal Identification of output-only systems using Frequency Domain Decomposition*. Proc. European COST F3 Conf. On System Identification & Structural Health Monitoring.

[6] Brownjohn, J.M.W., Lee, J., Cheong, B., (1999); *Dynamic performance of a curved cable-stayed bridge*. Engineering structures,(21), pp. 1015-1027.

[7] Brownjohn, J.M.W., (2007); *Structural health monitoring of civil infrastructure*. Phil.Trans.of the Royal Society, 365, pp. 589–622.

[8] Caesar, B., (1986); *Update and identification of dynamic mathematical models*. IMAC

IV, pp. 394-401.

[9] Carpinteri, A. et al., (2010); *Experimental and numerical analysis of a two-span model masonry arch bridge subjected to pier scour*. Advanced materials Research, 133-134, pp. 301-306.

[10] Ceravolo, R., Pescatore, M., De Stefano, A., (2009); *Symptom based reliability and generalized repairing cost in monitored bridges*. RELIABILITY ENGINEERING & SYSTEM SAFETY, 94(8), pp. 1331-1339.

[11] Cempel, C., Natke, H.G., Yao, J.T.P., (2000); *Symptom reliability and hazard for systems condition monitoring*. Mechanical Systems and Signal Processing, 14(3), pp. 495 – 505.

[12] Carmona, R., Hwang, W.L., Torrésani, B.P., *Practical time-frequency analysis*, San Diego, CA 92101-4495, USA Academic Press, 1998.

[13] Choi, H.I., Williams, W.J., (1989); *Improved time-frequency representation of multicomponent signals using exponential kernels*. IEEE Trans. Acoust. Speech Signal Process, 37(6), pp. 862-871.

[14] Cohen, L., *Time-Frequency Analysis*, Englewood Cliffs, NJ Prentice-Hall Inc., 1995.

[15] De Stefano, A., Actual trends in output only modal identification, in: Baratta, A., Corbi, O., Intelligent structures. An Overview on the Ongoing European Research, Fridericiana Editrice Universitaria, 2003.

[16] De Stefano, A., Ceravolo, R., (2007); *Assessing the Health State of Ancient Structures: The Role of Vibrational Tests*. Journal of intelligent material systems and structures, 18, pp. 793-807.

[17] De Stefano, A., Enrione, D., Ruocci, G., (2008); *Innovative techniques for structural assessment: the case of the Holy Shroud Chapel in Turin*. Proc. 6th Int. Conf. on Structural Analysis of Historical Construction (SAHC 2008).

[18] De Stefano, A., Enrione, D., Ruocci, G., Bottazzoli, F., (2007); *Robust stochastic model updating to face uncertainties: application to the Holy Shroud Chapel in Turin*. Proc.

2nd Int. Conf. on Structural Condition Assessment, Monitoring and Improvement (SCAMI-2).

[19] Diamantidis, D., *Probabilistic Assessment of Existing Structures.*, Diamantidis, Joint Committee on Structural Safety, RILEM Publications S.A.R.L., 2001.

[20] Deraemaeker, A., Reynders, E., De Roeck, G., Kullaa, J., (2008); *Vibration-based structural health monitoring using output-only measurements under changing environment*. Mechanical Systems and Signal Processing, 22, pp. 34-56.

[21] Enright, M.P., Frangopol, D.M., (1998); *Service-life prediction of deteriorating concrete bridges*. Journal of Structural Engineering ASCE, 3(124), pp. 309-317.

[22] Enright, M.P., Frangopol, D.M., Hearn, G., (1996); *Degradation of reinforced concrete bridges under aggressive conditions*. Materials for the New Millennium - ASCE, Vol. 2, pp. 978 - 987.

[23] Farrar, C.R., Worden, K., (2007); *An introduction to structural health monitoring*. Phil. Trans. R. Soc. A, 15(265), pp. 303-315.

[24] Felber, A.J., Ventura, C.E., (1996); *Frequency Domain Analysis of the Ambient Vibration Data of the Queensborough Bridge Main Span*. Proceedings of the 14th International Modal Analysis Conference, Dearborn.

[25] Ewins, D.J., *Modal testing*, Research Studies Press Ltd, 2000.

[26] Doebling, S.W., Farrar, C.R., Prime, M.B., Shevitz, D.W., (1996); *Damage Identification and Health Monitoring of Structural and Mechanical Systems from Changes in Their Vibration Characteristics: A Literature Review*. Technical Report LA-13070-MS , Los Alamos National Laboratory, Los Alamos, NM..

[27] Friswell, M.I., (2007); *Damage identification using inverse methods*. Philosophical Transaction of the Royal Society A, 365, pp. 393-410.

[28] Fassois, S.D., Lee, J.E., (1993); *On the problem of stochastic experimental modal analysis based on multiple-response data. Part II: the modal analysis approach*. Journal

of Sound and Vibrations, 161(1), pp. 57-87.

[29] Ghanem, R., Shinozuka, M., (1995); *Structural system identification II: Experimental verification*. ASCE J. of Eng. Mech., 121(2), pp. 265-273.

[30] Invernizzi, S., Lacidogna, G., Manuello, A., Carpinteri, A., (2009); *Damage assessment of a two-span model masonry arch bridge*. Proceedings of the SEM Annual Conference, Albuquerque, USA.

[31] Juang, J.N., Pappa, R.S., (1984); *An eigensystem realisation algorithm (ERA) for modal parameter identification and modal reduction*. NASA/JPL Workshop on identification and control of flexible space structures.

[32] Jolliffe, I.T., *Principal Component Analysis*, II, Principal Component Analysis, 2002.

[33] Lawless, J.F., *Statistical models and methods for lifetime data*, New York J. Wiley & Sons, 1982.

[34] Larimore, W.E., (1990); *Canonical Variate Analysis*. Proceedings of the 29th IEEE Conference on Decision and Control, Honolulu, Hawaii, 635-639.

[35] Ljung, L., *System identification theory*, Prentice Hall, 1999.

[36] Maeck, J., Peeters, B., De Roeck, G., (2001); *Damage identification on the Z24 bridge using vibration monitoring*. SMART MATERIALS AND STRUCTURES, 10, pp. 512–517.

[37] Mares, C., Mottershead, J.E., Friswell, M.I., (2006); *Stochastic model updating: Part 1 - theory and simulated example*. Mechanical Systems and Signal Processing, pp. 1074-1095.

[38] Matta, E., De Stefano, A., Quattrone, A., (2009); *Improvement of Time-Frequency domain identification through PCA*. Proceedings IOMAC09, 3rd International Modal Analysis Conference, Ancona (Italy).

[39] Matta, E., De Stefano, A., Quattrone, A., (2009); *Reliability issues in vibration-based sys-tem identification: lessons from the JETPACS case study*. Proc. 4th Int. Conf. on

Structural Healt Monitoring on Intelligent Infrastructure (SHMII-4).

[40] Natke, H.G., Cempel, C., *Model – Aided Diagnosis of Mechanical Systems*, Germany Springer, 1997.

[41] Natke, H.G., Yao, J.T.P., (1986); *Research topics in structural identification*. Proceedings of 3rd Conference on dynamic response of structures ASCE, New York, 542-550.

[42] Natke, H.G., Tomlinson, G.R., Yao, J.T., *Safety evaluation based on identification approaches*, Braunschweig/Weisbaden Vieweg & Sohn, 1993.

[43] Nowak, A.S., Collins, K.R., *Reliability of Structures*, Mc Graw Hill International Editions, 2000.

[44] Peeters, B., DeRoeck, G., (1999); *Reference-based stochastic subspace identification for output-only modal analysis*. Mechanical Systems and Signal Processing, 13, pp. 855-878.

[45] Quattrone, A., Ruocci, G., Ceravolo, R., Worden, K., De Stefano, A., (2010); *Non-Linearity detection in a masonry arch bridge subject to artificial settlements*. Proceedings of Fifth European Workshop Structural health Monitoring, Sorrento, Italy, 1133-1138.

[46] Ruocci, G., (2010); *Application of the SHM methodologies to the protection of masonry arch bridges from scour*. Politecnico di Torino PhD Thesis.

[47] Rucker, W., Hille, F., Rohrmann, r., (2006); *Guideline for Structural Health Monitoring*. Samco.

[48] Reynders, E., Pintelon, R., De Roeck, G., (2008); *Uncertainty bounds on modal parameters obtained from stochastic subspace identification*. Mechanical Systems and Signal Processing, 22, pp. 948-969.

[49] Ruocci, G. et al., (2011); *Experimental testing of a masonry arch bridge model subject to increasing level of damage*. 4th International Conference on Advances in

Experimental Structural Engineering, Ispra, Italy.

[50] Salawu, O., (1997); *Detection of structural damage through changes in frequency: a review*. Engineering Structures, 9(19), pp. 718–723.

[51] Smith, L.M., (1996); *In-service monitoring of nuclear-safety-related structures*. Structural Engineering. 74, pp. 210-211.

[52] Sohn, H. et al., (2003); *A review of structural health monitoring literature: 1996-2001*. Los Alamos National Laboratory Report LA-13976-MS.

[53] Spiridonakos, M.D., Poulimenos, A.G., Fassois, S.D., (2010); *Output-only identification and dynamic analysis of time-varying mechanical structures under random excitation: A comparative assessment of parametric methods*. J. of Sound and Vib., 329, pp. 768-785.

[54] Stewart, M.G., Rosowsky, D.V., (1998); *Time-dependent reliability of deteriorating reinforced concrete bridge decks*. Structural Safety,(20), pp. 91-109.

[55] Thoft-Christensen, P., Jensen FM, F.M., Middleton , C.R., Blackmore, A., Assessment of the reliability of concrete slab bridges, in: Frangopol D.M., C.R.B..R.R., Reliability and Optimization of Structural Systems, 1997, pp. 321-329.

[56] Thoft-Christensen, P., (1998); *Assessment of the reliability profiles for concrete bridges*. Engineering Structures, 20(11), pp. 1004-1009.

[57] Val, D.V., Stewart, M.G., Melchers, R.E., (1998); *Effect of reinforcement corrosion on reliability of highway bridges*. Journal of Engineering Structures, 11(20), pp. 1010 – 1019.

[58] Van Overschee, P., De Moor, B., *Subspace Identification for Linear Systems: Theory and Implementation - Applications*, Kluwer Academic Press Dordrecht, 1996.

[59] Vu, K.A.T., Stewart, , (2000); *Structural reliability of concrete bridges including improved chloride-induced corrosion models*. Structural Safety,(22), pp. 313-333.

[60] Wei, F.S., (1990); *Structural dynamic model improvement using vibration test data*. AIAA Journal 28, pp. 175-177.

[61] Welch, P.D., (1967); *The use of Fast Fourier Transform for the estimation of Power Spectra: a method based on time averaging over short modified periodograms*. IEEE Transactions on Audio and Electro-Acoustic, 15, pp. 70-73.

[62] Worden, K., Manson, G., Fieller, N.R.J., (2000); *Damage detection using outlier analysis*. Journal of Sound and Vibration, 229(3), pp. 647-667.

[63] Yuen, K.-V., Beck, J.L., Katafygiotis, L.S., (2002); *Probabilistic approach for modal identification using non-stationary noisy response measurements only*. Earthquake Engineering & Structural Dynamics, 31(4), pp. 1007-1023.

[64] Eurocodice, *Criteri generali di progettazione strutturale*. UNI EN 1990:2006.

[65] ISO 13822, (2010); *Bases for design of structures - Assessment of existing structures*. International standard ISO 13822.

[66] *EN 1991-2:2003; Eurocode 1: Actions on structures - Part 2: Traffic loads on bridges*.

[67] *EN 1990; Eurocode 0: Basis of Structural Design*.